QUASAR Deliverable D5.4

Final Report on Models with Validation Results

Project Number:	INFSO-ICT-248303
Project Title:	Quantitative Assessment of Secondary Spectrum Access - QUASAR
Document Type:	

Document Number:	ICT-248303/QUASAR/WP5/D5.4/120514
Contractual Date of Delivery:	30.06.2012
Actual Date of Delivery:	30.06.2012
Editors:	Marina Petrova (RWTH), Andreas Achtzehn (RWTH)
Participants:	Andreas Achtzehn (RWTH), Tizazu Alemu (Aalto), Vladimir Atanasovski (UKIM), Niclas Björsell (KTH/HiG), Torsten Dudda (EAB), Liljana Gavrilovska (UKIM), Mohamed Hamid (KTH/HiG), Tim Irnich (EAB), Riku Jäntti (Aalto), Jörgen Karlsson (EAB), Jussi Kerttula (Aalto), Konstantinos Koufos (Aalto), Jonas Kronander (EAB), Pero Latkoski (UKIM), Reihaneh Malekafzaliardakani (EAB), Guilberth Martinez (RWTH), Evanny Obregon (KTH), Alexandros Palaios (RWTH), Nikos Perpinias (RWTH), Marina Petrova (RWTH), Mikael Prytz (EAB), Kalle Ruttik (Aalto), Ljiljana Simic (RWTH), Ki Won Sung (KTH)
Workpackage:	WP5
Estimated Person Months:	30 MM
Security:	PU[1]
Nature:	Report
Version:	1.0
Total Number of Pages:	124
File:	QUASAR_D5.4_120630

Abstract

This deliverable reports final results of the assessment of spectrum whitespaces in various bands for their potential exploitation by specific secondary systems. A generic software tool to aid similar studies is presented. Furthermore, the project's findings

[1] Dissemination level codes: **PU** = Public
PP = Restricted to other programme participants (including the Commission Services)
RE = Restricted to a group specified by the consortium (including the Commission Services)
CO = Confidential, only for members of the consortium (including the Commission Services)

from several measurement campaigns on the accuracy of the underlying propagation and transceiver models are explained.

Keywords List

<List of keywords>

Executive Summary

Deliverable D5.4 summarizes and extends the quantitative assessment of secondary spectrum opportunities for various European countries. Building on the assessment methodology developed in the QUASAR project, this deliverable provides tangible conclusions on the feasibility of deploying specific secondary systems in the European spectrum whitespaces. For this purpose, scenarios for the exploitation of underutilized spectrum resources through macro-cellular deployments in TV whitespaces, Wi-Fi like use of TV whitespaces, and indoor broadband in radar as well as aeronautical spectrum, have been explored in accordance with the defined objectives of the project. Additionally, this deliverable offers new insights into aggregate interference modelling, which has turned out to be of major relevance for the reported studies. A generic software tool to aid the quantitative analysis by implementing the developed assessment workflow is presented and discussed. Verification of the methods has been conducted by means of extensive measurement campaigns for the considered frequency bands the project carried out in various locations throughout Europe.

The project concludes that the aggregate interference constraint seriously hampers potential deployments of cellular networks in TV frequency bands. Common objectives such as contiguous coverage and high throughput cannot be achieved. However, it has become apparent that TV whitespaces could be considered for micro-cellular capacity boosting in urban scenarios. Low-rate applications are a plausible target for Wi-Fi-like multi-user secondary networks, where current solutions provide insufficient ranges. Here, dense deployment studies in Macedonia have revealed that throughputs of approximately 1.7 Mbps are achievable under the currently proposed regulatory frameworks. Radar bands and aeronautical bands may lend themselves for dense low-power urban deployments due to the specific geometry and low density of primary transmitters. Even under conservative assumptions approximately 50 MHz of bandwidth would be available in urban areas as shown by example of Germany and Sweden.

The project's measurement campaigns show that large discrepancies exist between estimated and measured signal strengths of primary systems. Even with highly sophisticated propagation models, shadowing and local effects are not sufficiently captured. This may impose a serious threat to primary deployments if not taken into account by secondary systems' power budgeting. Shadowing correlation measurements have the potential of improving coverage prediction, and provide more robust protection requirements, as derived from measurement data acquired through the campaign. It was found that spectrum leakage and intermodulation products has an additional, serious impact to outdoor operations of whitespace devices operating in the proximity of TV transmitters. Studies for DME radars show that it is very difficult to reliably estimate spatio-temporal characteristics of these primary systems.

Contributors

First name	Last name	Affiliation	Email
Jonas	Kronander	Ericsson AB	jonas.kronander@ericsson.com
Jörgen	Karlsson	Ericsson AB	jorgen.s.karlsson@ericsson.com
Reihaneh	Malekafzaliardakani	Ericsson AB	reihaneh.malekafzaliardakani@ericsson.com
Tim	Irnich	Ericsson AB	tim.irnich@ericsson.com
Torsten	Dudda	Ericsson AB	torsten.dudda@ericsson.com
Mikael	Prytz	Ericsson AB	mikael.prytz@ericsson.com
Liljana	Gavrilovska	UKIM	liljana@feit.ukim.edu.mk
Pero	Latkoski	UKIM	pero@feit.ukim.edu.mk
Vladimir	Atanasovski	UKIM	vladimir@feit.ukim.edu.mk
Mohamed	Hamid	KTH/HiG	modhad@kth.se
Niclas	Björsell	KTH/HiG	nbl@hig.se
Ki Won	Sung	KTH	sungkw@kth.se
Evanny	Obregon	KTH	ecog@kth.se
Marina	Petrova	RWTH	mpe@inets.rwth-aachen.de
Ljiljana	Simic	RWTH	lsi@inets.rwth-aachen.de
Alexandros	Palaios	RWTH	apa@inets.rwth-aachen.de
Nikos	Perpinias	RWTH	npe@inets.rwth-aachen.de
Guilberth	Martinez	RWTH	gma@inets.rwth-aachen.de
Andreas	Achtzehn	RWTH	aac@inets.rwth-aachen.de
Tizazu	Alemu	Aalto	Tizazu.Alemu@aalto.fi
Jussi	Kerttula	Aalto	Jussi.Kerttula@aalto.fi
Konstantinos	Koufos	Aalto	Konstantinos.Koufos@aalto.fi
Kalle	Ruttik	Aalto	Kalle.Ruttik@aalto.fi
Riku	Jäntti	Aalto	Riku.Jantti@aalto.fi

Table of contents

1 Introduction

Due to the increased demand of broadband wireless services and the exponential growth of data traffic, the spectrum allocation policies and regulations need to be revisited in order to enable more flexible use of spectrum. Secondary spectrum sharing in different frequency bands has been intensively discussed and researched as a potential solution for providing additional capacity by spatial and temporal reuse of already allocated but underutilized spectrum.

Before adopting any new spectrum rulings, it is important to understand how much unutilized spectrum is out there in different locations and under what conditions it is available for use. Due to the strict protection rules for the primary users on one hand and the requirements to provide a certain quality of service to the potential secondary users, extensive quantitative analyses are need to determine if there exist real secondary opportunities for the desired secondary system realizations under a certain level of allowed interference.

The main goal of the project has been to address these questions and provide a detailed quantitative assessment, which can be used to draw tangible conclusions, both from scientific and regulatory point of view. For that purpose WP5 developed methods and tools for the assessment of the secondary spectrum based on the inputs from other technical WPs and provided tangible results about the spectrum availability. In the previous deliverable D5.1, basic framework and methodology for the quantitative assessment was proposed and some preliminary assessment results were presented [D51]. The basic methodology and results were elaborated in the deliverable D5.2, where four detailed secondary use scenarios were selected, and assessment methods were refined and fine-tuned in order to account for the specific aspects of each scenario [D52]. The results provided in D5.2 were an intermediate step towards the analyses of a multi-user secondary system in the sense that only a single secondary user was considered. In D5.3, the impact of multiple secondary users was thoroughly investigated for the scenarios chosen in D5.2, namely *macro cellular use of TV white spaces*, *WiFi-like use of TV white spaces*, *indoor broadband in radar spectrum* and *indoor broadband in aeronautical spectrum*.

1.1 Scope and organization of D5.4

This deliverable builds on the analyses in D5.3 and provides additional details and results from the spectrum assessment of multi-user secondary systems for the above-mentioned scenarios. Since this document is a final report about the work conducted in WP5, at the beginning we summarize the final design of the assessment work including new insights about the aggregate interference modelling. Furthermore we outline the main findings of the quantitative spectrum assessment carried out for a number of European countries, frequency bands and scenarios. To demonstrate the feasibility of the spectrum assessment methodology developed we have designed a generic software tool for calculation of spectrum availability and spectrum opportunity. Here we report on the main components of the software tool, show the implemented workflow that is aligned to the assessment methodology, and give the design parameters for two secondary deployment scenarios, namely cellular and Wi-Fi-like systems, that have been included in accordance with the scenarios developed in the project. Finally to support our approach in finding out the truth about the secondary spectrum opportunities a number of verification measurement campaigns were carried out in different locations throughout the duration of the project. An extensive overview of propagation measurements in TV bands, co-existence measurements reporting on the influence of a white-space device to a primary TV receiver and shadow-correlation measurements is given in this document.

The reminder of the deliverable is organized as follows. In Section 2 we discuss the main results from the quantitative secondary spectrum studies. In Section 3 we discuss a prototype implementation of a spectrum assessment software and aligned visualization tool. In Section 4 we present results from various measurement studies on spectrum availability, coexistence of secondary devices and better estimation of spectrum usage through shadow estimation. Finally we conclude the document in Section 5.

2 Spectrum availability assessment framework and summary of outcomes

This section provides a brief overview of the assessment framework that has been employed in QUASAR in the assessment activities to derive the usefulness of secondary spectrum access in the various scenarios. This section also summarizes the findings detailed in previous deliverables [D51][D52][D53] and state the main conclusions regarding the considered use cases and scenarios.

The main outcomes of the evaluations are as follows:

From the assessments of for using TV Whitespace (TVWS) opportunities to operating a mobile cellular network it is found that the business case, using reasonable assumptions on cost structures, is in almost every situation more promising for using licensed spectrum than TVWS opportunities. Hence, from the perspective of a cellular operator a second digital dividend, opening up TV bands for more licensed dedicated cellular spectrum is more beneficial than allowing secondary access to TV white spaces.

Through simulation of a nationwide cellular network in Germany and Finland it was found that the main hindrance to wide-scale deployments of cellular networks is the aggregate interference they evoke. Traditional planning tools for cellular networks require extensive modifications to allow for a policy-compliant configuration of the secondary network. Furthermore, the maximum transmit power budget for each base station permissible under the secondary usage policy is not sufficient for mixed microcellular/macrocellular deployments. It was found that mostly microcells in urban areas with low coverage requirements would benefit from TVWS, but that the requirements for universal coverage and high data rates cannot be fulfilled with the current plans for regulations. Especially, the adjacent channel interference constraint tends to limits the available power for cellular systems making deployment of large cells challenging.

The investigations of operating Wi-Fi-like secondary networks in TVWS in Germany show that outdoor operation is not viable. It is also found that indoor operation might be viable, but only for low-rate applications.

It is concluded from the studies of Macedonian situation that the existing significant interference in the band makes the average throughput of a secondary access point only reach a maximum of 1.7Mbps. Comparing with today's Wi-Fi systems operating in the ISM bands this maximal average throughput indicates that the solution will not be competitive alternative to operating in ISM bands.

A large part of the 2.7-2.9GHz radar band, used by air traffic control (ATC) radars, is found to be available for dense deployments of low-power secondary users. This in particular applies to secondary users in urban areas, which are typically far from the primary radars.

The investigations of the possibilities of secondary spectrum access to the aeronautical spectrum band (960-1215 MHz), used by distance measurement equipment (DME), have shown that under conservative assumptions a bandwidth of at least 50MHz would be available to a dense deployment of secondary users in any location of Germany or Sweden.

In summary: The radar and aeronautical bands provides promising opportunities for low-power secondary systems. However there are still large regulatory issues to be sorted out before the opportunities may be realized in practice, cf. [D14]. On the other hand, it seems to be difficult to realize good secondary performance in the TV bands, both for Wi-Fi like systems and for macro cellular systems. The latter indicates that it may be more beneficial to repurpose the TV bands, via a second digital dividend, to open up for more efficient use of the spectrum than to allow secondary TVWS usage. Such an alternative would comprise eliminating, or at least reducing the amount, of TVWS and provide more dedicated spectrum for mobile broadband services.

Before going into a more detailed overview of the above conclusions we start with a recapitulation of the assessment methodology and highlight some aspects of particular importance to the modelling of the scenarios.

2.1 Design principles of spectrum assessment methodology

In the following, we provide a short recapitulation of the spectrum assessment methodology and its main design principles. A comprehensive description is provided in D2.2 [D22] to which we refer the reader for further information.

The spectrum assessment methodology builds on the following requirements for a feasible evaluation of secondary spectrum usage opportunities

- A primary system as incumbent to the studied frequency bands shows to have a number of deployment and technological features that need to be taken into account before analysing secondary opportunities. Here, particularly the location of the network components (transmitters and receivers) needs to be studied as they imply the spatial extent of spectrum usage. However, the location is not the sole delimiter of primary usage characteristics. Links between primary devices are subject to path loss and other environmental challenges which affect the protection requirements. For systems with unknown component locations, e.g. due to mobility or broadcasting-type of deployments, the assessment needs to make worst-case assumption. These assumptions need to go beyond simple coverage-edge calculations as applied in current regulations, e.g. for TVWS, because the radio propagation environment is significantly more complex and effects of terrain, indoor/outdoor deployment, etc. may lead to considerably different protection requirements.
- The primary system technology and communication paradigm (unidirectional, bidirectional, broadcasting, etc.) must be included in any holistic study. The applied radio standards and transceiver technologies specify the achievable performance of the primary system under defined environmental conditions. A holistic study must go beyond simple maximum-interference calculations to find the user-level impact of secondary operations on the primary user. The observable degradation in service quality of the primary system needs to be accounted for beyond binary “coverage-no-coverage” studies. Here, also probabilistic models of service-level degradation that include more sophisticated primary transceiver chain models will be a feasible extension for secondary studies. Since practical transceiver implementations make, for reasons of cost-efficiency, tradeoffs on their achievable performance, (a set of) more realistic transceiver models needs to be derived for any primary system under consideration.
- It was found that the configuration of the secondary systems in terms of deployment scenario, power and resource allocation, and other transmitter characteristics plays a significant role in the secondary opportunity calculation. Model-based deployments need to be tested in their entirety to find the possible impact on primary performance and the achievable gains through secondary operations. Abstract secondary system models regularly fail to cover all necessary facets of secondary network operations, hence simulation-based studies need to sacrifice abstract representations to conduct large-scale studies with a multitude of different possible/plausible secondary configurations instead.
- Only after the secondary deployment has been defined, its impact on the primary system can be derived. This process requires an iterative circle that tests secondary configurations for their compliance to the considered usage regulations, and modifies the secondary configuration in order to match the primary constraints and/or improve secondary performance. Decision-making at this level is highly complex, because technical as well as economic objectives of the secondary system design affect the design process. While for local or

simplified problems this may be described in terms of mathematical optimization algorithms, the holistic approach that is the objective of the QUASAR project will require also human interaction. This can only be achieved by providing the relevant stakeholders, i.e. regulators and industry, with a set of tools to study the complex scenarios of secondary operations.

The design principles described above have led to the definition of the spectrum assessment methodology, which we are going to describe in the following. Furthermore, as the QUASAR project also favours finding a set of tools to allow in-depth studies of secondary opportunities, a prototypic implementation of a spectrum assessment tool has be conducted. We will discuss the mapping of the implementation to the spectrum assessment methodology in detail in section 2.2 below.

2.2 Spectrum assessment methodology

The spectrum assessment methodology can be described by four consecutive steps that require individual inputs and create outputs that are inputs to the subsequent execution steps. We will list them here for sake of completeness, but refer for a more detailed explanation to the relevant QUASAR deliverables.

As a first step, the primary system is specified, which is comprised of primary transmitters/receivers that employ a known radio technology (e.g. DVB-T) for communication. If the locations of the primary devices are unknown, worst case assumptions are made, e.g. assuming that TV receivers exist in any location that is covered through the TV broadcasting signal. At this point, models of the radio environment are included to calculate the performance of communications links without the impact of the secondary network. This will build the baseline of the assessment. If required, the primary system model is additionally described through a reference geometry and reference technical implementation that may cover antenna heights, decoding capabilities and Signal-to-Noise Ratio (SNR) requirements. By reversion of the spectrum usage, i.e. by finding those spectrum resources that are spatially or temporarily unused, and through application of the regulation policy with a simplified single-secondary transmitter model, the raw **spectrum availability** can be determined.

The second step is to define the secondary system that is planned to be deployed. Here, only the fundamental configuration, i.e. the basic parameters of distribution and transmitter/receiver technology limitations are specified. The secondary system may be deployed according to an existing deployment plan (as is the case if “boosting capabilities” of existing networks are analysed) or a probabilistic model with locations according to point-process models are applied. Part of the specification of the secondary system is also the description of the performance metrics that will be used in subsequent steps for the feasibility analysis. The secondary transceiver capabilities in terms of the supported transmit powers, the antenna configuration as well as the primary-interference rejection capabilities are additional inputs to this assessment step.

In a third, and computationally complex step, the spectrum allocation to the secondary system as well as the power budgets are calculated. The regulatory policy of the primary system will define these constraints, but additional constraints due to the secondary system technology, can be integrated here. This step requires some level of optimization if the solution space of allocations is non-singular. The optimization may be conducted manually, or through application of generic optimization algorithms with adequate utility functions for the secondary operator. The comprised spectrum usage of the secondary system defines the **secondary opportunity**, which is a subset of the spectrum availability described above. The third step may require manual intervention and review to find an allocation that maximizes utility while protecting the primary system. It may lead to a reversion to the second assessment step if no suitable solution is found.

The final step takes more advanced metrics that do not influence the secondary system design and produces a holistic analysis of the configuration found. The results of this step may be compared to other assessments with similar parameters but other

realizations of probabilistic terms. The final step can be conducted offline and integrates the business analysis of the scenario. Higher-level statistics of multiple test runs will build the foundation for further system-level discussions, e.g. on opportunities of policy review. Here, also the quantitative impact on primary system performance is used as a metric to gauge potential acceptance of the secondary deployment.

2.3 **Modelling**

The modelling and assumptions that goes into the assessments is of high importance for the relevance of the obtained results. Hence it is important to make the reader aware of the models used. In previous deliverables the models have been presented in detail. In D5.2 [D52] the modelling related to accurately describing the radio propagation environment, the parameters and models describing primary and secondary systems are described in detail, and we refer the reader to that deliverable for information on the models. In this section we limit ourselves to giving an overview of the developed models for one of the most important aspects of secondary spectrum access; how to model the interference caused by secondary transmitters to primary receivers. The complexity of the model stems from the difficulty to accurately and computationally efficiently estimate the aggregated interference from a large set of secondary transmitters. The presented models have been shown to accurately describe the interference situation experienced at primary receiver locations.

2.3.1 **Interference modeling**

In D4.3 we proposed two new models for computing the aggregate secondary interference: the exclusion region model and the power density based model. The exclusion region model is applicable when multiple secondary transmitters interfere with a single primary receiver and it is suitable to describe aggregate interference in the radar and aeronautical spectrum. The power density based model proposes to group multiple secondary transmitters together and describe their interference as a function of the spatial power density emitted from their deployment area. It has been validated in the TV spectrum [D43].

One of the clear outcomes of QUASAR is that the key bottleneck in secondary spectrum access would be the aggregate secondary interference under a massive secondary use. In D4.3 we have proposed a method to approximate the aggregate interference in a terrain-based propagation environment with non-uniform spatial user service demand. In the present deliverable we illustrate the results for a study area in Helsinki using realistic household density maps.

The secondary system is assumed to be of WLAN type. Each household has single WLAN transmitter. To get a first assessment of the aggregate interference the secondary MAC scheme is ignored. In order to compute the aggregate interference the location and the activity of each secondary transmitter has to be known. This kind of information is usually not available and statistical approaches are utilized instead. The Poisson point process (PPP) [Kingman1993] has been widely used to model the aggregate interference from independent and randomly located transmitters.

The PPP model assumes that the transmitters are uniformly distributed inside their deployment area. Because of that, a PPP model is not able to capture the statistics of the interference distribution in environments with non-uniform spatial service demand. One way to overcome this issue is to consider a clustered PPP model [Gulati2010]. The clustered PPP describes the aggregate interference as a sum of the interference from multiple clusters.

Our system set up is illustrated in Figure 2-1. We consider a single TV transmitter outside Helsinki, Finland and 10 test pixels inside its coverage area. The TV test pixels are used to emulate the potential locations of TV receivers. Around each pixel we deploy a grid of 100 test points for modelling the effects of slow fading. We compute the aggregate interference level due to the secondary transmissions at all 1000 points. We

will express the distribution of the aggregate interference by computing the histogram of these 1000 values. The parameter settings for the TV and the secondary system can be found in D4.3.

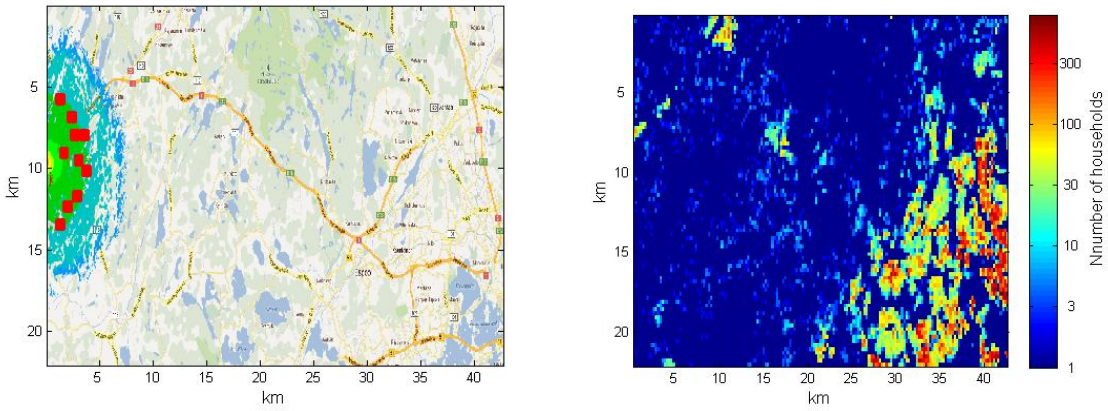

Figure 2-1: Terrain, TV coverage area and TV test points (left). Density of the households (right).

Outside of the TV protection area the secondary network is deployed and operates co-channel to the TV transmitter. Following the approach adopted by ECC the deployment area is covered by square pixels. The number of households inside each secondary pixel is depicted in Figure 2-1 (right). The emitted power from each pixel is computed by scaling the transmission power level of a single secondary transmitter with the amount of households in that pixel times the activity factor.

Due to the non-uniform density of the households, a PPP model cannot describe the aggregate interference distribution sufficiently well. We separate the deployment area into multiple groups of pixels and compute the aggregate interference from each group. For illustration, we split the secondary deployment area into equally-sized squares, see Figure 2-2. For each group of pixels the density of the PPP can be computed by multiplying the activity factor with the amount of households inside that group.

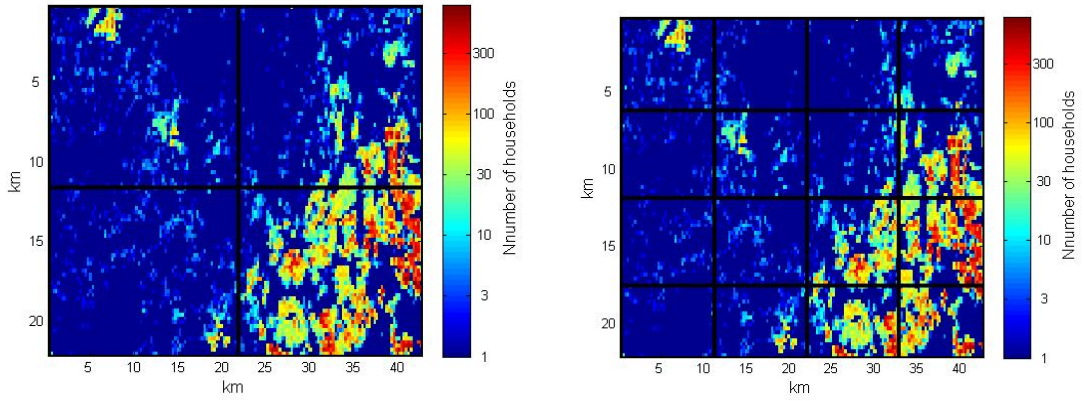

Figure 2-2: Splitting the secondary deployment area into 4 and 16 groups of pixels.

In Figure 2-3 (left) the distribution of the aggregate interference is depicted. In our system set up, see Figure 2-1 (right), most of the households are located far from the TV coverage area. As a result, the PPP model overestimates the aggregate interference. The mean interference level is overestimated by 8 dB approximately. By increasing the number of groups, better approximation is achieved because the density of the PPP would be small for groups located close to the TV coverage area and higher for groups located far from the TV coverage area. One can see that 25 groups are already sufficient to approximate the exact interference distribution. Note that we are practically interested in a good match at the upper tail of the interference distribution because the

upper tail would determine whether the Signal-to-Interference Ratio (SIR) target is violated or not.

In Figure 2-3 (right) the corresponding SIR distribution is depicted. In Figure 2-3 the activity factor is taken equal to 10 % while, in Figure 2-4 the activity factor is taken equal to 5 %. One can see the impact of activity factor on the interference and corresponding SIR distribution.

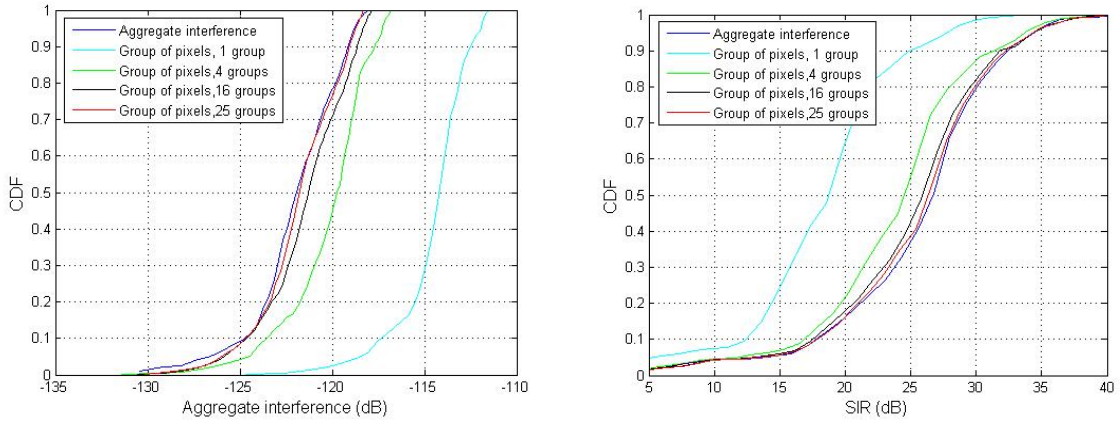

Figure 2-3: Distribution of the aggregate interference at the TV test points (left). SIR distribution at the TV test points (right). The activity factor is taken equal to 10%.

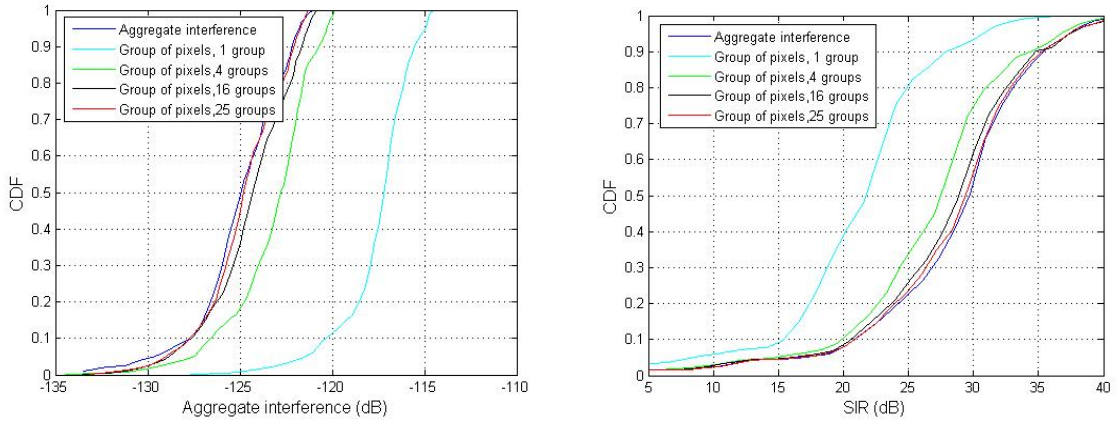

Figure 2-4: Distribution of the aggregate interference at the TV test points (left). SIR distribution at the TV test points (right). The activity factor is taken equal to 5%.

2.3.1.1 Matching the terrain-based model to power law based attenuation

So far, the attenuation from each secondary pixel to each TV test point has been computed using terrain-based propagation. Usually, a PPP model assumes power law based attenuation with slow fading. The power law model parameters, pathloss exponent, attenuation constant and slow fading standard deviation can be computed by fitting the terrain-based attenuation to the power law model. The computation details can be found in QUASAR D4.3 [D43].

In our computations the attenuation exponent is fixed to 3.6 while the attenuation constant and the slow fading standard deviation are computed assuming that the aggregate interference follows the log-normal distribution. The transmissions originated from pixels belonging to the same group are characterized by same propagation model. Some exemplary values for the attenuation constant when 16 and 64 groups are used can be found in Figure 2-5. Note that the values of the attenuation constant can be different when transmission to different TV test point is considered. Exemplary values for the slow fading standard deviation can be found in Figure 2-6. As expected, the larger is

the size of the group, the larger becomes the standard deviation characterizing transmissions from that group.

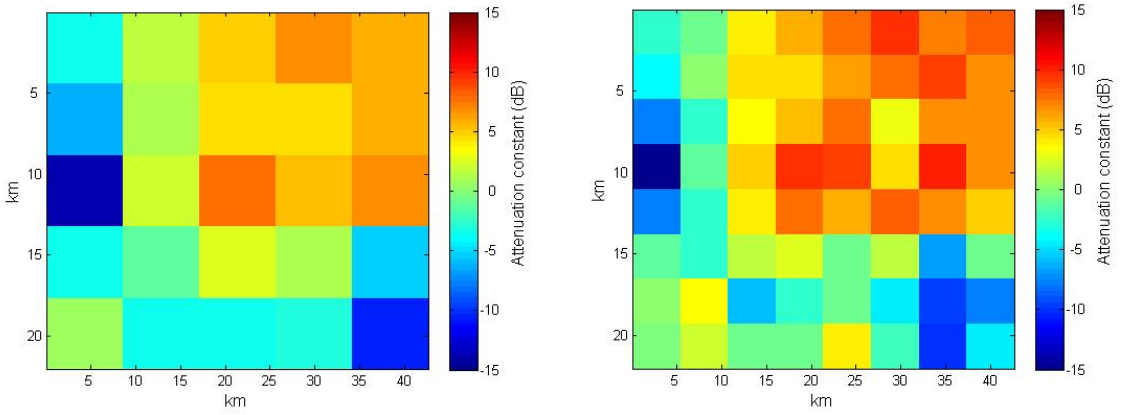

Figure 2-5: Pathloss attenuation constant (dB) from each secondary area towards one TV test point. 25 clusters (left). 64 clusters (right).

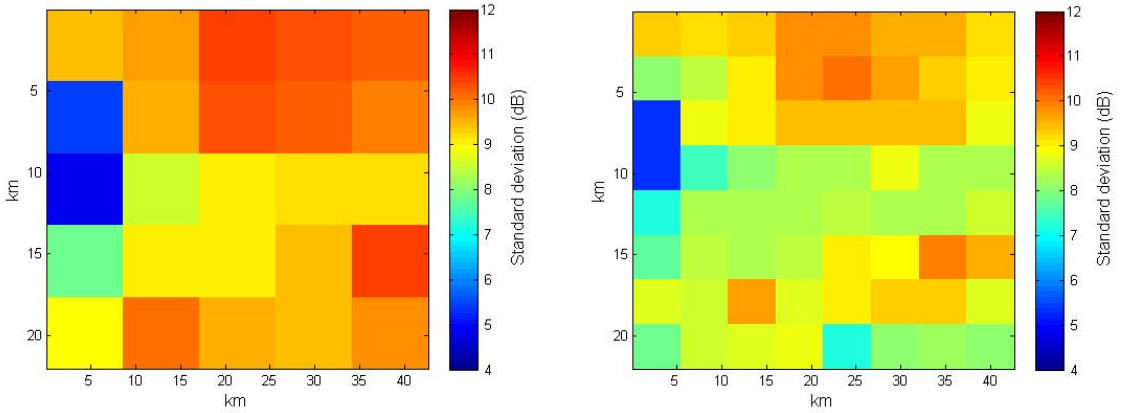

Figure 2-6: Slow fading standard deviation (dB) from each secondary area towards one TV test point. 25 clusters (left). 64 clusters (right).

We can repeat the fitting process by considering each pixel as a group. One can see in Figure 2-7 and Figure 2-8 that neighboring pixels experience similar propagation conditions.

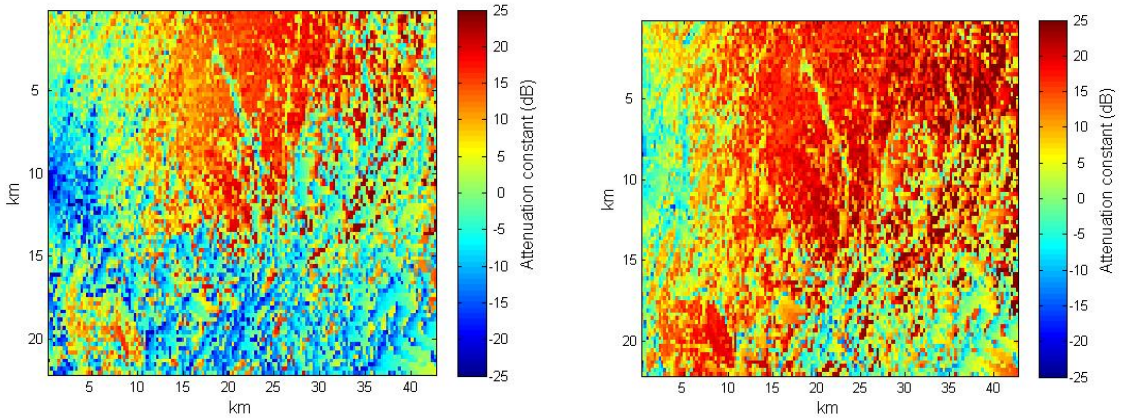

Figure 2-7: Pathloss attenuation constant (dB) from each secondary pixel towards two TV test points.

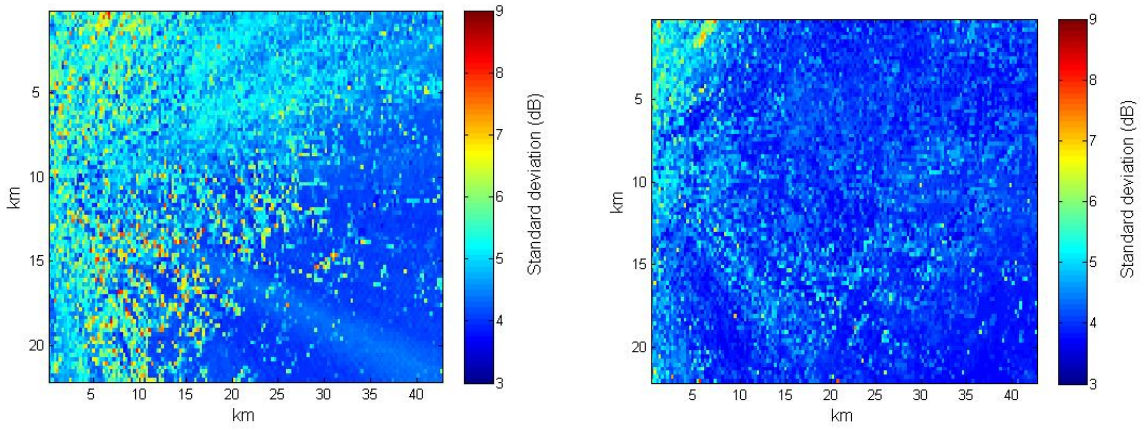

Figure 2-8: Slow fading standard deviation (dB) from each secondary pixel towards two TV test points.

Finally, in Figure 2-9 we approximate the distribution of the aggregate interference by using the power law channel model for the PPP. Due to the additional approximation error in comparison with Figure 2-3 and Figure 2-4, the match to the aggregate interference distribution becomes worse in the lower tail. This is not critical from the perspective of primary system protection as the approximation in the upper tail still remains good.

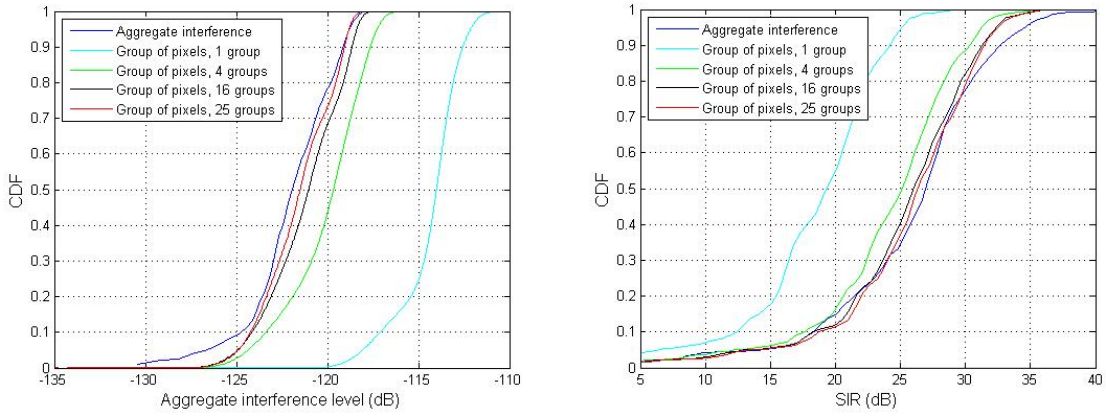

Figure 2-9: Distribution of the aggregate interference at the TV test points (left). SIR distribution at the TV test points (right). The activity factor is taken equal to 10%.

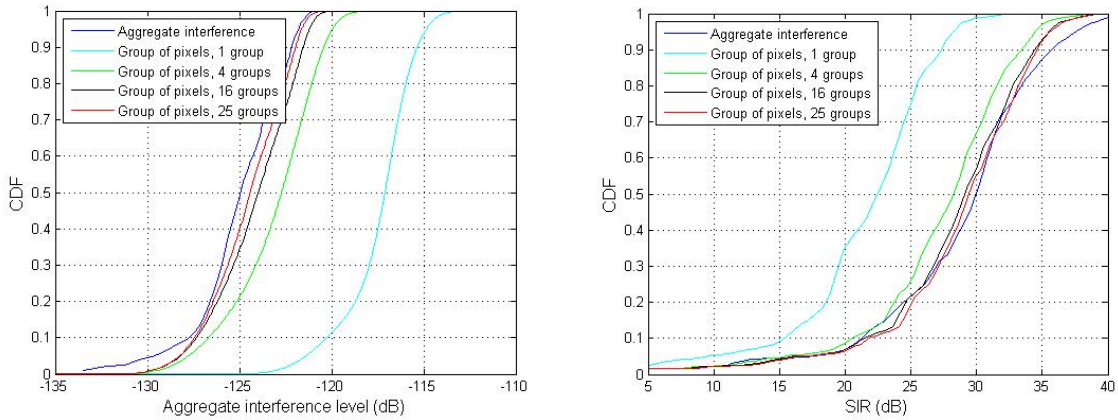

Figure 2-10: Distribution of the aggregate interference at the TV test points (left). SIR distribution at the TV test points (right). The activity factor is taken equal to 5%.

Overall, our results indicate that separating the secondary area into few groups of pixels is sufficient to capture the impact of non-uniform spatial service demand and approximate well the aggregate interference distribution. In our example, the secondary deployment area has size approximately equal to 1000 km^2 and 25 areas are sufficient to approximate the interference distribution with good accuracy particularly in the upper tail.

2.4 Cellular networks as secondary user in TVWS

The studies carried out during the QUASAR project on using TVWS for cellular systems are presented in this section. They follow two tracks: The first uses high level system modelling and emphasizes the number of available channels, cell sizes, and the aggregate interference caused by a large number of secondary transmitters in exposed positions. It investigates the achievable theoretical link level spectral efficiencies through holistic optimization of the secondary transmit power and channel allocation in the cellular network. After an initial analysis in a focus area, a methodology is derived that can be applied to a country-wide network.

This approach differs from the second track of investigations in that the latter instead places the emphasis on the quality of the TV channels, from the secondary system perspective, and investigates the achievable spectral efficiency and performance of a macro cellular LTE system using a state-of-the-art LTE system simulator applied to TVWS. This line of investigations also maps the results to the business feasibility of the scenarios and compares with the option of investing in licensed spectrum.

The investigations presented in this section may thus be seen as complementary and bring focus to, and insight into different aspects of operating a cellular network in TVWS.

2.4.1 Generic cellular network as a secondary system

In this section we report on the QUASAR project's findings on the feasibility of cellular network deployments in TVWS scenarios. We summarize our results from a study conducted in Germany for a focus area at the Western edge of the country and a large-scale deployment over the entire country. An extended description can be found in earlier deliverables [D52] and [D53].

2.4.1.1 Focus area results

In our initial focus area study we considered a cellular network deployed in the Southern Rhineland of Germany. The region exhibits large variations in population density with the city of Cologne as largest agglomeration. Furthermore, the TV broadcasting system is extensively used, e.g. to host local news stations. The region is sharing national borders with the Netherlands and Belgium, and state borders with Rhineland-Palatine and Hessia. The latter is of relevance due to the independent planning of broadcasting in the federal states of Germany.

The aforementioned peculiarities, combined with a highly varying terrain profile, lead to variances in the number of used channels in the area. In particular, the central region of the focus area exploits large quantities of the available TV channels. The whitespace availability hence differs significantly. In Figure 2-11(a), we show the number of available channels for secondary reuse if a SE43-type of regulatory policy is assumed. Under the proposed rulings, channels are considered "available" if the point lies outside the protection contour of the TV coverage region. We notice that fractional large whitespaces are available in the Eastern and Southern parts of the area and low availability is given in the center region.

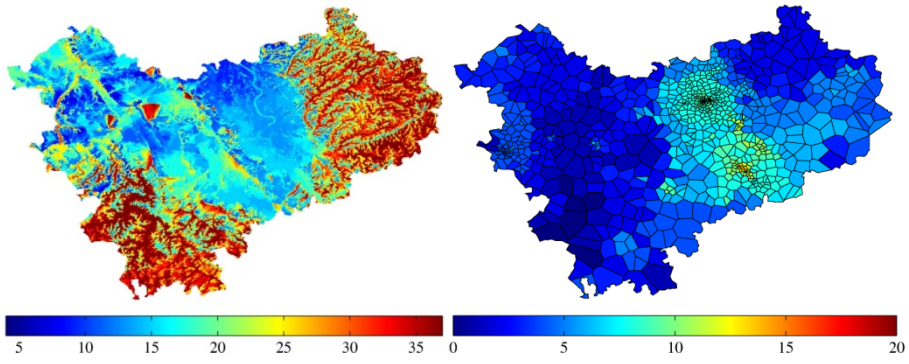

(a) (b)

Figure 2-11 The left-hand figure shows the number of available channels for secondary use if SE43-type of regulatory policy is assumed. The right-hand side shows the allocated number of channels per base station after optimization for cell-edge SINR of 23dB.

Our focus area study continued with an analysis of the potentials to boost the capacity of a cellular system in the focus area. The locations of the base stations were provided to use by a local operator. The distribution of cells exhibits the typical macro-cellular structure in rural areas and micro-cellular configuration in the urban environment. We defined the optimization task of the system model as to optimize the channel allocation per base station with the target of maximizing the capacity of a user located at the cell edge. The cell-edge user case was considered to be the worst-case assumption for cellular usage and hence optimization of this objective may maximize overall expected secondary capacity. Cells were allowed joint access to a TVWS channel (a) if they are non-adjacent in order to avoid in-system interference and (b) if their aggregate interference does not cause unacceptable outage in the primary system. We assume a fixed SINR target for each cell that can be reversely mapped into a cell size-dependent minimum required transmit power of the base station. For a more detailed description of the optimization objective we refer to [D53].

As can be observed in Figure 2-11(b), the cellular deployment for high Signal-to-Interference+Noise Ratio (SINR) scenarios (here SINR=23dB) is turned out to be feasible only for small cell sites. Centrally located cells in the urban environment have a 2-4 channels assigned to them. The rural deployments with large cells and hence large transmit power requirements are only rudimentarily exploiting the whitespaces. The chosen optimization method and the channel allocation strategy hence cause inferior coverage. This assumption is supported by a plot of the cell size over the number of accessible channels for the above-mentioned configuration as depicted in Figure 2-12.

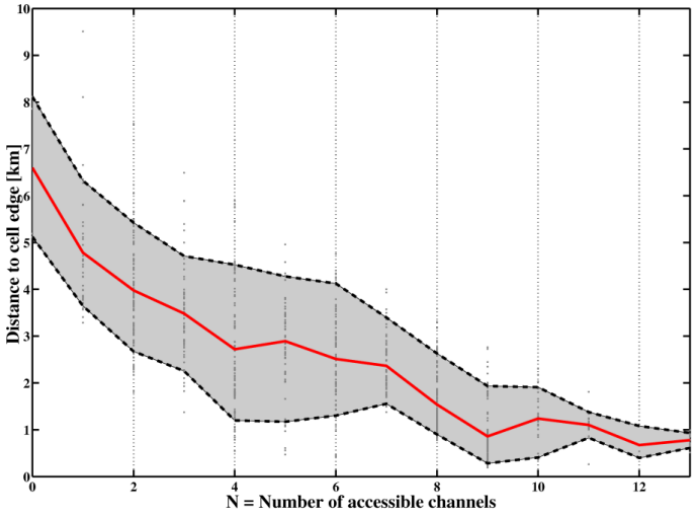

Figure 2-12 Number of accessible channels given the distance to the cell edge for an SINR target of 23 dB.

To judge on possible improvements to the allocation strategy, we applied in the following a weighting to test whether rural area coverage may be improved. We additionally considered two different possible interpretations of regulatory policy regarding the protection of neighbour-country TV stations. In the NPR (No-Neighbour Protection) case, a TV channel was only protected if it was used by a tower within the focus area. Neighbour region channels were only protected up the border of the region, thereby building an intersection between country borders and protection contours. The general protection case (GPR) was treating foreign and local channels equally.

While the different interpretations of the policy resulted in improvements in the overall channel availability, see Figure 2-13, the optimization did not significantly change the number of allocated channels. Visual inspection of the regional distribution of channels showed only slight improvements in border areas between macro-cellular and micro-cellular deployments. Otherwise, the rural areas did not exhibit better performance figures.

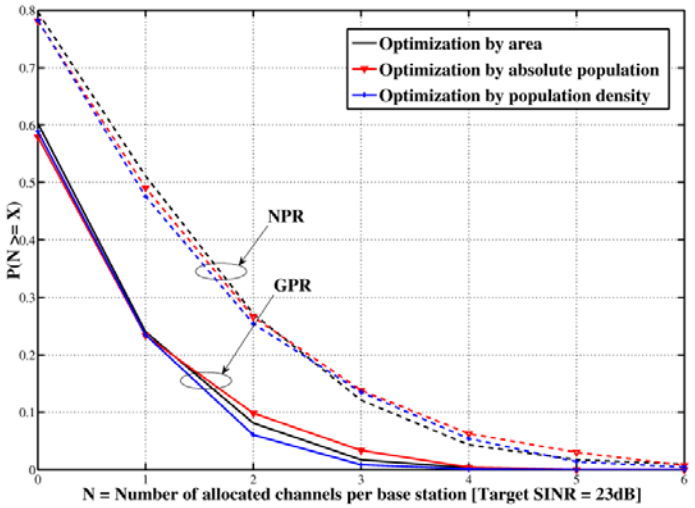

Figure 2-13 Number of allocated channels per base station for SINR target of 23dB and different optimization weighting and policy interpretations.

We conclude from this focus area assessment that a generic coverage strategy with the abovementioned constraints, even if weighting is applied, does not suffice to provide good performance for urban and rural scenarios alike. Only micro-cellular scenarios, as predominantly found in urban environments, are capable of exploiting whitespace

resource while maintaining the required protection to the primary system. We assume that the rural coverage will not be feasible if entire cellular systems are considered, but only if they are boosting the capacity of few selected base stations. This will make the economic viability questionable due to the additional costs of provisioning and end user device support.

2.4.1.2 Study area results

The results of the focus area study were not encouraging, hence we continued by refining the optimization problem and extending it to the study area of an entire country. The latter extension was considered necessary to even out effects specific to the focus area and discussed above. Again, we have used the country of Germany as reference for the cellular deployment.

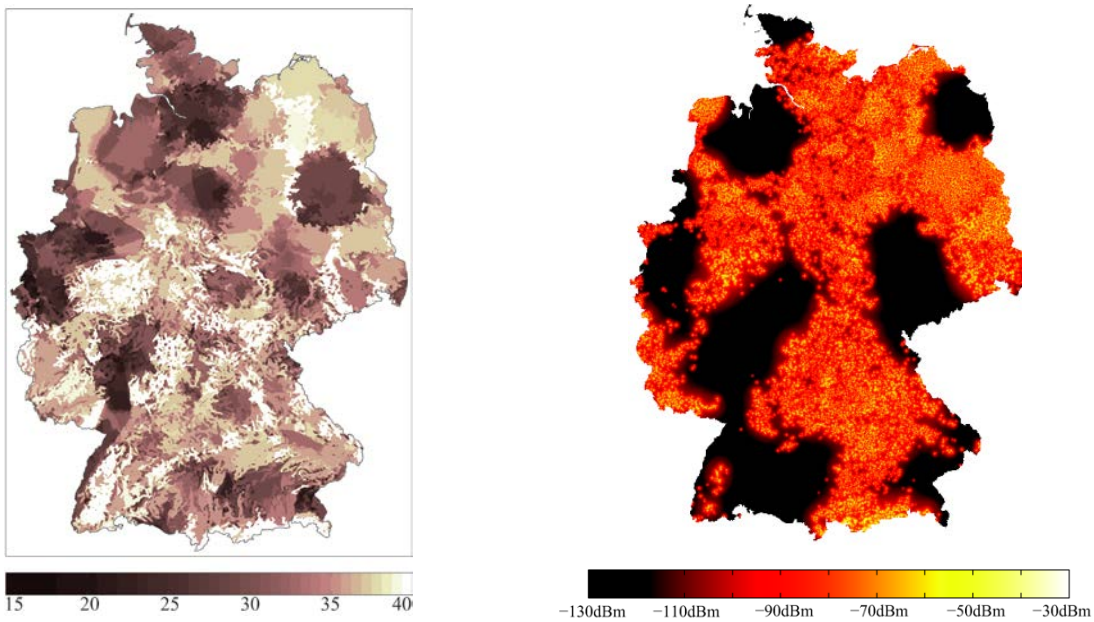

Figure 2-14 Channel availability and channel exploitation in study area of Germany. Figure (a) shows the number of available channels assuming SE43-type of protection policy. Figure (b) shows the received power from secondary transmitters after optimization for channel 21.

The country's channel availability differs between Eastern and Western states with high availability figures in the North-Eastern region as depicted in Figure 2-14(a). As visible in the figure, the previous focus area can be considered particularly challenging due to the extensive primary spectrum usage.

We have extended the original optimization problem by redefining it as multiple-choice nested knapsack problem (MC-NKP). For each base station we initially derive the required transmit power to achieve a particular spectral efficiency at the cell edge in units of bps/Hz. Unit size is normalized and quantized to allow equal steps in lowering/increasing the allocated power budget in terms of the objective function. The objective was hence to maximize the number of "units" of spectral efficiency in the secondary system. The maximization is constrained by a newly defined coupling matrix between the secondary system transmitters and the coverage contour points of the primary system. Each element of the coupling matrix gives the fraction of secondary power that is received at the contour point, i.e. the secondary interference at this location. We have developed a novel heuristic algorithm that searches for efficiency-maximizing solutions for which the sum interference calculated at the contour points is

below the regulatory threshold. The description of the algorithm as well as an analytical formulation of the optimization problem can be found in [D53].

To even out effects of secondary deployment irregularities, we conducted the optimization for different number of base stations as well as different location distribution strategies. To maximize the potentially allowed power budget for each cellular base station, we applied a Poisson Point Process for distribution weighted by the average distance of the location to protection contours of the different channels. This way, we aimed at operating more base stations in the "center" of the whitespaces. As reference, we reused the locations of a real cellular system.

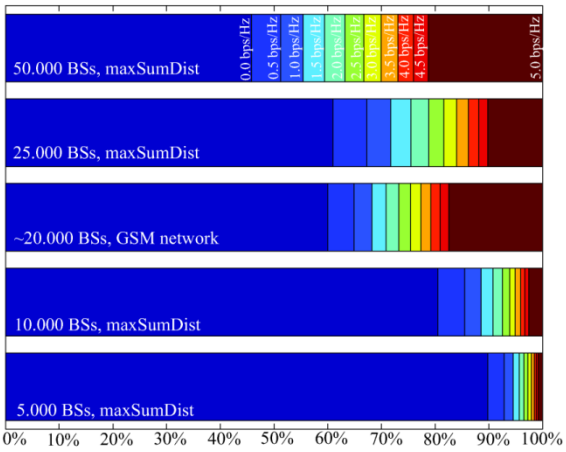

Figure 2-15 Fractions of cellular base station/channel combinations operating at the specified spectral efficiency level for different number of base stations and location distributions.

In Figure 2-15 we show the fractional distribution of achieved spectral efficiencies through the optimization process, i.e. the ratio of (channel/spectral efficiency) tupels taking a particular value. We found that only for large number of base stations, the cell sizes remain small enough to achieve high spectral efficiencies. Instead, a similar behaviour as in the original focus area study was observed with large number of unused channels for particular base stations.

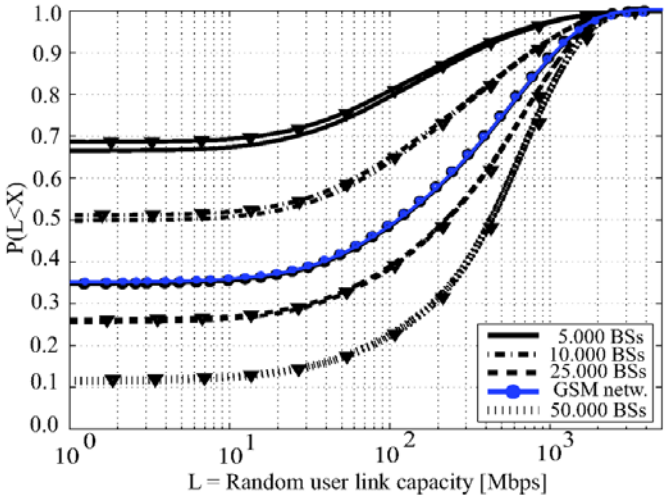

Figure 2-16 Cumulative distribution function of the link capacity of a user that is randomly placed within the study area. Marked lines denote the distance-to-protection contour maximizing placement strategy.

The achievable theoretical link capacity of a randomly placed used within the studied country shows the scattering of whitespace usage opportunities within the country. While in some locations, large capacities can be achieved (most notably close to the base

station locations and furthest from the protection contours), significant fractions of the country remain unserved by the cellular system. Only with high cell-site densities in the order of 50,000 sites coverage of around 90% of the country can be achieved. Compared to a dedicated spectrum allocations, whitespaces are hence inferior in terms of coverage.

Our extended study for an entire country confirms our assumption that whitespace usage for cellular systems is only feasible for regional deployments. Continuous coverage may only be achieved through dense secondary transmitter deployments. Given the costs of base stations and the comparably low exploitation capabilities of the whitespaces, cellular systems will not be able to achieve acceptable performance for large-scale deployments.

2.4.2 **Macro LTE network as a secondary system**

The present assessment considers a LTE network operating in Germany and that either uses only TVWS for its operation or uses TVWS to extend its legacy operation to achieve additional capacity where available. The details of the evaluation are given in D5.3 [D53] and here we only highlight the main outcomes and conclusions. Here we summarize the most important results from the studies that have been obtained.

The methodology described in this section is used for assessment of the amount of white space available in the UHF broadcasting bands, in particularly applied to the European situation. The considered regulatory rule sets that are used in this part of the evaluation are the CEPT SE43 proposed rules [ECC159].

This section outlines the methodology employed when studying the available capacity for a LTE cellular system using the TVWS for either providing coverage as a stand alone network or to use as a capacity booster. The latter is referred to as a DSA enabled cellular network and the former as a stand alone cellular network. To clarify: A stand alone network uses the opportunities provided by TVWS as the only spectrum resource available to provide coverage and capacity. A DSA enabled network has in addition to TVWS opportunities also access to dedicated licensed spectrum that serves the purpose of providing basic cellular service. In locations when TVWS opportunities are not available the DSA enabled network uses the licensed spectrum as a fallback, and where TVWS opportunities are available they are used to enhance the performance of the network.

A high level overview of the methodology employed to derive the results related to operating a LTE macro cellular network in TVWS is illustrated in Figure 2-17 below. This methodology has been applied to derive the reported results in Section 2.1 of [D53] and in the extension to business feasibility in [D13].

The achievable performance of cellular networks has been studied in D5.3 [D53] with emphasis on accurately modelling the intra-system interference arising from simultaneous use by multiple White Space Devices (WSDs) on a given channel. Not all TV channels have been considered as useable by the secondary cellular system due to interference from TV transmitters.

The methods applied to derive the number of available TV channels, the quality of these channels in with respect to interference level from TV transmissions, allowed secondary transmit powers EIRP has been described in [D51] and we refer the reader to that deliverable for details.

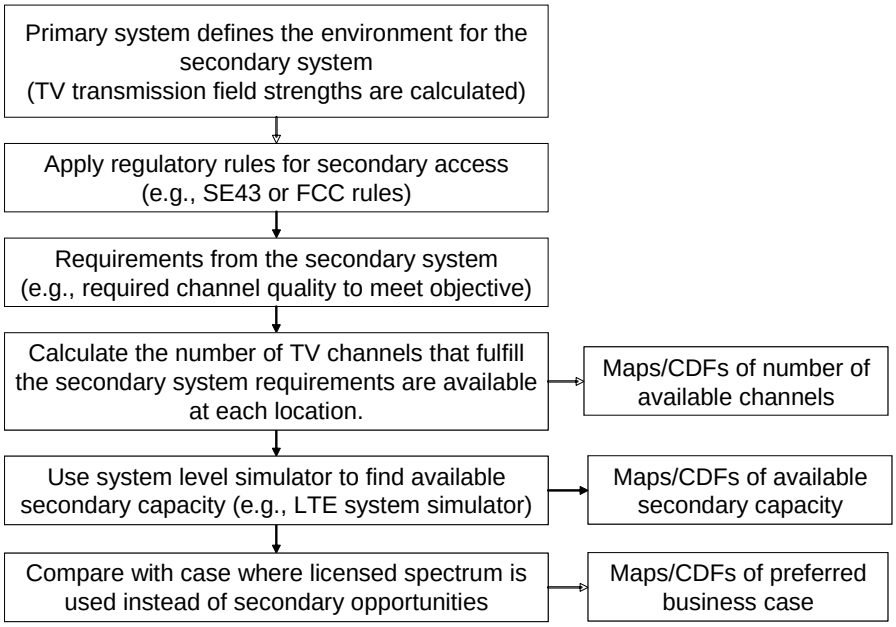

Figure 2-17: High level overview of the employed assessment methodology for analyzing cellular use of TVWS opportunities

The two first steps are covered in [D51] and the reader is referred there for details on the rules and how to employ them in cellular scenarios.

The next step, related to the requirements from the secondary system, comprises detailing requirements stemming from the objective of the secondary system. To reflect the objective of the service that is to be offered by a secondary system we introduce channel selection criteria for the TV channels.

The rationale for introducing channel selection criteria is that not all, by regulatory rules available TV channels are useful in all circumstances due to potentially large interference levels caused by TV transmissions. For a stand alone network the investigated channel selection conditions ensure that the network may provide coverage over the entire area, while for a DSA enabled network the conditions aim to select channels that are useful to provide a reasonably high performance increase. In the latter case a certain overall spectral efficiency in a cell must be supported by the extension carrier, so that a reasonably large amount of the users in the cell benefits from the additional spectrum.

Apart from respecting the maximal EIRP limits specified in [ECC159] for selected each channel the used TV channels that are used by the secondary system are a subset of the channels that are available according to proposed regulation [ECC159].

The options for channel selection criteria that are applied to the stand alone network case are:

- If the outage probability (in both uplink and downlink) is smaller than 5% (or 1%), the coverage is considered contiguous and the channel is used. The outage probability is the percentage of the user-bit-rate distribution, which corresponds to 0 bit/s. The bit-rate distribution is the distribution of the achievable bit-rate for users randomly deployed in the system. A TV channel is considered available for cellular network use, if the criterion is met for the minimum required ISD in the corresponding location and under the local circumstances of maximum WSD EIRP limitation and TV interference.
- If the achievable cell edge user-bit-rate is higher than 10 % (or 50 %) of the achievable cell edge user-bit-rate in the interference-limited case, the coverage is considered contiguous and the channel is used. The interference-limited case is defined as the performance of the LTE system with given ISD with optimally dimensioned BS transmit power.

The options for channel selection criteria for a DSA enabled cellular network are:

- When using TVWS the system's cell spectral efficiency must be at least 25% (or 50%) of the cell spectral efficiency achievable in a LTE system deployed in dedicated spectrum for the channel to be considered as useful.
- If the median of the user-bit-rate distribution is higher than 25% (or 50%) of what can be achieved in the dedicated spectrum reference case the channel is used.

For a more extensive description of the channel selection conditions, see Section 2.1 in [D53] and [Dudda12].

By employing the channel selection criteria we get a set of usable channels for the secondary system and we may find the number of channels fulfilling the requirements in each geographic location. Figure 2-18 illustrates this for the case of a DSA enabled cellular network in Germany.

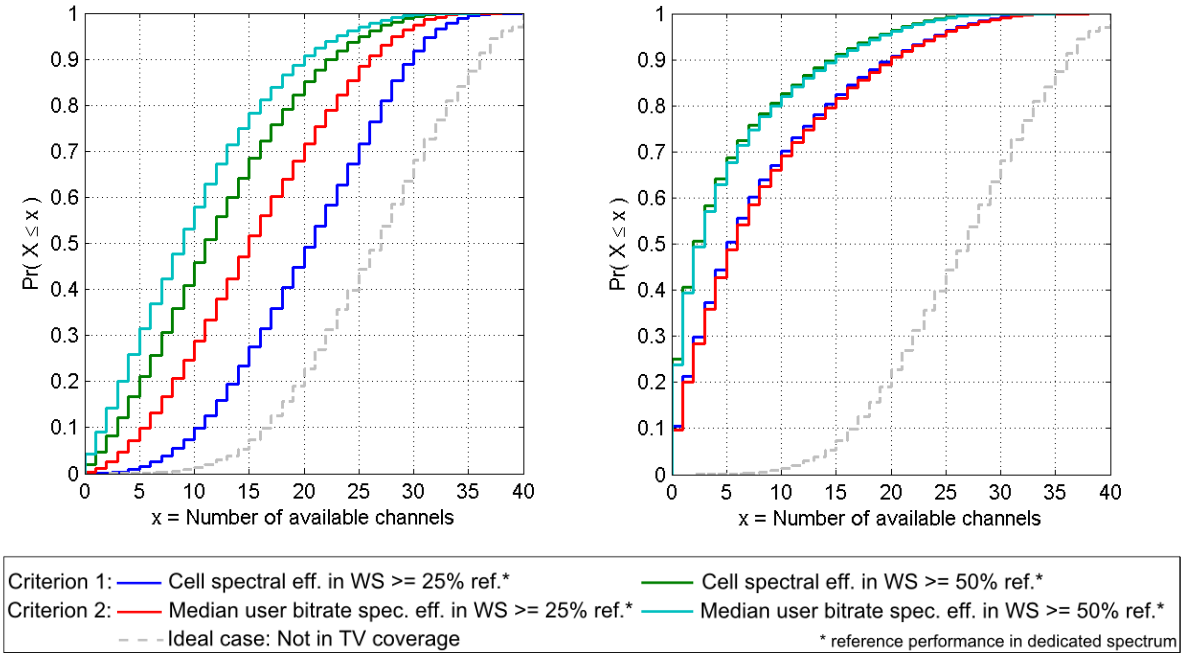

Figure 2-18: CDF of the number of available channels for downlink (left) and uplink (right) in German locations for a DSA enabled alone macro cellular network according to different channel selection criteria. (Figure from [D53]).

From the above figure it is evident that the number of useful channels under the various selection criteria is larger for the downlink than for the uplink. This is due to the fact that the base station antennas are more exposed to interference from TV transmitters, since they are mounted at high locations, than the receivers in down link. Thus, the number of useful channels depends greatly on the possible isolation from interfering TV transmissions.

Next we use a LTE system simulator to map the available secondary bandwidth and population density to a capacity in the secondary system. The population density is only used to make a realistic assumption on the inter site distance in the cellular system. For more details on the system simulations the reader is referred to [D53] and [DI12]. An illustrative result obtained in this step for a DSA enabled macro cellular system extending its operation to TVWS is shown in Figure 2-19.

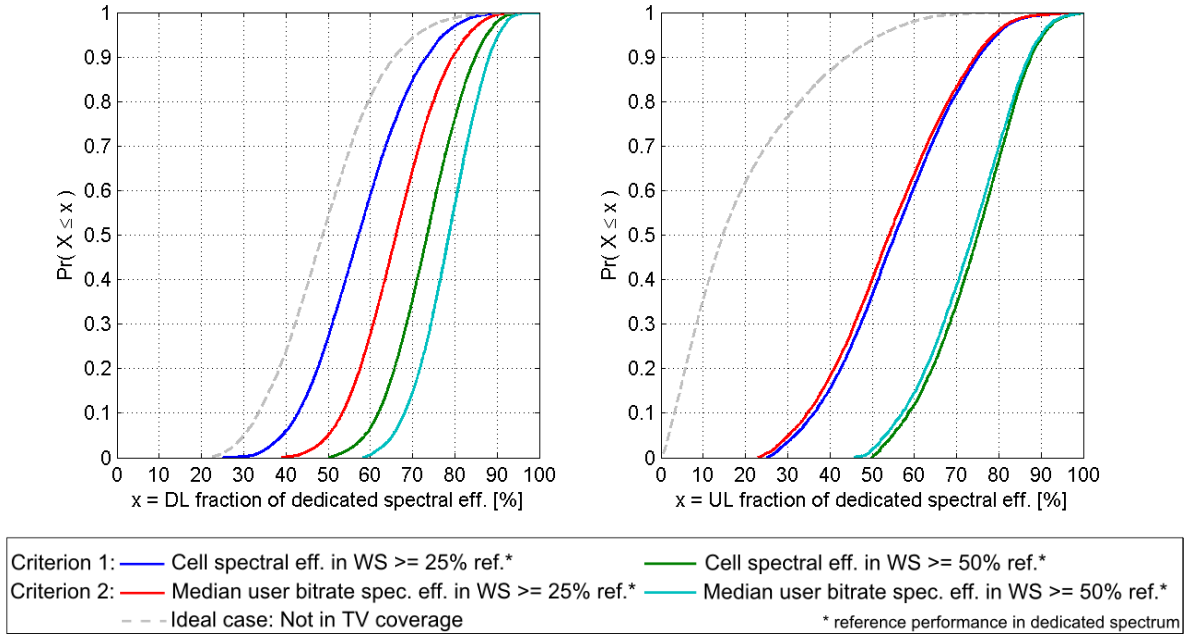

Figure 2-19: CDF of the available relative spectral efficiency for DSA enabled LTE cellular network in downlink (left) and uplink (right). (Figure from [D53]).

From the above figure we find that the median spectral efficiency of the DSA enabled LTE network in UL (DL) is in the order of 55-80% (55-74%) of what is achievable in dedicated licensed spectrum.

For this case a capacity boost of up to ~100 Mbit/s in DL and 65 Mbit/s in UL as the sum of the cell throughputs for all available channels (both values represent the 95% percentile of the CDF over locations), has been observed [D53]. On average we find 9-21 channels available (depending on channel selection criterion) that on average provide a link spectral efficiency of 55-80% of what can be achieved in dedicated spectrum for the DL direction. In the UL we have 3 to 5 channels available for the same channel selection criteria. Thus it seems to be a lot of capacity that can be achieved by using TVWS, but keep in mind that the spectral efficiency is not as good as in licensed spectrum, indicating that this form of the usage is not the best way to use the spectrum. Turning again to the case where the LTE network uses TVWS to extend capacity (the DSA enabled case) when available the situation looks better. The main reason is due to the legacy spectrum being around to function as a fallback for the operation.

The final step in the applied methodology is useful to compare various business cases to find which is more beneficial for an operator looking for business opportunities.

Even though it may be reasonable to expand LTE operation to use TVWS as an additional resource in some areas, it must be compared to the alternative business case of using licensed spectrum. For the case of a LTE macro cellular system operating in TVWS (DSA enabled or stand alone) we compare with a business case where the operator uses licensed spectrum instead of TVWS. To make the cases comparable we assume that it will be possible to license the TVWS spectrum in regions corresponding to a pixel in the study. This implies that the amount of spectrum that needs to be licensed varies over the considered area. In each location a bandwidth of licensed spectrum is assumed to be acquired that gives the same performance as the system using TVWS opportunities would have in that same location. This corresponds to a second digital dividend, where TV services are squeezed together into a smaller bandwidth and the remaining bandwidth is licensed to other services, and the assumption that the spectrum may be licensed on smaller regions than countries. These assumptions give the same performance in the two cases and hence the same revenue and OPEX is assumed. This means that only the CAPEX cost associated with a TVWS enabled LTE network is relevant

for the comparison. For details on the modeling and what parameters are considered the reader is referred to [D13].

The obtained results are statements on which business case is the most promising in each studied area element. A comparison between the business cases for using licensed spectrum and TVWS for the case of a DSA enabled LTE macro cellular network is shown in Figure 2-20.

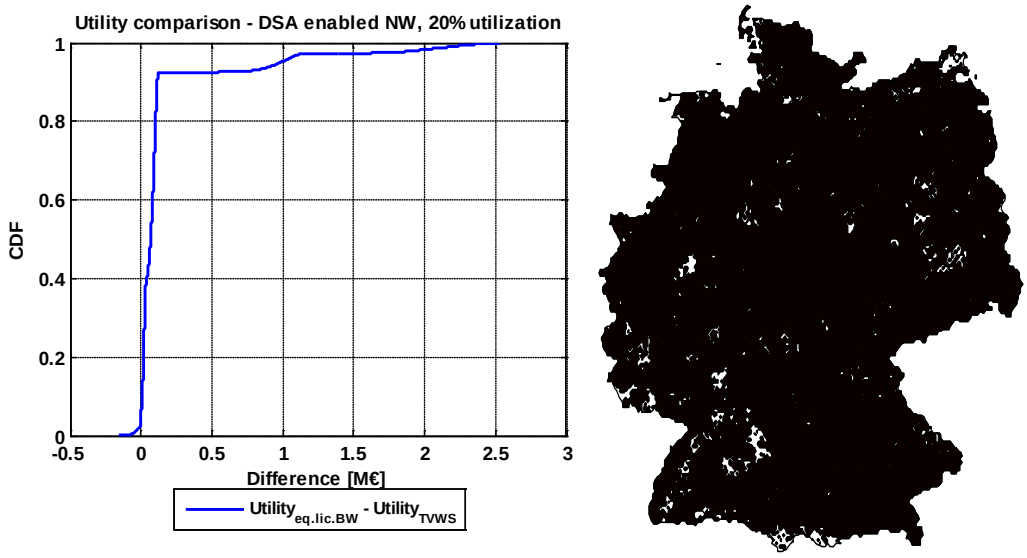

Figure 2-20: Comparison between utilities for use of licensed spectrum vs. TVWS opportunities for a macro cellular network in Germany. The CDF (left) shows the difference between the utilities for the two cases and the map (right) shows regions where using licensed spectrum is preferable (black areas) and where using TVWS opportunities is preferable (white areas). (Figure from [D13]).

For the case illustrated in Figure 2-20 it is clear that using licensed spectrum is almost everywhere preferable to using TVWS opportunities. This conclusion holds as long as the upgrade cost of a TVWS site is more than 10 k€ (~1.4 times) larger than the upgrade cost for a site using licensed spectrum, the price for licensing spectrum price is less than ~1.70€/MHz/capita and the spectral efficiency of the system is above 1 bps/Hz. It should however be remembered that this conclusion is based on the assumption that spectrum could be licensed in areas smaller than the entire Germany and that the price for these licenses is comparable to the price per MHz and capita paid in previous auction in Germany [Kronegger10]. But if that will be the case in the future, a second digital dividend is surely preferable from a macro cellular perspective.

In D1.3 [D13] it is further shown, under reasonable assumptions, that the business case for using licensed spectrum, when the same amount of spectrum is licensed in the whole country, still outperforms the business case of using TVWS.

2.4.2.1 Conclusions regarding operating a macro LTE cellular network in TVWS

It is not recommended to try to build a cellular LTE network relying only on TVWS opportunities.

Overall it can be observed that TVWS is much better suited for offloading than for stand-alone networks. However the spectral efficiency of the system is not as good as in licensed spectrum.

Under almost all circumstances a second digital dividend and using licensed dedicated spectrum is preferable based on a cost comparison to macro cellular network operator over using TVWS opportunities.

2.5 Wi-Fi-like secondary system using TVWS

As when studying the case of operating a cellular system in TVWS the present case of operating a Wi-Fi-like system in TVWS follows two separate, complementary, tracks.

The first line of investigation aims to assess the viability of Wi-Fi-like secondary networks in TVWS for three different use-case scenarios: outdoor urban, indoor urban, and outdoor rural deployments. The investigation culminates in estimating the realistically achievable rate and range of multiple Wi-Fi-like APs (access points) operating in TVWS using the *permissible* secondary AP transmission power as determined by aggregate secondary user interference constraints on the TVWS channels available in the example study regions. The estimates of achievable range and rate are based on real estimates of TVWS channel availability from example urban and rural study regions in Germany, the application of the Wi-Fi auto-rate function defined in the IEEE 802.11g/a standard, and explicitly taking into account the impact of congestion and interference among co-channel secondary APs.

The second investigation track uses the Macedonian TV band conditions when evaluating the performance and realizable throughput of a set of proposed channel sharing schemes for Wi-Fi-like systems employing the CSMA/CA MAC protocol. Also here the aggregated interference from secondary transmitters plays an important part by severely limiting the achievable throughput.

As such the investigations presented in this section are complementary, together bringing a more complete insight into the benefits and difficulties of operating Wi-Fi-like systems in TVWS.

2.5.1 Performance analysis of a Wi-Fi-like secondary network

In this section we summarise our analysis of the performance of a system of multiple Wi-Fi-like secondary users operating in TVWS, thus concluding our earlier studies reported in QUASAR Deliverables 5.2 and 5.3 [D52, D53]. In order to obtain a robust estimate of the achievable range and downlink rate of such a secondary system, we use real TVWS availability estimates (calculated within the German focus area studied in our earlier case of cellular deployments) and consider the effects of interference and congestion among secondary APs (access points) sharing the same TVWS channel [Simic12]. Importantly, we also take into account the impact of aggregate secondary interference on the *accessibility* of TVWS channels, thereby evaluating the real-world viability of a secondary Wi-Fi-like network in TVWS, in terms of its realistically achievable performance.

We consider three deployment scenarios (outdoor urban, indoor urban, and outdoor rural) and take the city of Aachen and the area around Wipperfürth in Germany as examples of an urban and rural study area, respectively; each scenario is characterised in Table 2-1 in terms of its salient parameters. In the interest of conciseness, we omit a more detailed description of our system model and instead refer the reader to Section 2.3.1 of [D52] and Section 3.1.1 of [D53]. However, it should be noted that, whereas in the preliminary analysis presented in [D53] we assumed that the maximum aggregate secondary user interference to the primary system of -105.2 dBm was allowed for our secondary network, our present analysis is based on the more realistic assumption that other Wi-Fi-like secondary networks may concurrently be operating elsewhere outside the protection contour of those TVWS channels used by our network. Thus we assume that only a fraction of the total maximum secondary interference budget is allocated to the secondary network operating in our bounded study area, proportional to the population density; the budgets assigned to our study areas in this manner range from about -140 to -130dBm (for further details, please refer to [AchtzehnSimic12]).

Table 2-1: System model parameters for different deployment scenarios for a Wi-Fi-like secondary network in TVWS.

	Outdoor Urban	Indoor Urban	Outdoor Rural
Propagation	k = 3	k = 4, 18 dB wall	k = 2.5
AP density	λ = 12.5/km^2	λ = 125/km^2	λ = 0.25/km^2
Study area	2 km x 2 km	500 m x 500 m	5 km x 5km

Figure 2-21 shows simulation results of the typical performance of the Wi-Fi-like secondary network in TVWS, as characterised by the mean estimated downlink rate over the whole network of $|A|$ APs, $\overline{R}_A$, and the mean cell-edge AP coverage range over the network, r_{max}^{A} (as defined in [D52]). Each curve was generated by varying the transmission power of the secondary APs, P_{tx}={0,5,10,15,20,25,30} dBm (i.e. each point represents the achievable mean rate and coverage range for a given fixed P_{tx}). Figure 2-21 shows the performance for a real example of TVWS channel availability (thick solid curves) compared to no inter-AP interference (best-case reference; dashed curves) and all APs being co-channel (worst-case reference; think solid curves). As previously discussed in [D53], these results reveal that although greater AP coverage is expected from operating in the lower frequency TV bands compared to IEEE 802.11 Wi-Fi in the 2.4 GHz ISM band, this range extension is significantly diminished once we consider the impact of inter-AP interference and congestion. Accordingly, owing to increasingly overlapping shared contention domains among multiple secondary APs, the AP downlink throughput is increasingly reduced for higher AP transmission powers.

The red curves in Figure 2-21 show the performance results for *permissible* secondary Wi-Fi network operation on "accessible" TVWS channels only, where the aggregate secondary interference constraint to the primary is respected for the given P_{tx}. The number of such "accessible" TVWS channels is presented in Figure 2-22, as compared to the number of "available" channels originally advised by the TVWS database. Figure 2-22 reveals that when aggregate secondary user interference is considered, there is a dramatic decrease in the number of TVWS channels available to the secondary network. For the outdoor urban scenario, Figure 2-22(a) shows that no 16 MHz or 24 MHz TVWS remain accessible, whereas the number of 8 MHz TVWS channels reduces from 17 to at most 4, with the highest permissible P_{tx} being 25 dBm when operating on the single remaining accessible channel. Figure 2-22(b) reveals that for the indoor scenario, no 24 MHz channels remain accessible and three 16 MHz channels are accessible only at P_{tx} =0 dBm; of the 17 "available" 8 MHz channels, the number that remain accessible progressively reduces from 10 to 1 as P_{tx} is increased. Lastly, Figure 2-22(c) shows that for the outdoor rural scenario, of the 14 "available" 8 MHz channels at most 3 remain accessible, with the highest permissible P_{tx} being 5 dBm when operating on the two remaining accessible 8 MHz channels; of the 4 "available" 16 MHz channels, only one remains accessible at the lowest P_{tx} of 0 dBm.

Given the number of practically accessible channels presented in Figure 2-22, the red curves in Figure 2-21 represent the realistically achievable performance of a Wi-Fi-like secondary network in TVWS. Considering the rate versus range trade-off when operating at various P_{tx} and channel widths, the results in Figure 2-21 indicate that for competitiveness with 2.4 GHz Wi-Fi, the best-case feasible operating points in TVWS are: (i) outdoor urban: P_{tx} = 10 dBm, four 8 MHz channels; (ii) indoor urban: P_{tx} = 25 dBm, four 8 MHz channels; and (iii) outdoor urban: P_{tx} = 5 dBm, two 8 MHz channels.

Let us benchmark the performance of the Wi-Fi-like secondary network operating in TVWS using these best-case feasible parameters against that of IEEE 802.11g Wi-Fi operating at the European regulatory transmit power limit in the 2.4 GHz ISM band of P_{tx} = 20 dBm. For the outdoor urban scenario in Figure 2-21(a), best-case feasible

operation in TVWS affords only a marginal coverage range extension over IEEE802.11g (112 m vs. 100 m) and yields a 60% lower average throughput[2] (6.8 Mbps vs. 17 Mbps). Figure 2-21(c) shows that for the outdoor rural scenario, best-case feasible operation in TVWS also yields a 60% lower average throughput (6.5 Mbps vs. 16 Mbps) and provides a *lower* coverage range than IEEE802.11g (202 m vs. 290 m). **Our results therefore suggest that outdoor operation of a Wi-Fi-like secondary network in TVWS is not viable**. For the indoor urban scenario in Figure 2-21(a), best-case feasible operation in TVWS yields a 60% lower average throughput (8.6 Mbps vs. 22 Mbps) but does afford a substantial coverage range extension over IEEE802.11g (30 m vs. 12 m). This indicates that the TVWS Wi-Fi variant will provide a substantial range extension for an equivalent rate compared to IEEE 802.11g. **Our results thus suggest that operation of Wi-Fi-like secondary devices in TVWS might be viable for extending range in indoor environments, but only for low-rate applications. Nonetheless, given the abundance of underutilized spectrum in the 5 GHz unlicensed band, it is debatable whether allowing secondary operation in TVWS is justified by this use-case alone.**

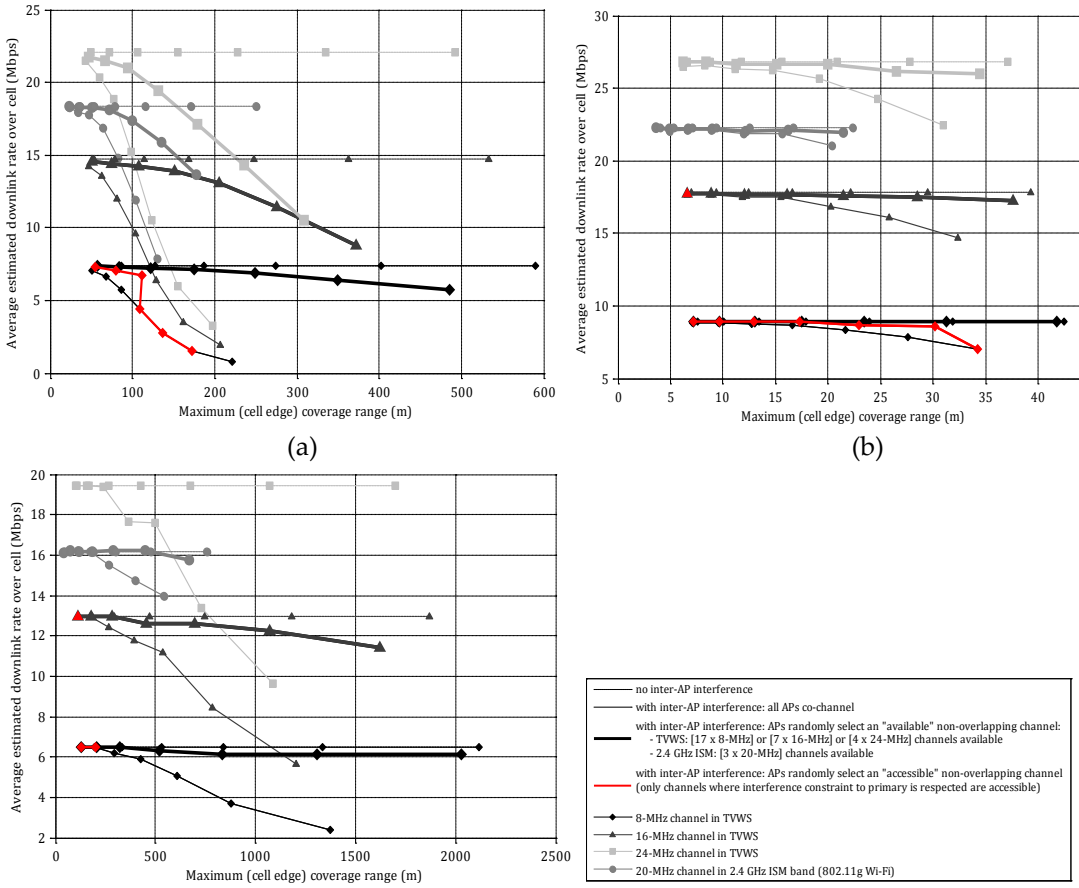

Figure 2-21 Average downlink rate for a covered user vs. maximum AP coverage range (corresponding to secondary AP transmission power P_{tx}={0,5,10,15,20,25,30} dBm), for the deployment scenarios of (a) outdoor urban, (b) indoor urban, and (c) outdoor rural. Performance results for *permissible* secondary Wi-Fi network operation on "accessible" TVWS channels only (*cf.* Figure 2-22), where the aggregate secondary interference constraint to the primary is respected for the given P_{tx}, are shown in red.

[2]This is of course consistent with the channel width of 8 MHz in TVWS being 60% of the 20 MHz channel width in the 2.4 GHz ISM band.

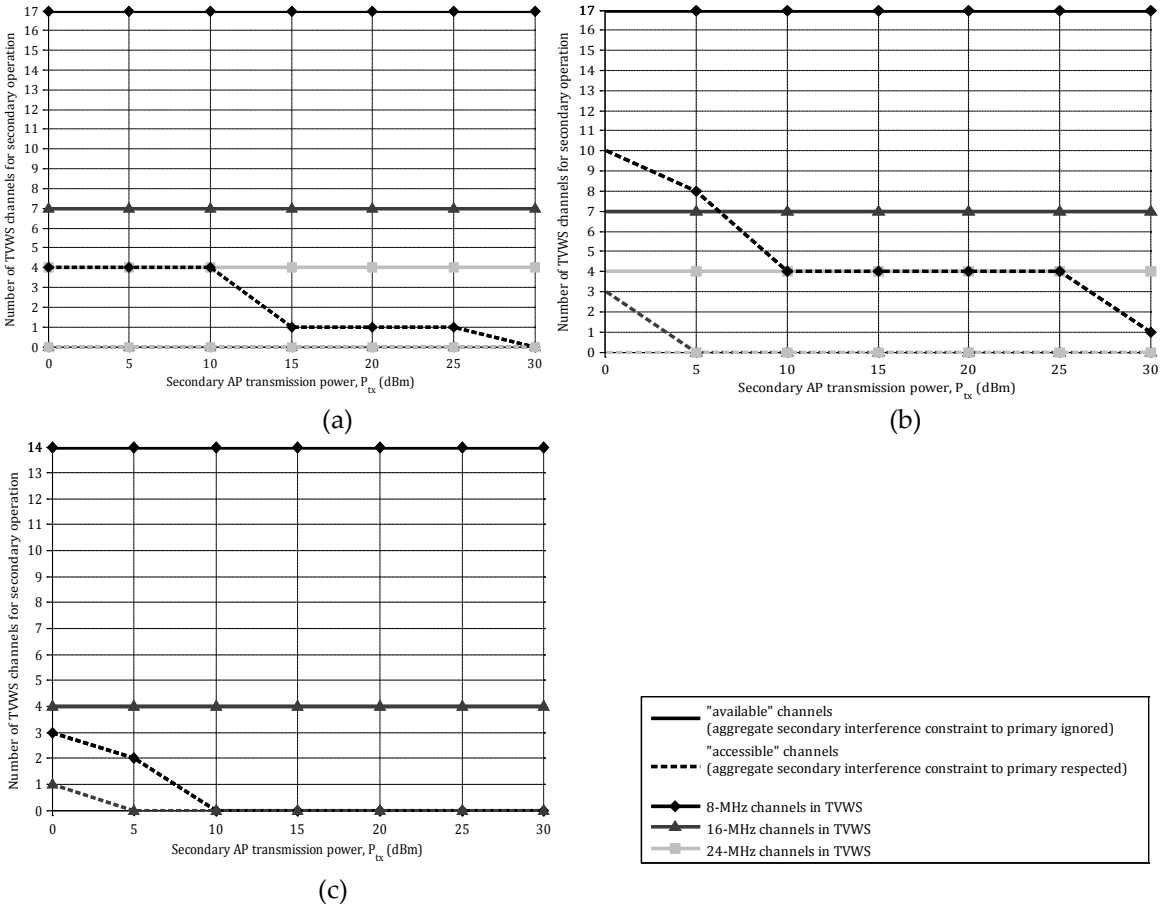

Figure 2-22 Comparison of the number of "available" and "accessible" TVWS channels for secondary operation vs. secondary AP transmission power, for different TVWS channel widths and the deployment scenarios of (a) outdoor urban, (b) indoor urban, and (c) outdoor rural. A TVWS channel is "available" if the secondary network is outside the primary protection contour of the corresponding TV channel(s); an "available" TVWS channel is "accessible" if the aggregate secondary interference constraint is respected for the corresponding TV channel(s).

2.5.2 **Achievable Throughput of Wi-Fi-like secondary system in TVWS using channel sharing schemes**

This section summarizes the main outcomes regarding the spectrum availability assessment in Macedonia. The target territory for spectrum availability research is interesting mainly due to its geographical position and terrain specifics, variability in population densities and its current phase of television digital switchover process. The assessment framework targets the television frequency spectrum and the possibility to implement a Wi-Fi-like secondary system in TVWS.

The initial assessment of available TVWS in Macedonia was reported in deliverable D5.1 [D51]. The performed calculations use the input data of television transmitters provided by the Agency for Electronic Communications-Macedonia (AEC). The territory of Macedonia is divided into a grid of 100x100m cells (pixels). The calculations in D5.1 apply the FCC rule set for coverage and protection area definition. The initial results reveal that the amount of available channels in Macedonia is not excessive. This outcome was explained by the adopted approximations of flat terrain and omnidirectional antennas in the calculations.

Deliverable D5.2 [D52] contains more realistic results implementing the actual terrain of the target territory in the analysis. While the results in D5.1 were entirely obtained by MATLAB, D5.2 relies on the Radio Mobile freeware to accurately predict the coverage area maps using Longley-Rice terrain-based model. The maps were later processed in

MATLAB. Additionally, D5.2 provides the number of available TV channels throughout Macedonia in form of colour-coded maps according to the FCC and ECC rules. D5.2 considers one Wi-Fi-like secondary system operating per TVWS frequency chunk consisting of one Wi-Fi-like access point communicating with one Wi-Fi-like user. In particular, it is assumed that one such secondary link operates in every available frequency chunk. There is no interference between secondary links since the chunks are non-overlapping. As a result, the analysis shows that there is a substantial TVWS opportunity, which can be exploited by short-range Wi-Fi-like secondary systems where the single-existing secondary user can exploit up to 50 Mbps [Latkoski12]. Furthermore, D5.2 reveals that the achievable throughput for Wi-Fi-like secondary systems highly depends on the organization of the detected secondary spectrum.

Finally, deliverable D5.3 [D53] analysed the possibility to use a Wi-Fi type of secondary network containing multiple SUs in the TV band extending the case study in Macedonia. In particular, the analysis investigates the limitations imposed by the aggregate interference caused by multiple SUs to the primary system assuming different levels of penetration of the secondary system. Targeted as the most economic viable case, the investigation inspects a limited area, which co-locates with the capital of Macedonia, Skopje. The target area is 15 km by 20 km and belongs to urban type of environment. The goal of D5.3 was to find the probability that a particular set of multiple SUs (a realization) would cause degradation of the location probability for the primary TV receivers and show the possible improvement reached through various sharing schemes (only ECC rules were investigated).

The current deliverable investigates all aspects necessary for a comprehensive spectrum availability assessment in Macedonia. The analysis builds on the findings presented in D5.3 introducing more realistic models of the secondary system, e.g. CSMA/CA medium access control protocol. The CSMA/CA procedure changes the performance of the sharing schemes previously presented in D5.3 in terms of their realization acceptance rate.

Figure 2-23 depicts the new realization acceptance rate of all three sharing schemes introduced in D5.3 (Random based sharing scheme, Power-weighted uniformly distributed channel sharing scheme and Power-weighted non-uniformly distributed channel sharing scheme). Evidently, the power-weighted schemes still outperform the random channel allocation, but only up to Secondary Access Point (SAP) density of 80 SAPs/km^2. The random channel allocation scheme provides better realization acceptance rate for higher SAP densities.

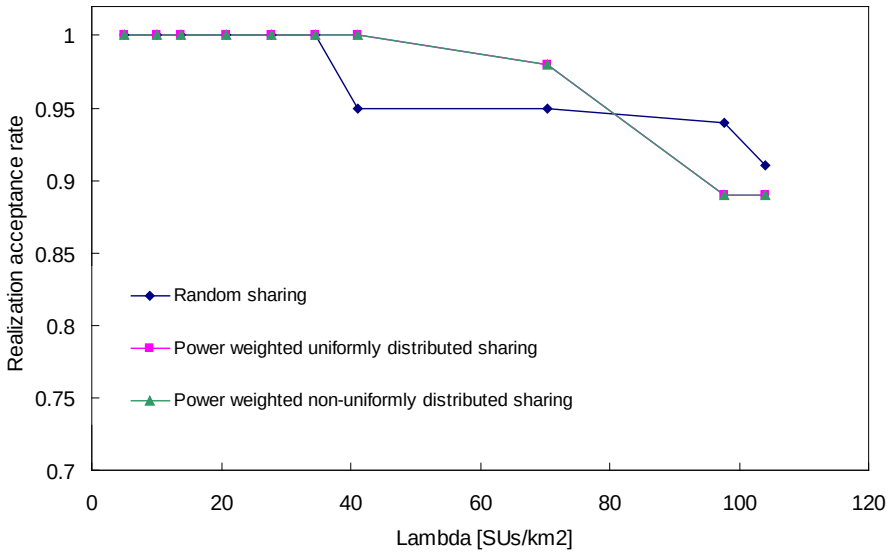

Figure 2-23 Influence of the aggregate interference (with CSMA/CA),

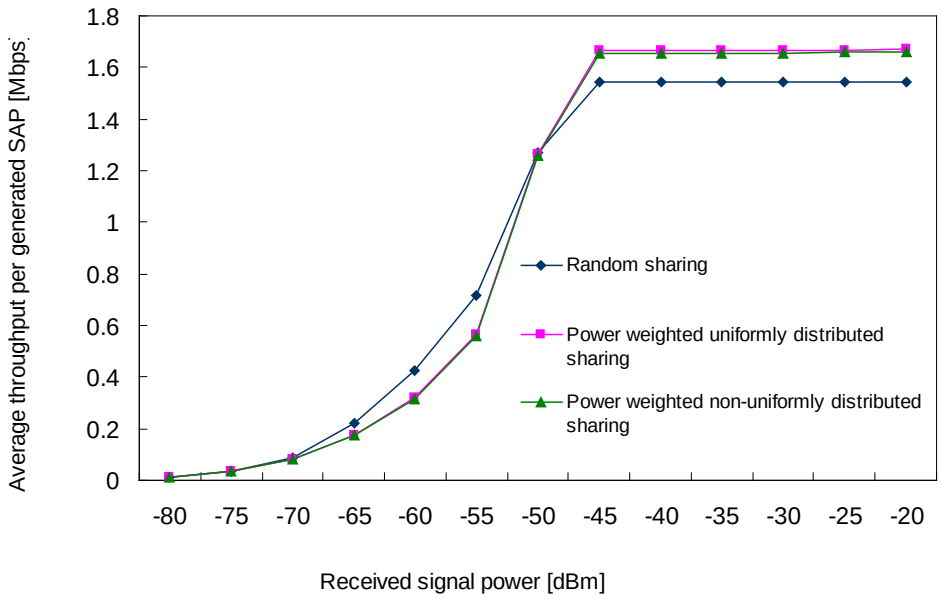

Figure 2-24 Average throughput per SAP.

Figure 2-24 depicts the impact of the aggregate interference from multiple secondary users to the secondary system via the average throughput per generated SAP. The throughput analysis assumes implementation of the CSMA/CA procedure. Evidently, the random channel allocation scheme outperforms the power-weighted schemes in terms of average throughput when the secondary system receiving signal power is lower than -50 dBm. For received signal power higher than -50 dBm, the power-weighted schemes outperform the random channel allocation. However, in each case the obtained values for the average throughput are relatively low (below 2 Mbps).

2.5.2.1 Conclusion

ECC defines the maximum allowed transmission power for a secondary user based on a controlled degradation of the location probability of the primary system reception. Since the criterion defined by the SE43 (Report 159) [ECC159] for geolocation database approach originally takes into consideration only single SU, it is possible that multiple SUs for which the ECC database has allowed separate operation might produce intolerable level of total aggregate interference (co-channel and adjacent-channel) towards the primary system. The results of Macedonia case study (presented in D5.1, D5.2, D5.3 and D5.4) revealed that adjacent channel interference is usually higher than the values of co-channel interference and introduces limitations in the secondary usage of TVWS. The presented analysis investigated the percentage of acceptable random SAPs realizations regarding the produced aggregate interference for different densities of SAPs within the analyzed territory. Implementing a combination of intelligent channel sharing schemes and CSMA/CA MAC protocol improves the SAPs acceptance rate. This assures a relatively high level of secondary spectrum technology penetration, even comparable to the current Wi-Fi. However, the analysis proved that the conditions involving limited TVWS frequency chunks in urban areas, along with the existence of significant interference (for density of 30 SAPs/km^2), limit the average SAP throughput to values below 2 Mbps.

2.6 Secondary use of radar and aeronautical bands

In this section, we summarize the results of availability analysis on the secondary access to radar and aeronautical spectrum bands. Substantial amount of useful spectrum, i.e. lower than 6 GHz, is primarily allocated to radar and aeronautical navigation systems. In

QUASAR, we focused on the two primary systems operating on the frequency bands as shown below:

- 2700-2900 MHz for air traffic control (ATC) radars,
- 960-1215 MHz for aeronautical navigation, in particular distance measuring equipment (DME).

ATC radar is normally located near airport, and used for watching airplanes in the air. It emits strong pulses and receives the reflected rays to locate the target objects. DME is a type of two-way radar which estimates the distance between two entities (ground station and aircraft) by exchanging the Gaussian pulses and measuring the round-trip delay of the pulses.

Unlike the assessment of TVWS, the secondary access to the radar and aeronautical spectrum has not been discussed well thus far. Therefore, we first studied opportunity detection schemes and primary protection rules that are suitable to the ATC radar and DME. Then, the feasibility of secondary usage was assessed based on the proposed detection and protection mechanisms. For both primary systems, low-power secondary systems for indoor capacity provision (such as Wi-Fi access point and LTE HeNB) are considered. It is assumed that the secondary users are distributed in a large geographical area and simultaneously want to use the spectrum.

The assessment methods applied the ATC radar and the DME are quite similar because they operate under similar working principles. In this section, we describe the technical aspects that can be commonly applied to the ATC radar and DME. Then, we present the assessment results for these systems.

2.6.1 **Opportunity detection methods**

Generally speaking, there are three candidate technologies for the secondary users to discover the opportunities of spectrum access, namely spectrum sensing, geo-location database, and sensing + database.

2.6.1.1 Sensing-only detection

Radar relies on the reflected rays to locate or shape the objects. This means that a radar transmitter is usually collocated with a receiver. Thus, detecting the radar is equivalent to detecting the interference victim, which is completely different from the case in TVWS where sensing TV transmitter does not give relevant information about the TV receivers. It makes the spectrum sensing a feasible and favourable opportunity detection option in the radar spectrum. It is noteworthy that the sensing-only detection method has already been adopted by the dynamic frequency selection (DFS) mechanism for secondary use of 5 GHz radar band [ETSI08].

Despite the fact that it is feasible and already in use, the sensing-only method is not a desirable method of opportunity detection. First, it is difficult to prevent a wrongful transmission nearby the radar. Since the radar pulses are short and bursty, there is always a risk that the pulses are not detected by the secondary users even with the high signal strength. Second, aggregate interference is not properly controlled by imposing a fixed sensing threshold to individual secondary devices. It could be possible to prevent excess aggregate interference by setting an extremely conservative margin, but it will severely reduce the secondary access opportunities.

2.6.1.2 Database-only detection

The geo-location database is the most feasible form of opportunity detection in TVWS. Similar type of database can be constructed in radar and aeronautical spectrum. The database will be effective in regulating the wrongful transmissions by nearby secondary users and controlling the aggregate interference. However, it does not fully utilize the characteristics of the radar favourable to the spectrum sensing.

2.6.1.3 Sensing + database detection

It is shown in D5.2 [D52] that the combination of sensing and database can significantly improve the opportunity of secondary users compared to the pure database method. Therefore, we propose the sensing + database method for the detection of opportunities in radar spectrum. With this method, secondary users are assumed to be attached to a geo-location database and fed information about the radar, e.g. location, center frequency, maximum pulse power, pulse shape, antenna gain, and rotating pattern. Then, the secondary users will be able to make an accurate estimation of propagation loss in slow time scale, i.e. distance-based path loss and shadow fading via spectrum sensing. The database also gives the secondary users an interference threshold which is adaptive to the traffic load. Finally, each secondary user decides whether it can use the frequency band with a certain transmission power based on its estimation on the propagation loss and the sensing threshold given by the database.

2.6.2 **Protection rule for the primary system**

We propose a simple protection rule that was inspired by the DFS mechanism in D5.2 [D52] and D5.3 [D53]. The basic principle is that the radar should be protected from the harmful interference that could potentially be generated by the aggregation of interference from multiple secondary users. Due to the random nature of the radio propagation, we proposed a rule based on the probability of interference violation:

$$\Pr\left(I_{su}^{agg} \geq THR_{rad}\right) \leq \beta_{rad} . \qquad (2\text{-}1)$$

Notations used above are:

I_{su}^{agg} : aggregate interference power received at the radar from the secondary users,

THR_{rad} : interference threshold value for the radar,

β_{rad} : maximum allowable probability of interference violation.

The value of THR_{rad} is determined by the required interference to noise ratio (INR). This corresponds to approximately -110dBm for typical ATC radars [M1464]. In addition to the required INR, protective margins such as apportionment margin and fast fading margin can be applied.

Although the proposed protection rule is based on probabilistic approach, the allowed interference violation β_{rad} should be sufficiently low to ensure the proper protection of the radar because ATC radar performs a function concerning safety-of-life. Reasonable value of β_{rad} has not been fully investigated in the literature. In [D52][D53], we used β_{rad} =0.001% as used in [ITU07], though it may result in a pessimistic result. It means almost zero violation from a practical point of view. Moreover, β_{rad} does not necessarily represent the event of radar failure. It rather means the probability that I_{su}^{agg} exceeds THR_{rad}, which is already conservative due to the protective margins.

The aggregate interference I_{su}^{agg} depends on the decisions of secondary users on the transmit powers. Here, we employ an assumption that that every secondary transmitter uses the same power $P_{tx,su}$, and then it makes an individual ON/OFF decision based on its estimation of propagation. Let us consider an arbitrary secondary user j. We define ξ_j as the interference power that the radar would receive from the user j if it were to transmit. Also, let $\overline{\xi_j}$ be the estimate of ξ_j which is measured by j. The decision of j relies on the individual interference threshold I_{thr}, which is given to every secondary user in the system by the central database. A proper value of I_{thr} should be determined depending on radar protection parameters (THR_{rad}, β_{rad}) and the aggregate interference

caused by the secondary users. As a result of the decision, the actual interference from the SU j to the radar is given by

$$I_j = \begin{cases} \xi_j, & \text{if } \overline{\xi_j} \le I_{thr}, \\ 0, & \text{otherwise.} \end{cases} \quad (2\text{-}2)$$

Then, the aggregate interference can be expressed by

$$I_{su}^{agg} = \sum_{j=1}^{N} I_j \ , \quad (2\text{-}3)$$

where N denotes the total number of the SUs in the investigated area.

As mentioned earlier, the above protection rule resembles the DFS which is specified in ETSI standard EN 301 893. However, our scheme differs from the DFS in the sense that we consider adaptive adjustment of I_{thr} depending on the intensity of secondary traffic in order to ensure the protection or the radar and to maximize the opportunity to the secondary users.

2.6.3 **Assessment results: secondary access to 2.7-2.9 GHz ATC radar spectrum**

The protection mechanism we proposed results in a propagation-dependent exclusion region within which the secondary use of spectrum is prohibited. Thus, the feasibility of secondary access can be evaluated in terms of minimum required exclusion region for massive deployment of the secondary users. Figure 2-25 illustrates the minimum required separation between the radar and the secondary users in dB scale as a function of the traffic intensity of the secondary users. In this figure, the secondary users are assumed to be uniformly distributed over a large area, and all of them want to have access to a frequency channel overlapping the radar operation. It is observed that the separation of around 170 dB is required to accommodate 100 simultaneous secondary transmissions per square kilometre. This corresponds to a physical exclusion distance of a few kilometres when the secondary users are located below the rooftop level. Considering the ATC radars are usually located near airports that are at least a few kilometres away from downtown, it suggests that the massive use of low-power secondary systems in downtown is feasible on the same frequency of radar operation.

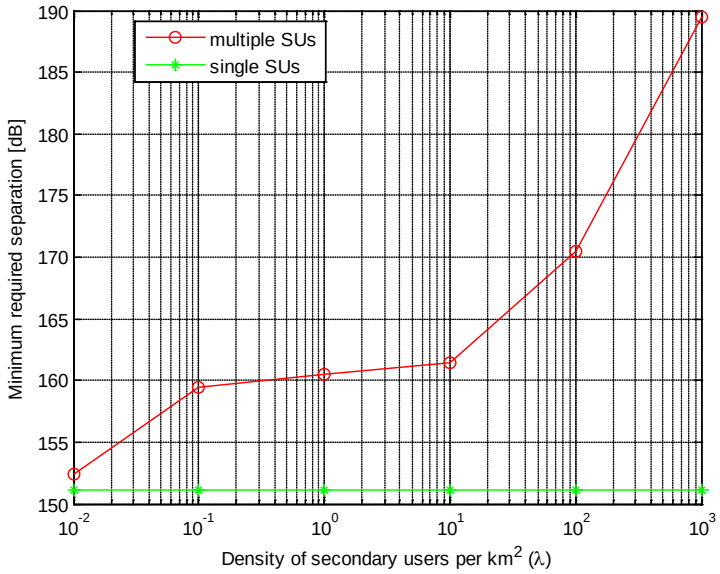

Figure 2-25: Minimum required separation between radar and secondary users as a function of secondary user density; this figure was copied from [D53] where the experimental parameters can be found.

The ATC radar employs an antenna with very sharp azimuthal (horizontal) beam width, which rotates 360 degrees in a regular and predictable manner in many cases. Exploring this feature can further enhance the feasibility of radar spectrum usage. Assume that the secondary users have an accurate knowledge of the radar rotation pattern. The probability of accessing spectrum varies over time as illustrated in Figure 2-26. The availability of the radar spectrum dramatically increases during most of the time, and slightly decreases only when the SUs face the main beam as demonstrated in the figure.

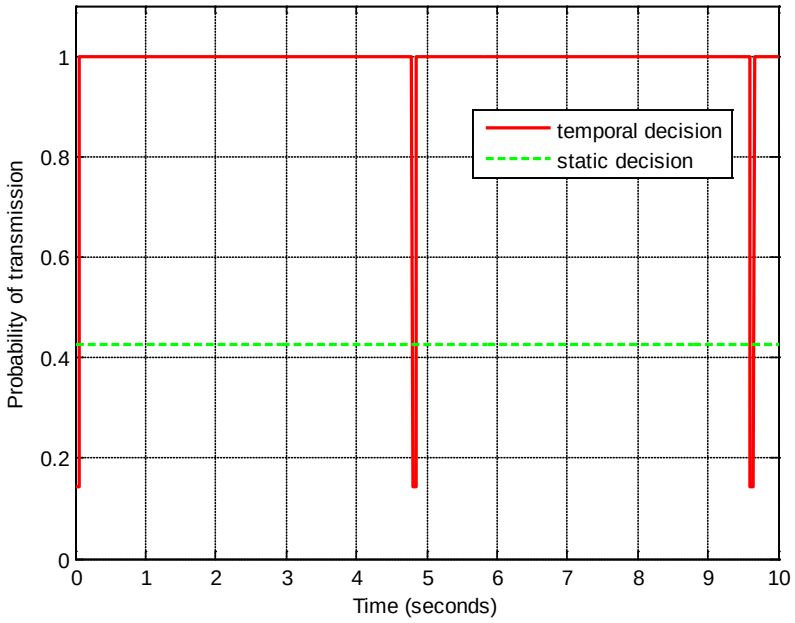

Figure 2-26: Probability of transmission as a function of time for a secondary user 3 km away from the radar; This figure was copied from [D53] where the experimental parameters can be found.

In the above figures, the required separation was calculated by assuming that the secondary users transmit on the same channel that the victim radar employs. Additional frequency-dependent rejection can be applied if they use non-overlapping channels. Therefore, the feasibility of the radar spectrum significantly increases if the frequencies are non-overlapping between the radar and the secondary users. In fact, the opportunity of such a non-overlapping channel access is abundant because the radars are sparsely assigned over the frequency band of 2700-2900 MHz.

2.6.4 **Assessment results: secondary access to 960-1215 MHz DME spectrum**

The availability of large scale secondary usage in the DME spectrum is examined in this section. In our assessment, a DME channel is considered as *available* channel if the secondary user, under the applied opportunity detection method, is able to successfully access the channel without violating the primary protection criterion.
We consider that secondary users share the spectrum with the DME system via spectrum sensing with the help of geo-location databases. DME consists of two types of interference victim, namely ground transponder and airborne interrogator, which is the main difference from the ATC radar. For the ground transponder case, the secondary users detect the primary transmissions on the reply (sensing) frequency but the interference is given on the interrogation (interfering) frequency. Since there is 63 MHz frequency offset between the sensing and interfering channels, *uncertainty* in the fading estimation still remains. The correlation (ρ) between the fading values in these two channels will depend on the characteristics of the environment. For the airborne interrogator case, secondary users are assumed to share the DME spectrum via a real-time database. Secondary users could experience *uncertainty* or imperfect information

on the location of the primary victim due to high speed of the airplanes. The level of uncertainty will depend on the update delay (t_u) in the communication between the geo-location database and the secondary users [D53].
In Figure 2-27, we illustrate the availability by area in Germany and Sweden. For our evaluation, aggregate interference in the spatial and spectral domain has been taken into account which is combined with the demographics information. In Table 2-2, the impact of the uncertainties on the average secondary usage availability is summarized. A more detailed explanation on the methodology for availability assessment and simulation parameters can be found in [D53] [Obregon12].

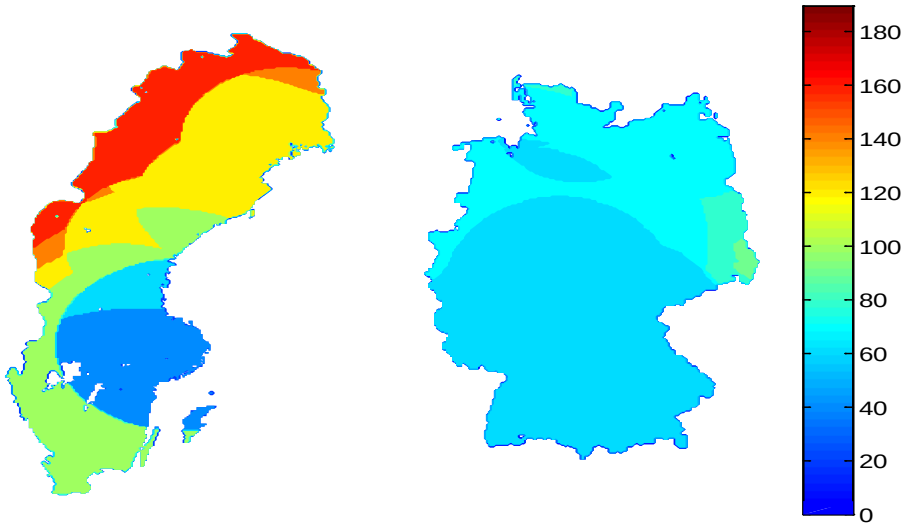

Figure 2-27: Availability by area (MHz) in Sweden (left) and Germany (right) ($P_{tx,su}$ =0dBm/MHz, ϱ=1 and t_u=0min)

Table 2-2: The average availability by area and population

Country		Average availability by area (MHz)	Average availability by population (MHz)
Sweden	ρ=1, tu=0min	117.6970 (61.30%)	85.6323 (44.60%)
	ρ=1, tu=2.5min	110.1365 (57.36%)	81.2953 (42.34%)
	ρ=0, tu=0min	114.5914 (59.68%)	83.0755 (43.26%)
Germany	ρ=1, tu=0min	69.0680 (35.97%)	68.5318 (35.69%)
	ρ=1, tu=2.5min	68.7083 (35.78%)	68.1942 (35.51%)
	ρ=0, tu=0min	58.1505 (30.28%)	57.8966 (30.15%)

According to our results, the availability for low-power secondary usage is at least 30% of the total DME spectrum (50 MHz) in any location of Germany and Sweden. The availability highly depends on the distribution of the population and the secondary system parameters and requirements. The potential uncertainties in the estimation of propagation loss have a negative but not critical impact on the availability. For high levels of uncertainty, the availability only decreases up to 6%.

2.6.5 **Concluding remarks on radar and aeronautical spectrum**

In QUASAR, we investigated the availability of 960-1215 MHz DME spectrum and 2.7-2.9 GHz ATC radar band for massive secondary use of low-power broadband devices. First,

we examined opportunity detection methods, and concluded that the geo-location database aided by individual sensing is the most promising means to find the opportunities. Then, we proposed a primary system protection rule which ensures the aggregate interference is below a certain threshold. The rule takes into account the stringent protection requirement for the safety-of-life primary systems. Finally, we developed an assessment framework based on aggregate interference models, and illustrated the availability of the target spectrum bands.

For DME in 960-1215 MHz band, it is observed that the available spectrum for dense deployment of secondary users ranges from 50 to 100 MHz depending on area, but at least 50 MHz is available in any location of Germany and Sweden. However, a good carrier aggregation capability is required to fully enjoy the availability.

For ATC radar in 2.7-2.9 GHz band, the availability of the same type of secondary service looks better than 960-1215 MHz spectrum. Co-channel access to the radar frequency requires an exclusion region of a few kilometres. Thus, the co-channel usage is feasible in most of downtown areas. Moreover, a separation in frequency domain and an exploitation of temporal interference characteristics offer additional availabilities to the secondary users. Considering sparse frequency occupancy of the ATC radars, a substantial portion of 2.7-2.9 GHz band is expected to be available for the massive low-power secondary users particularly in urban areas.

It should be emphasized that our assessment employed conservative parameters and protective margins to protect the safety-of-life primary systems. However, enforcement of the proposed protection rule remains as a challenge in this spectrum. More discussions about the regulatory issues can be found in [D14].

3 Prototyping the framework

To demonstrate the feasibility of the spectrum assessment methodology developed in the QUASAR project, we have developed a generic software tool for calculation of spectrum availability and spectrum opportunity. In this chapter, we introduce the main components of the software tool, show the implemented workflow that is aligned to the assessment methodology, and give the design parameters for two secondary deployment scenarios, namely cellular and Wi-Fi-like systems, that have been included in accordance with the scenarios developed in the project.

3.1 Workflow concept and common terminology

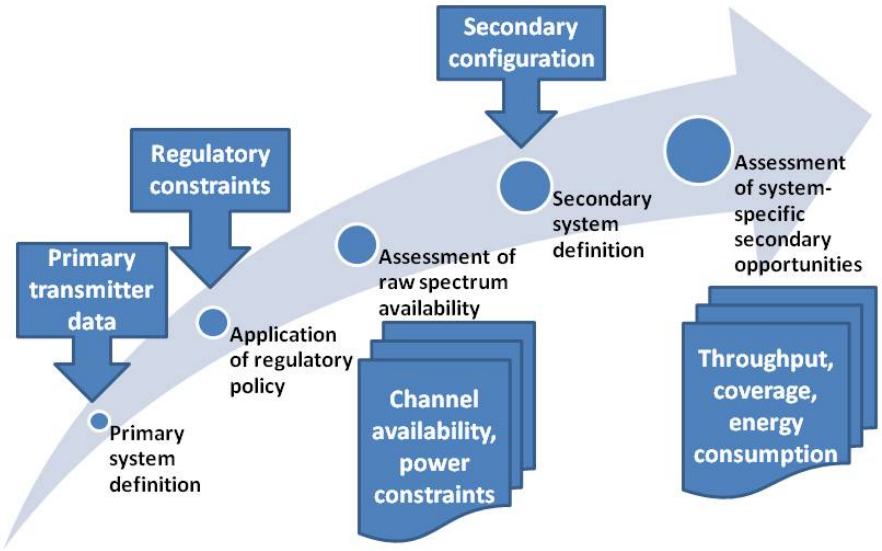

Figure 3-1 Workflow of spectrum assessment

In Section 2.2 we have discussed the process of generating spectrum availability/opportunity estimates based on a stepwise modelling of the relevant system components. The assessment methodology can be mapped into a workflow for the evaluation as depicted in Figure 3-1 and integrated into a generic software tool for spectrum assessment. The spectrum assessment tool we have implemented builds upon this workflow and reflects it in its user interface. Each modelling step is represented by a single pane/tab of the tool interface. One aspect we found to be of particular interest was the possibility to assess intermediate results through visual inspection in a graphical interface and derive preliminary conclusions on how the model parameters affect the spectrum usage/reusability. Unfortunately, there is a limitation to this approach, which is the computational complexity of scenario calculation. One focus of the implementation work was therefore to integrate a caching/storage infrastructure that will handle changes efficiently and require only lightweight recalculation steps after initialization.

At this point, we shortly revisit the necessary workflow steps for the spectrum assessment tool.

Primary system definition, regulatory policy and spectrum availability

In this step, the initial location and transmission patterns of the primary system are specified and, based on this information, the spectrum usage in terms of the signal strength at certain locations is derived. The primary network will include predefined transmitters from local databases, provided e.g. by the national regulators or operators of the primary system. Propagation modelling is either conducted offline through application of sophisticated terrain-aware models such as the Longley-Rice model or through online-calculation which computationally less demanding models such as the ITU P.1546-3 model. The applied propagation model for signal propagation estimation is freely selectable by the user in order to allow studying the effects of different parameter sets on the availability of resources for secondary reuse. Note at this point that the signal strength calculation is separated from the regulatory policy calculations for reasons of modularity and flexible adaptation to the study scenario.

The background calculation of the propagation characteristics keeps as much data as possible in a buffer to alleviate the heavy computation tasks. We have revised the underlying propagation models to identify opportunities for streamlining the propagation calculation and keeping most transmitter-specific information in pre-calculated databases. The final primary system calculations are carried out through a Primary Spectrum Resource Usage Server entity. The design of our database enables easy extension towards other propagation models. Future extensions may also allow to integrate data derived through measurement campaigns into the database with only minimal modifications to the database interface.

The application of regulatory policy completes the derivation of **spectrum availability estimation**. The regulatory policy does not affect the primary system spectrum usage characteristics, hence we outsourced it into a separate workflow step. The user can select the type of regulatory policy which should be applied in the scenario. Due to their good availability and the ongoing debate about the advantages of one regulatory policy over the other, we have implemented both, an FCC-type of regulatory policy [FCC10] as well as a policy framework according to the EC SE43 proposal [SE4310] for the spectrum assessment tool. The FCC-type of policy defines a set of allowed combinations of minimum-distance to coverage protection zone, secondary transmit power and secondary antenna height, a secondary device must comply with in order to be allowed to access a particular spectrum resource. The spectrum assessment tool allows to define the rule sets and display the resulting spectrum availability in terms of the number of accessible channels in a particular point and the permissible transmit power for a certain secondary transmitter. Statistics for an entire study area can be generated, displayed, and exported for further processing. The SE43 proposal for secondary operations defines an upper boundary on the decrease in primary signal quality that is acceptable due to secondary operations. Our spectrum assessment tool will calculate the individual resulting transmit power budget and create similar statistics as before to be reviewed and exported.

Secondary system definition, secondary-specific opportunity assessment

The secondary system is modelled on a node-level where the user can load secondary node locations from a file or apply a probabilistic distribution model. A model at this granularity brings some additional computational burden such as the requirement for small-step aggregate interference calculation. On the other hand, it opens many more parameters to be included in the description of the secondary system and a more precise evaluation. The most challenging task in this respect is the calculation of the aggregate interference that evolves from the parallel operations of multiple secondary transmitters. Each secondary system, i.e. each multi-transmitter configuration, will have to have means to control the interference to the primary system to an acceptable level. This can

be achieved either through more restrictive power budgets or centrally coordinated power allocation schemes.

Our spectrum assessment tool implements two complementary secondary system models to demonstrate different design philosophies based on the type of assumed secondary deployment. The selected models are a subset of the scenarios developed in the QUASAR project, see [D11]. The initial model is a cellular system where the network operator tries to boost the network capacity by using secondary resources. Due to the fixed and known locations of the transmitters, comparably high transmit antennas, and the high power requirements to achieve universal coverage, this model lends itself as prototype for other studies with similar deployment layouts such as rural broadband setups. The second model supported in the prototype is intended for dense deployments of low-power transmitters such as those found in Wi-Fi-like deployments. In those scenarios, the capability of aggregating channels for low-cost transceivers and the secondary-to-secondary interference play a more significant role. The second deployment scenario is hence computationally more complex and is mostly studied in small deployment areas.

Visual review

The visual review capabilities are one of the strengths of the graphical user interface. We allow the user to *interactively* review some primary and secondary model parameters effects and observe the changes on spectrum availability in a map visualization of the study area. Not only does this require extensive features of the map interface, e.g. by allowing to select individual transmitters and review their properties in a separate dialog. The most critical part is the background calculation of delta-adjustments to the review pane. We have used openly available APIs such as the Google Maps interface for this purpose.

Statistics

Statistics can be generated from the given configuration of primary system in a graphical representation, e.g. as complementary cumulative distribution functions or bar plots, and be exported through a generic interface to other applications such as Excel. This allows for more detailed and comparative studies for different parameter set configurations and make the tool a good extension to other existing toolchains for whitespace assessment. It allows it to act as foundation for more extensive studies, e.g. on the effects of policy decisions on whitespace deployment feasibility.

3.2 Terminology for area definition

To converge towards a common terminology in the assessment of spectrum resources, we in the following define the different types of “areas” used in the spectrum assessment tool. All of these can be set dynamically in the respective configuration tabs of the applications. A graphical representation is shown in Figure 3-2.

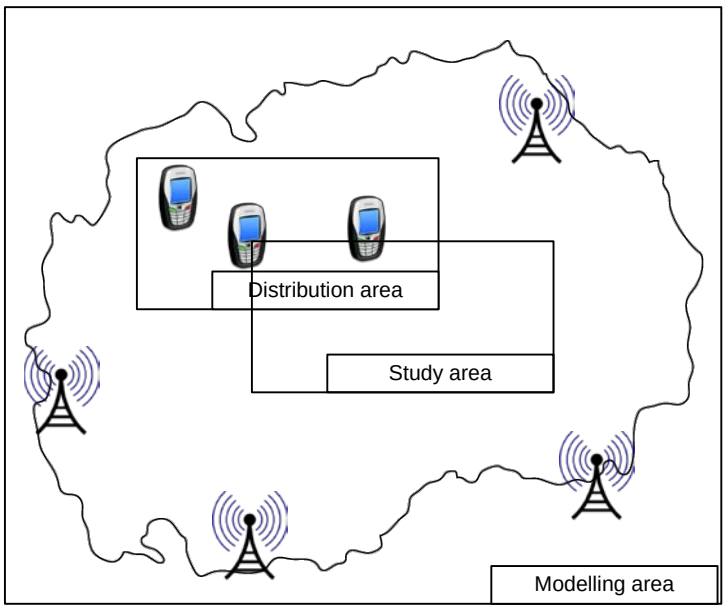

Figure 3-2 Terminology visualization for "area" in spectrum assessment tool

Modelling area

The modelling area is the largest area we foresee for the application. It describes regions of the size of e.g. an entire country with all relevant parameters of the primary system, in particular the locations and characteristics of the primary transmitters. If datasets for the primary system are included, they are aligned to the modelling area. Primary data are made available either by national regulators or by primary network operators. The modelling area will also allow specification of the type of spectrum resources that may potentially be available, e.g. the different TV channels, their center frequencies and bandwidths.

Distribution area

This is a secondary system parameter that defines in which area secondary nodes are operating. The distribution area is a subset of the modelling area and may be a state, a city or the country itself. The distribution area may also be implicitly defined through the locations of the secondary transmitters if they are fixed as is the case e.g. for the cellular system model.

Study area

The study area is a initially defined for the review. Only for the study area statistics are being generated and displayed. The user will be able to decide on whether the study area coincidences with the distribution area. The study area is defined prior to creation of the more demanding statistics.

3.3 System architecture

The dichotomy between the speed and visualization requirements of the tool and the reuse of existing codebases and integration of existing workflows in data-oriented programming environments such as MATLAB [Matlab12] requires for a modular, heterogeneous design with different data-providing facilities and a central visualization/control application.

We found it reasonable to separate the large data volumes that need to be stored for the primary system signal strength prediction by means of building an independent entity, the **Primary Spectrum Resource Usage Server**. The server is an extension to the comparably static geolocation databases that allow only queries for the availability of certain spectrum resources in a single point in space. The PSRUS offers a web-based control interface via an HTTP server through TCP/IP to allow running it on a separate host machine and provide a holistic view of the primary spectrum usage. We have developed a new tripartite XML schema to describe queries to the server that comprises the primary model definition, primary system definition and definition of a set of queries on the primary dataset. We will describe those in detail below.

For data-centric tasks, industry and academia make heavy use of MATLAB given its easy programming language and large in-memory and parallel processing capabilities. For this reason, we have selected MATLAB to implement our **Secondary System Models and Evaluation Toolkit** which builds the core of the spectrum assessment tool. MATLAB unfortunately lacks good graphical visualization and user interaction toolsets hence we have decided early in the development of the prototype to separate computation and outsource display tasks and user interaction to a separate **GUI**. Interaction of an external application with MATLAB is unfortunately challenging. MATLAB implements a small-scale TCP server, but is unable to provide larger datasets through this interface to other applications. Fortunately there are several methods to exchange data through inbuilt interfaces of MATLAB, most notably the MATLAB automation server communication with its MATLAB command line interface (CLI) [MatlabCLI12]. They do allow exporting data from a third-party application into the MATLAB workspace and executing functions from outside the MATLAB instance. Exchange of configuration data and execution control of native MATLAB code has hence been realized through this interface.

A native application for the visualization task is necessary due to its better integration into the operating system environment and the good availability of visualization classes and extensions. We have implementing the GUI in C# (Visual Studio) in order to benefit from Microsoft's Foundation Classes and the commonly used control handles. Furthermore, extensions to integrate the map services are available to C# programmers, making the GUI more natural to use and removing the burden to implement complex map interaction features.

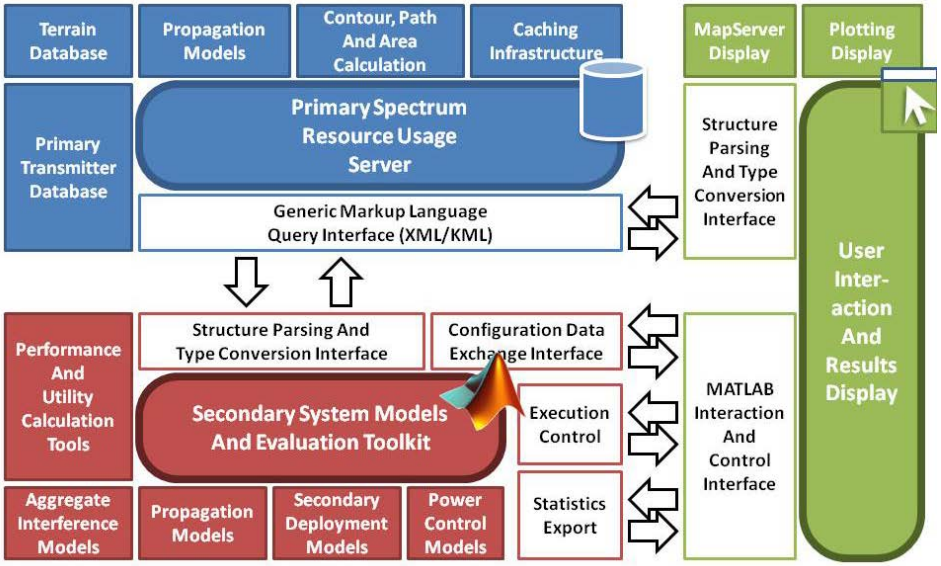

Figure 3-3 Spectrum assessment tool system architecture

The overall architecture of the spectrum assessment tool is depicted in Figure 3-3. At the right-hand side of the figure is the GUI through which the user interacts with the spectrum assessment tool. We have kept the GUI as light-weight as possible and leave all processing tasks to other services. This way, the GUI implementation can remain largely independent from the processing part of the spectrum assessment tool to allow later extensions and modifications. Central elements of the GUI are

- a set of tabs for the primary and secondary system definition that will guide the user through defining the scenario to be studied
- a map interface in which the user can zoom through the modelling area and study the primary signal strengths, interference power of the secondary and outage effects on primary receivers
- scenario-specific statistics panes which display statistics about various aspects of the primary/secondary relationship including but not limited to coverage statistics, outage statistics, channel usage statistics, distribution statistics etc.

Data for the GUI comes from two different sources. First, primary signal strength information is retrieved from the PSRUS with regard to the requested spectrum resource (e.g. a channel), location and time probabilities and environmental parameters. The GUI features a copy of the primary transmitter database to provide to the PSRUS and allow the user to select the entities of the primary system which should be included in the assessment. The server can either directly process this transmitter information in the request to calculate signal strength or it can use pre-processed data calculated earlier to answer the request. In the following, we will describe the format of the request coming from the GUI and/or Evaluation Toolkit and the format of the reply from the PSRUS.

More advanced processing, in particular the secondary modelling are conducted in a MATLAB instance that runs on the same machine as the GUI. Interfaces are able to exchange map information (similar to the PSRUS), function calls, data, statistics and status updates.

3.4 The Primary Spectrum Resource Usage Server

We have design a novel protocol for the PSRUS based on the exchange of XML files over a TCP/IP connection. This way, high compatibility is achieved and the GUI can make use of existing parsing tools for XML tree structures. The return format of the server is a XML variant known as KML. This map-oriented style format is used by popular map services such as Google Maps and Bing and can therefore be easily combined with their APIs. We intentionally deviate from other protocols for the whitespace data exchange that are currently under development, e.g. in the PAWS working group of IETF [PAWS12]. We took this step because the focus of these protocols is on providing spectrum availability information for single whitespace devices, not on exchanging data for statistical or modelling purposes. Furthermore, we also analyzed the database exchange format proposed by FCC for the US whitespace databases [FCCDB12]. We found that this format does not incorporate actual signal strength calculation data (which is done locally in each database instance) and is therefore not suitable for the purpose of our spectrum assessment tool.

3.4.1 Input format

We have taken the approach of building the PSRUS with a central webserver interface using the standard HTTP web protocol. Though not of primary relevance to the project, the database can be easily queried using other frontends, e.g. through a webpage if this methodology is applied. The communication protocol encompasses the exchange of a XML file with configuration and request details for the server. The server replies by sending a KML file that can be parsed easily by existing mapping tools. Upon opening a

HTTP connection the TVWS server, the GUI sends a XML file as a POST request that is processed by the TVWS server. The XML file follows a generic format we specifically designed for spectrum assessment purposes. It is easily extendible and can be used for TVWS studies, aeronautical radar bands and similar primary systems.

The input file is divided into three sections: The primary model definition captures general features of the propagation model used and specifies some design parameters, the primary system definition in which the primary system, i.e. the primary transmitters, are described and the output definition that contains the requested data sets that need to be calculated by the server.

Primary Model definition

The primary model definition provides information on the propagation model to be used for the modeling process. We support the Longley-Rice Irregular Terrain Model (ITM) l due to its integration of terrain data into the modeling process. In general as well as the ITU P.1546-3 model for generic calculations. The propagation model requires some general input data that applies to all transmitter which are included in the calculation. We split these into the environment-specific parameters and the probabilistic assumptions on primary receivers. Environment data describes those parameters that directly affect the physical properties of propagation. Among those are earth conductivity, relative permittivity and the radio climate. We adapted those parameters from the ITM model algorithm provided by NTIA. For more information on these parameters, we refer to the literature on the ITM model [Longley69]. In the scenarios we are going to show, these environmental parameters can be considered static for the whole operation time.

Of larger interest are the probabilistic parameters and receiver-side parameters defined in design specification section of the XML request. Here, we capture the statistical nature of the propagation model by defining the probability of exceeding a certain path loss at a certain location within the area represented by a data point (fraction of situations, area-dependent) and the fraction of time at which the path loss value is exceeded (fraction of time, mostly due to atmospheric and environmental effects). Also, the primary reference geometry is defined here in terms of the secondary receiver height. Antenna gains and similar static offsets may be applied later in the processing.

Primary system definition

In the primary system definition, we define the primary transmitters. We envision that the GUI will provide a list of transmitters with their respective transmission features. Of course, the server may internally hash these feature specifications, compare them to a list of pre-calculated datasets and use stored (raw) data to speed up the calculation process. Nevertheless, we want to leave as much freedom to the user in specifying primary transmitter characteristics as possible to study scenarios with select changes in the primary system, e.g. channel reallocations or transmit power reductions. To reduce the communication overhead, the GUI may refer to an existing database stored in the server.

Each list entry consists of the following information

- Unique name used to identify the primary transmitter, e.g. “Kilchillan”
- Location of primary transmitter (in latitude/longitude, WGS84)
- Height of foundation of antenna above sealevel in meters
- Height above average terrain in meters
- Polarisation: Valid values: horizontal,vertical,both

- Directionality of the transmitter: Directional, Omnidirectional
- The radiation pattern of the antenna (a list of radiation powers in angles from True north in dBW), intermediate angles are interpolated in the TVWS server
- The spectrum resource used

The spectrum resource is a generic definition of the spectrum occupation for the particular primary transmitter. We use a channel rasterization to be applied here. First, a channel number is defined, e.g. 23, which is the mapped to the center frequency that is used. To calculate the frequency band, a channel rasterization needs to be provided along with the channel. For example, for the European DVB-T system, the bandwidth of each channel is 8 MHz with an offset of 306 MHz, so channel 21's center frequency is

$$474\ [\text{MHz}] = 306\ [\text{MHz}] + 21 * 8\ [\text{MHz}]$$

Alternatively, the center frequency specified directly.

Output definition

The request to the database for signal strength information will require to define which information sets shall be returned. We allow three composite return types that consist of the primitives of a point or a (closed-shaped) polygon.
We found three different composite shapes, depicted in Figure 3-4, for specific spectrum resources to be useful as return values

- A signal strength contour, which is a polygon surrounding an area for which the signal strength is larger than a specified threshold, spectrum holes are not considered, multiple polygons can occur
- The shortest path between two points, where the signal strength values at equidistant points along the path are returned
    - Requires definition of starting and end point and distance between points
- A rectangular region bounded by a North-East and South-West point, where signal strength values for a raster of points is returned (given a certain resolution)
    - Requires definition of corner points as well as latitudinal and longitudinal resolution

For each request, a bounding box to match the study area can be specified.

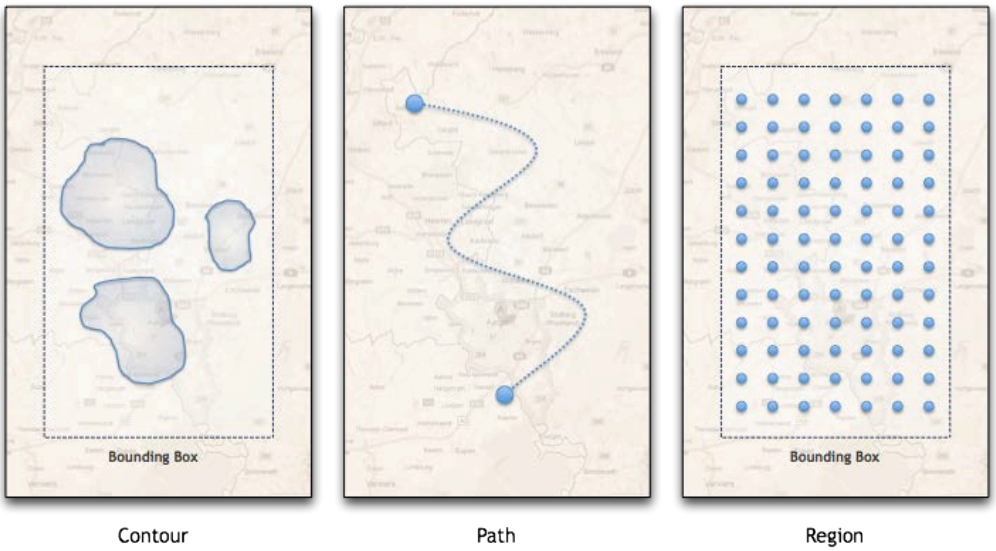

Figure 3-4 Returned output formats from PSRUS for a single spectrum resource.

3.4.2 **Output format**

The composite returned data set prototypes map directly into the basic shapes defined by the geography-oriented KML format. Hence, we consider it to be easiest to build the return type on this structure definition. Not only will KML allow to directly display returned data in tools such as Google Maps, Bing Maps or Google Earth, but due to it belonging to the family of XML definition we can use the same tools that are used for creating the original request for creation/extraction. Each output definition in the XML request contains a unique identifier, which is reused by the PSRUS in the returned KML file to distinguish between the different output values. The basic shapes of KML used are

- Polygon: Used for the contour levels. We encode the output ID in the folder, which contains the respective polygons for a contour level.
- Point: Single point values (along paths or in regions) are represented by Point primitives.

3.5 **Outlook: Caching of whitespace data**

One of the main difficulties we found for the server to perform at a bearable speed was the computational burden of calculating signal strengths if changes in the primary model parameters are allowed. We noted that the speed can be improved if intermediate variables of the signal strength calculation are stored and the final signal strength calculations are only partially updated. In this excursion we focus on the ITM model for terrain-based propagation modeling for a single transmitter to show the potentials for improving performance.

First, we note that signal strength calculation for a path between transmitter TX and receiver RX is at the highest abstraction level simply the subtraction of the path loss from the emitted signal power of TX in direction of RX (in dB scale) . Since this operation is fast, we only need to consider the path loss calculation for the speedup.

We have analyzed the implementation of the ITM model under computational aspects. In the open-source Splat! Implementation [Splat12], steps that deal with the calculation of terrain-dependent issues such as effective heights and distances consume most resources. All other steps, including those for dealing with the scenario variability, are lightweight and can easily be derived in an ad-hoc mode. In Figure 3-5 we depict the dependency graph of the ITM model with intermediate variables shown in black. Intermediate variables in red need to be stored and can be used to update the path loss value A if the variability parameters are changed.

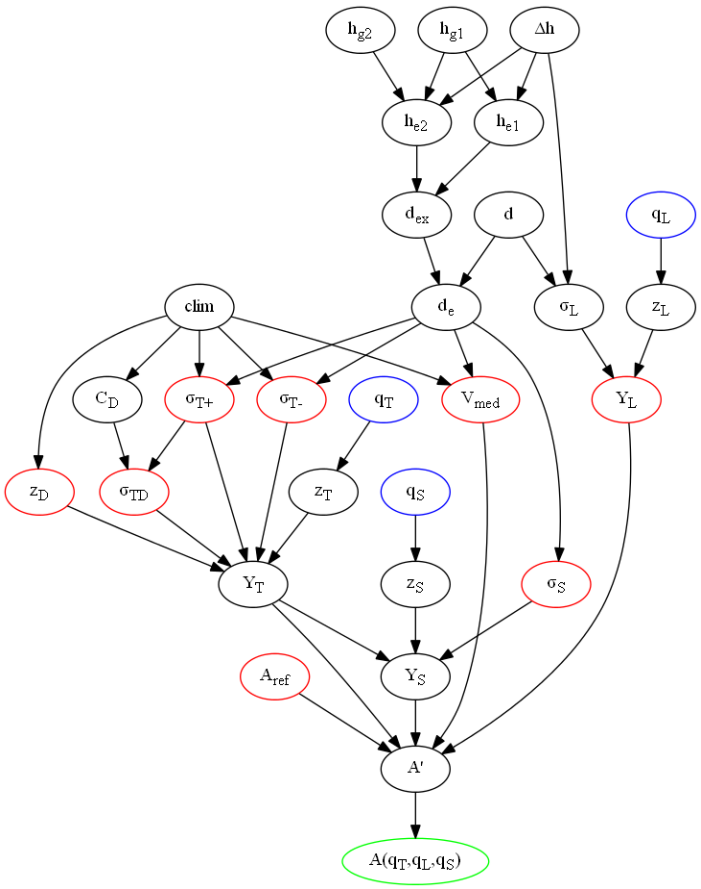

Figure 3-5 Dependency graph for ITM model (excerpt). Red nodes denote variables that need to be saved for the final path loss (A) calculation if the situation, location and time variability (q_S, q_L, q_T) are modified on the fly.

This methodology will allow the following parameters of the primary system to be adjustable in an ad-hoc manner

- Transmit powers of TV towers and antenna gains
- Variability figures for scenario, location and time

Following parameters need to be kept static or multiple copies for different configurations need to be stored

- Primary receiver height. Here, default values can be stored: 1.5m (for primary mobile receiver scenarios), 10m (for primary rooftop-mounted scenarios), 15m.
- Physical parameters (conductivity, climate, etc). We don't consider these parameters to be of primary interest to spectrum assessment studies.

3.6 Spectrum Availability Review

The spectrum assessment tool differentiates between interactive and non-interactive review facilities. Interactive reviews allow displaying data in a map-type of environment that can be either a geographic map (imported through the aforementioned APIs) or a heat map in case of high-density configurations. Non-interactive reviews builds upon a static graphs and raw data export. In the following we list the set of review opportunities that are possible for assessing the availability of spectrum for secondary reuse. The availability assessment assumes only a single secondary transmitter with a simplified usage model, comprised only of the transmitter height and maximum transmit power. For initial capacity estimates, a static pathloss between secondary transmitter and receiver is assumed.

Interactive display facilities	Non-interactive display facilities

- Display channel availability in color-coded map for single spectrum resource, e.g. a single channel
  o Possibility to select: No# of available resources, MHz available
- Display usage of particular resource in color-coded map (one by one, each resource can be visited)
  o For FCC, this review is based on the considered no-talk contour
  o For SE43, we consider the broadcasting coverage contour
- The user can click on the map to get available resources in a point and the allowable maximum transmit power
- Show color-coded capacity map assuming a simplified point-to-point link model for secondary system
	- Display CCDF of resource availability
	- Display CCDF of achievable capacity per pixel for a transmitter that
	  o can use all available whitespace resources
	  o The best N resources, assuming they are located arbitrarily in the frequency spectrum
	  o The best N resources, assuming they are located in adjacent locations in spectrum (carrier aggregation system)
	- Display CCDF of achievable capacity with population weighting

3.7 The Secondary Systems Model and Evaluation Toolkit

The Evaluation Toolkit provides several unified interface to exchange configuration information of primary and secondary system, map data, and statistics. The interfaces work bidirectional. In addition to being responsible for secondary system processing, the MATLAB instance is also the exclusive provider of statistics about coverage, outage and performance. For this purpose, the MATLAB instance may query the PSRUS for additional signal strength information if required. The multitude of statistical parameters makes it difficult to apply in-application data exchange. Instead, the evaluation toolkit stores several plots and data source files to disk for retrieval by the GUI. In the following, we present the map exchange format to give an example of the structure of the exchanged data sets. Furthermore, we provide a list of parameters for the secondary system models that are specified in the GUI and subsequently sent to the Evaluation Toolkit for calculation.

3.7.1 **Map exchange**

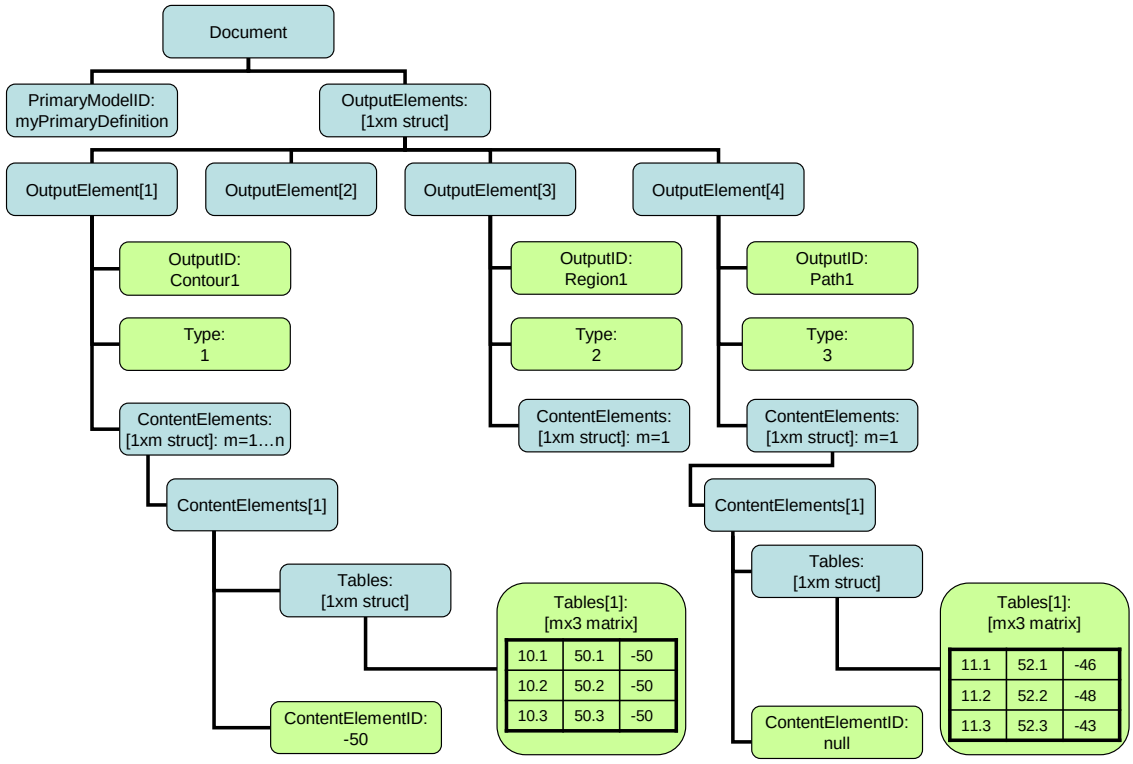

Figure 3-6 Data structure for map exchange

We have reviewed various methods for exchanging data between MATLAB and the GUI application and found that C# as programming language for the GUI limits the number of feasible options. In particular, the commonly used MATLAB Engine does, at the current stage, not support .NET SDK based applications [NETSDK12] due to the lack of a compiler. Therefore, we have decided to exploit the MATLAB Automation Server, an older method that provides a CLI to the MATLAB workspace and the exchange or fundamental data types. In Figure 3-6 we show the MATLAB struct created from the examples listed above upon conversion from the KML. The GUI will export the content of the KML file in this way. If data from a specific output element is accessed, it can be identified by a number of index identifiers. For example, in order to access the first contour polygon in the first contour request in the first output element, the MATLAB instance accesses `Document.OutputElements[1].ContentElements[1].Tables[1]` where the first column is the longitude information, second column is the latitude information and third column contains the signal strength value.
The “Type” token represents the type of output element that is queried, see Table 3-1.

Table 3-1 Type IDs of output definitions.

Type ID	Type
1	Contour: (a set of) polygons The signal strength value in the third column of each table is identical in all rows and identical to the ContourID in a PSRUS request.
2	Region: Contains a single content element with a single table in which the data points are stored,
3	Path: Similar to region, the path has a single content element with a single table of data points.

3.8 Spectrum opportunity review and secondary system models

The exploitation capabilities of the secondary system depend on a number of parameters. A simple analysis of the raw spectrum availability hence does not suffice to argue on the feasibility of secondary deployments in whitespace scenarios. As discussed before, we have implemented two different secondary deployment types that can be considered prototypic for other exploitation scenarios. In the following, we give the input parameters of the particular secondary system and the exploitation review facilities we have implemented. The spectrum assessment tool is flexible enough to allow for easy extension to further secondary system models if necessary.

3.8.1 Cellular system model

The cellular system model assumes a single secondary network composed of a wide spread configuration of secondary transmitters. Transmitters are usually mounted at exposed positions, e.g. at the roof of buildings or towers to cover large ranges. Besides high throughput, cellular system operators thrive for a maximization of the coverage of their network. Power-control between cells is optimized to the specific usage pattern of secondary cell users and highly dynamic. The analysis therefore abstracts from the actual power allocation and models only an upper boundary of the allowed power budget for each spectrum resource in downlink direction. In the following table, we give the set of parameters configurable through the GUI and the statistics that can be accessed after completion of the simulation run.

Table 3-2 Cellular system model - Inputs and generated statistics.

Inputs	Generated statistics

Transmitter Distribution
(Here, we select how the locations of the secondary transmitters are selected)
- From fixed locations (e.g. locations of deployed cellular network)
- Poisson point process
  o Homogeneous: needs specification of the density
  o Inhomogeneous: besides density, we define the weighting function, e.g. by population density or by broadband penetration in a country (inverse)
- Regular hexagonal
  o Only the cell sizes need to be specified in this case
 	
Transmitter configuration
- TX antenna height
- Maximum system-supported transmit power
- Resource usage opportunities
  o Specifies, whether a transmitter can use all available channels or needs
	Interactive
	- Graphical display of a power contour of the secondary systems
	- Graphical display of the intersection of a power contour of the secondary system and a power contour of the primary system (to find, e.g., areas that are interfered by the secondary system)
	
	Non-Interactive
	- Whitespace usage
	  o Statistics on how many resources are used by each secondary transmitters
	  o Statistics on allowed transmit power of secondary transmitters for each resource
	- Whitespace exploitation
	  o Statistics on the achievable downlink capacity for the secondary cell users
	  o Statistics on the achievable downlink capacity for the secondary cell users,

to limit itself to a subset due to constraints in the transceiver hardware. (Carrier aggregation) - Power allocation scheme o Specifies how the interference budget is distributed between secondary transmitters. ***Receiver configuration*** - RX antenna height - User distribution relative to transmitter location o Uniform o Gaussian - User Density o Either specified relative to the area, or specified by a total number users per cell site - WSD propagation model o Model to be used for secondary TX to secondary RX calculation: Okumura Hata or ITU P.1546-3 - Other WSD features o Residual noise floor o Noise figures and gains - Capacity model o The capacity model provides the mapping from SINR to capacity	normalized to the number of users in a cell (sharing) - Coverage o Statistics on the received power from the secondary cell towers in the distribution area, showing only the best spectrum resource in each case o Statistics on the average number of useable channels in a random point in the distribution area

3.8.2 **Wi-Fi-like system model**

The Wi-Fi-like system model is used in small-scale scenarios to model the effects of aggregate interface, low power, and penetration losses for secondary transmitters, considering the downlink connection. It additionally takes into account the MAC layer of the secondary devices, and considers the shared access of multiple Wi-Fi-like access points (APs) to the resource medium. A simple carrier aggregation model is offered where the user can select how many adjacent spectrum resources may be aggregated to a single spectrum allotment for the secondary APs.

Table 3-3 Wi-Fi-like system model - Inputs and generated statistics

Inputs	Generated statistics
Transmitter (AP) Distribution - Poisson point process (homogeneous): Definition of density either over area (APs per km²) or over population (APs per inhabitants) Note at this point that the secondary network distribution area is considerably smaller than compared to the cellular	***Interactive*** - Graphical display of a coverage regions where a given minimum estimated bit rate is provided to the user terminal associated with a secondary AP, for a given secondary transmit power (exclusive access and shared access)

scenario.

Transmitter Configuration

- Fixed power level
- Resource allocation
  - each AP randomly selects (is allocated) one of a number of "available" resources, as advised by a central coordination entity
  - carrier aggregation allows allocation of resource chunks of N adjacent resources (carrier aggregation)
  -

Receiver configuration

- User distribution according to uniform or Gaussian distribution, cut-off distance according to fixed threshold from AP, fixed number of users per AP
- log-distance path loss model, with
  - reference path loss @ 1m
  - pathloss coefficient
  - wall penetration losses
- Capacity model
  - SINR mapped to raw-rate provided by AP to user terminal using auto-rate function as specified in IEEE 802.11a/g, based on receiver sensitivity (spectral efficiency x bandwidth = raw rate in Mbps)
  - Contention domain limit for load-based estimation of channel access time

Non-Interactive

- Whitespace exploitation
  - for a given transmit power, rate vs. range curves
  - rate distribution over area
  - CDF Per-AP Resource Usage
  - CDF Per-Resource Secondary TX Power
  - CCDF Single User Capacity (exclusive access or shared within AP)

3.9 Web-based visualization tool

This section presents an integrated web-based Spectrum Availability Assessment Tool for TV White Space. The tool is a front-end visualization for time-intensive computational assessment - the white space spectrum availability and secondary capacity estimation made for Finland and UK on the digital TV coverage. The assessment methodology for the whole process involves considering the radio environment models, the DTT coverage and appropriate secondary system models as described in Section 2.2. The tool also includes visualization for primary system performance that is subjected to secondary system scenarios. This helps to compare the impacts of different parameters on the existing primary system. The graphical user interface of the tool is developed using standard, user-friendly and dynamic features to shorten the learning time for new users.

3.9.1 **Visualization tool architecture**

The main goal of the Spectrum Availability Assessment Tool is to visualize the findings of the undergoing research in TVWS for Finland, UK and possibility to extend into other areas as well without the need of installing any additional software. In this way the tool can be used in any computer with Internet connection by using normal web browser. There are few practical challenges for implementing this. The major one being the time requirement, it takes long time to generate any of the required outputs (roughly 0.5 - 3hrs), so that real time interaction is almost impossible. This is also a big hurdle to stand-alone applications. Secondly, it needs higher bandwidth requirement that is able to transport many gigabytes of DVB-T broadcast and population data in only few minutes. The direct implication is that we cannot make a timely browser-side computation. These limitations ultimately demand the computations to be on the server-side and cannot be real-time one. Consequently, a precomputed model has to be implemented. This approach uses ready outputs that are pre-calculated and stored in a database server. Practically, the need of the database can be compromised based on the data size (number of generated cases) and the features needed at the front end – browser based access. In this scheme, everything is calculated ahead. This gives a great level of flexibility to use either a server-side or browser-side mechanism to access the data. The model in Figure 3-7 uses browser-side scripting languages to fetch data from the web-server.

The architecture shown in Figure 3-7, presents the architecture model for realizing our technical requirements. The back-end computation takes population and TV broadcast data as inputs. By using the appropriate propagation models and relevant parameters, the computational outputs are stored in a web server. Overlay plots are stored as images and comparison curves are stored as text files. The web server can be accessed by any of the latest browsers.

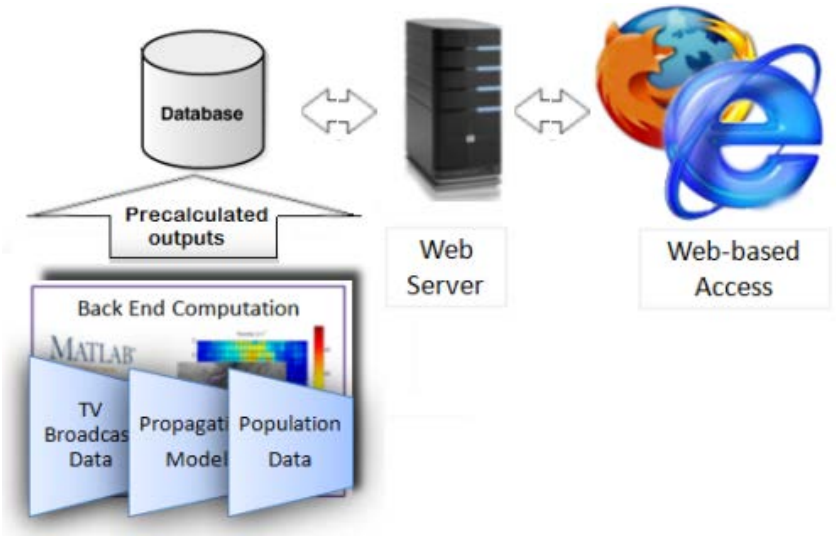

Figure 3-7 Visualization tool architecture

There are various free map service providers to visualize the capacity plots; Google Maps, Bing Maps, OpenStreetMap, WikiMapia, Nokia Maps and others. We chose Google Maps for its customizable web-based visualization experience. Google Maps provides its own Google Maps API (Application Package Interface) that can be used to embed the mapping service on non-commercial third party websites. Google Maps API uses Javascript technology, which is a scripting language (lightweight programming language) very well compatible for most browsers. Apart from becoming a scripting language of choice in Google Maps environment, Javascript is very popular tool in dynamic web-based applications. The World Wide Web Consortium (W3C) standard known as

Document Object Model (DOM) is a language-neutral interface that allows scripting languages like Javascript to dynamically access and update content, structure and style of HTML documents. Javascript uses an API for browsers, called XMLHttpRequest, to submit request to web-servers and to load server-side files to the browser. For the SINR plotting functionality, we can make use of XMLHttpRequest protocol and any of the Javascript plotting libraries; specifically we used a library named as flot. Moreover, Javascript is executed in the browsers without preliminary compilation. This has greatly eased its portability across different systems. The combination of HTML, CSS and Javascript allows a very flexible web-based GUI visualization. An HTML document presented by the three technologies is named as Dynamic HTML (DHTML). DHTML enables faster content fetching from server without the need of refreshing the page. It is the main tool in dynamic web formatting and visualization.

One other alternative to DHTML is Java applet, which can offer a more dynamic client-side GUI. They have an advantage of giving the programmer more control of the UI and with capability of handling computation intensive visualizations. Java applets run in a web browser using Java Virtual Machine (JVM), a platform-independent code execution component for Java codes. However, applets are with many limitations. Firstly, the user must have JVM enabled browser. Secondly, they are restricted by many security issues in the face of malicious intents using applets; they work under security sandbox model. Besides these, applets lack the flexibility of dealing with on-line map services.

3.9.2 **Visualization tool description**

The tool can be accessed on the web by using a universal resource locater (URL) address. URL is a specific character string, in our case http://quasar.netlab.hut. The content is hosted on an Apache HTTP Server. Apache is an open source (allows access to the source code, medication and free redistribution) web server. Web servers are software that serves requests from browsers by organizing content residing in them. They only serve requests and hence they remain in listening mode until they receive them. The requests are sent from browsers to web servers using the URL addresses.

Web tool is capable of plotting overlay plots over a map and compare cumulative distribution function curves of different scenarios. Overlay plotting is done by using Google maps Application Programming Interface (API). Google maps API has built-in zooming and panning functionality that allow the map to be focused into desired area. Graphical user interface (GUI) of the tool can be seen in Figure 3-8. Left side of the interface has the options for selecting the wanted usage scenario and it also has different plotting buttons for presenting the results. Results can be seen as coloured overlay images on the map, or the selected parameter combination can be added for comparison. Comparison plotting allows comparing the CDF curves of different scenarios. Right side of the GUI consists of the actual overlay plotting map and its controls. Map controls are shown in Figure 3-9.

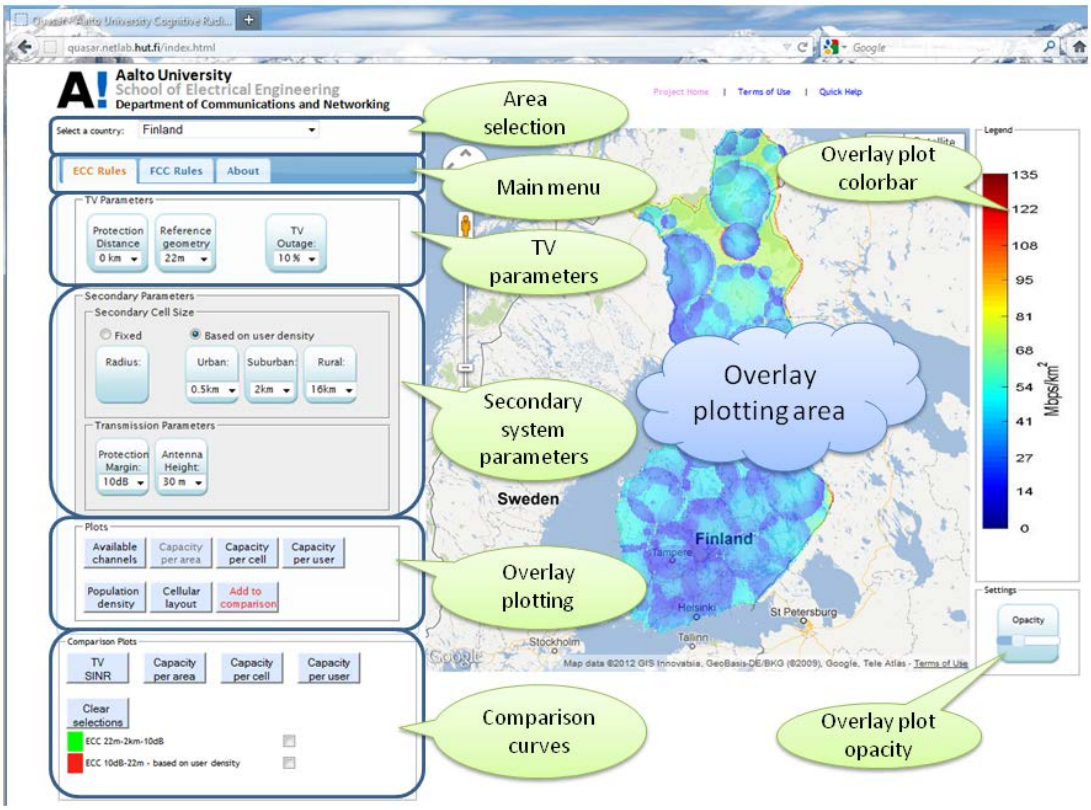

Figure 3-8 Graphical User Interface of Spectrum Availability Assessment Tool

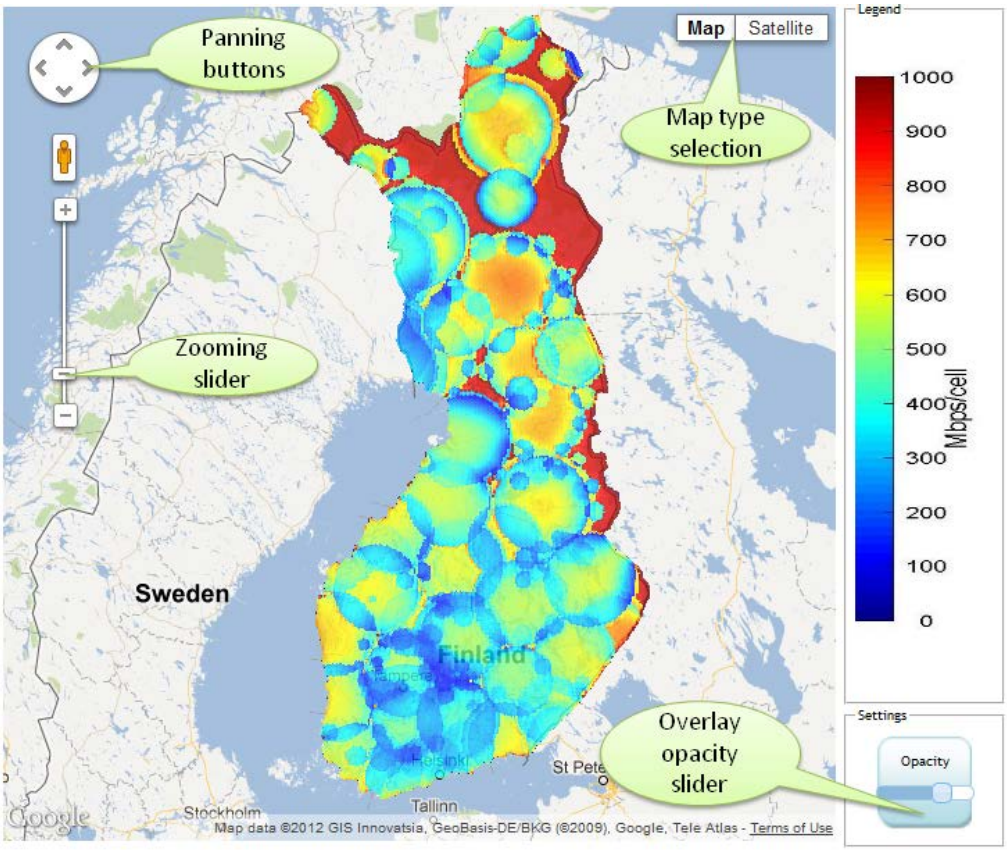

Figure 3-9 Map controls

3.9.3 Scenario parameters and overlay plotting

The panel showing the different parameters and overlay plotting options is shown in Figure 3-10. First thing that the user can choose is whether the secondary usage scenario is based on ECC or FCC rules. These rules can be selected by choosing the right tab on top of the panel. Below the rules are the parameters that are being used. Some of the parameters can be changed by selecting different value from the drop-down menu. At the bottom lies different plotting buttons that place the overlay image on top of the map. If some plot is not available or it is not computed, the button is disabled.

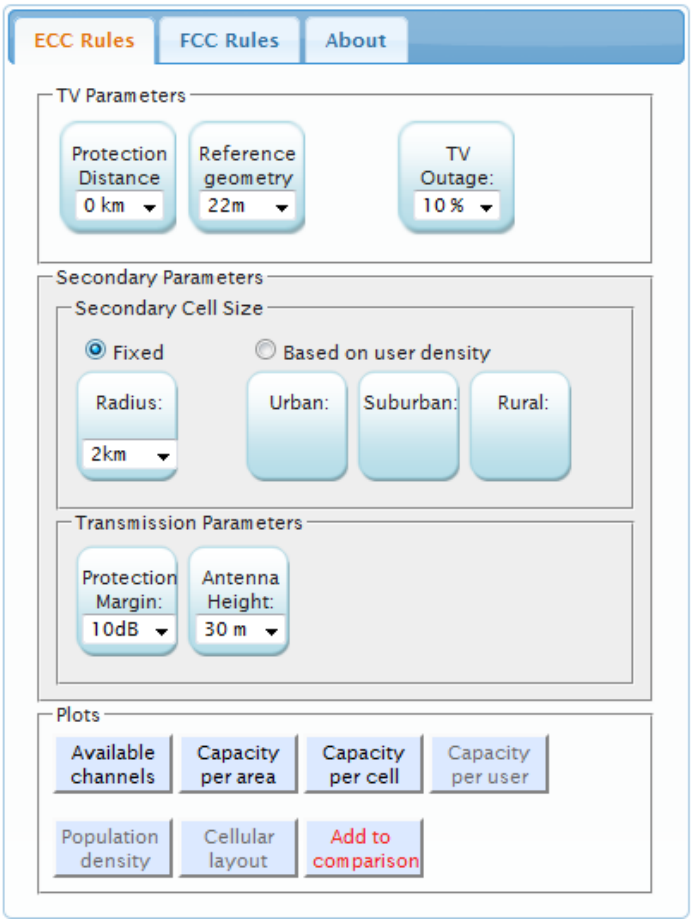

Figure 3-10 Scenario parameters and map overlay plotting options

The parameters and buttons shown in Figure 3-10 are

- Protection Distance - the minimum radial distance between a secondary transmitter and an intended TV receiver operating on the same channel
- Reference geometry - the minimum separation between the primary receiver and the secondary transmitter working in adjacent channel
- TV Outage - target outage probability at the TV coverage area border in the presence of secondary transmitter
- Fixed Radius - refers to the homogeneity of cellular radius of the secondary system across the country. It can have constant values of 2km, 5km or 10km.
- Based on user density - the cellular radius of the secondary system is dependent on population density. The secondary cells can have radius of 0.5km for densely populated urban areas, 2km for suburban areas having medium population density and 16km for sparsely populated rural areas.

- Protection Margin - the extra power margin added in the calculation of power emission level for a secondary device, for protecting the primary system from harmful interference. It includes the safety margin, SM, and the aggregate secondary system interference, MI. Refer equation
- Antenna Height - the height of secondary device above average terrain level
- Available Channels - the number of free TV channels, in a specific geographic location
- Capacity per Area - the secondary capacity (data rate) on the available channels, when homogeneous cellular size is used across the country.
- Capacity per Cell - the average capacity in the TVWS available to the whole secondary cell, when the cell-size is based on population density.
- Capacity per User - the average capacity of the TVWS available to each user in a cell. It is obtained by dividing the capacity per cell with the number of users in a cell.
- Population density – the number of inhabitants living per square kilometer
- Cellular layout – cellular layout when cell sizes are selected based on the user density
- Add to comparison – adds selected parameter set into comparison plots where CDF curves can be plotted and compared

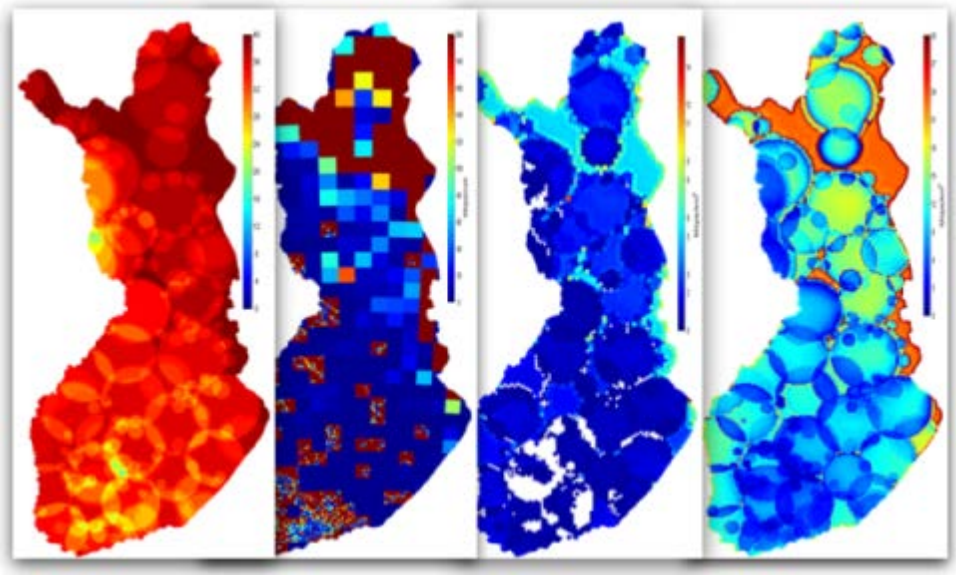

Figure 3-11 Examples of overlay plots (available channels, capacity per cell with user density based secondary cell layout, capacity per area 2km and 5km)

3.9.4 **Comparison plotting**

Since different overlay plots are difficult to compare with each other, there is a possibility to compare the cumulative probability distributions of different usage scenarios. The comparison plot panel is shown in Figure 3-12. Add to comparison – button adds the selected parameter combination for comparison and allocates different colour to each set. Different sets can be choosed for plotting by ticking it. A new popup window then opens with the ticked sets when one of the comparison buttons are pressed. Clear selections button removes all sets.

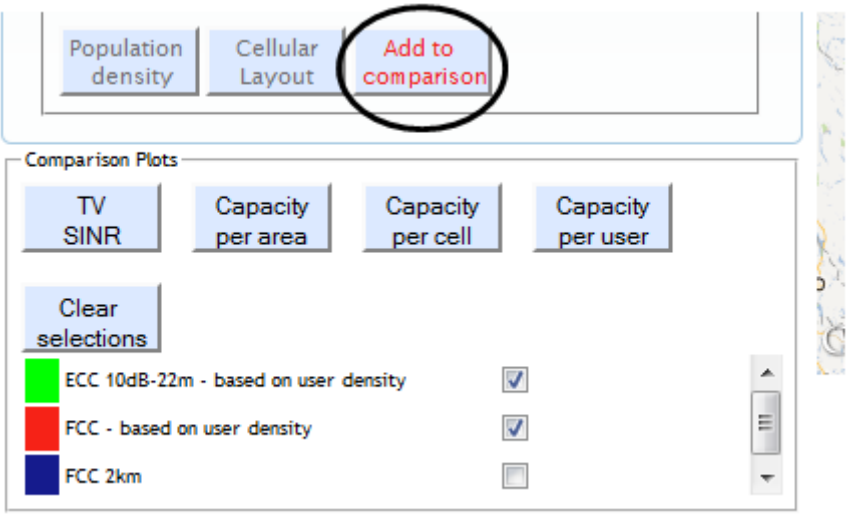

Figure 3-12 CDF comparison options

The tool allows comparison of the following statistics:

- TV SINR – Television coverage edge SINR CDF
- Capacity per area – Average secondary capacity per area CDF
- Capacity per cell – Average secondary capacity per cell CDF
- Capacity per user – Average secondary capacity per cell divided by the number of users CDF
- Clear selections – Removes all selections

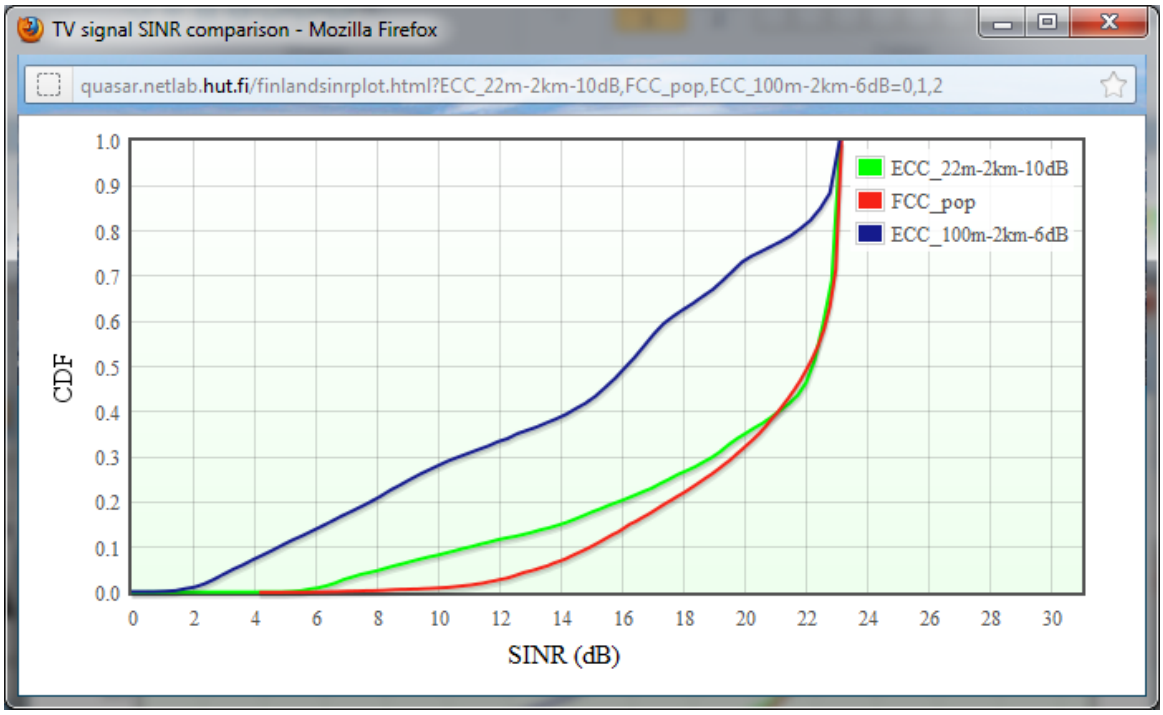

Figure 3-13 Example plot of TV cell edge SINR comparison

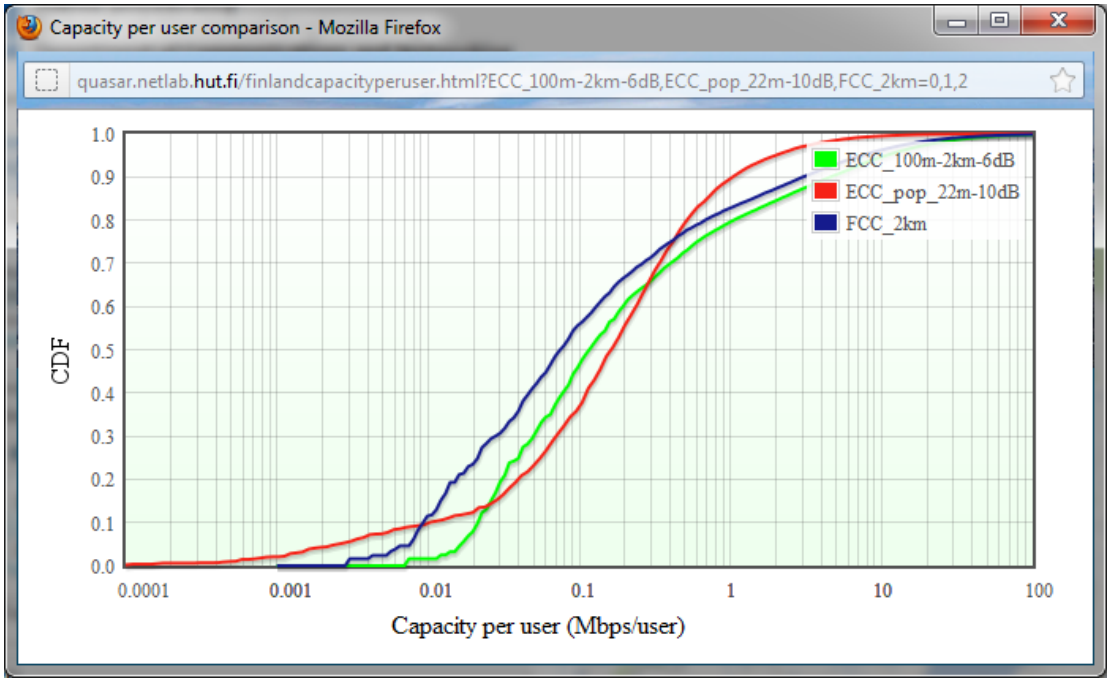

Figure 3-14 Example plot of capacity per user comparison

4 Verification Measurements

The QUASAR project has not reported until now about the conducted measurements by several partners. This section presents the verification measurements including the used measurement equipment, measurement locations and the obtained results. Generally, the measurement efforts are organized in three groups: verification of propagation models measurements (reported in Section 4.1), co-existence measurements (reported in Section 4.2) and shadowing measurements (reported in Section 4.3).

4.1 Verification of propagation models

Secondary system will exploit spectrum resources in various frequency bands. At the current stage, mostly TV frequencies have been considered for this deployment scenario due to the semi-static transmitter locations, transmit powers, and good propagation characteristics in the UHF bands. Planned and effective rulings on the fair access to these bands make heavy use of the concept of geolocation databases. Secondary devices will query these entities to retrieve allowed transmit powers and channels for the license-exempt access. For this purpose, the databases will need to correctly estimate the primary usage of spectrum by accurately predicting the radio propagation in the relevant bands. Depending on the level of abstraction and the complexity of the environment, the employed radio propagation models may perform quite well, but they require significant fine-tuning and auxiliary information. Inconsistent estimation may result in primary outage or hamper secondary deployments due to low capacities.

The QUASAR project has carried out a measurement campaign in several European countries and cities to assess the accuracy of the widely used propagation models when used for whitespace prediction. Additionally, configurations of multiple towers serving a coverage area by means of an SFN network are examined as they are often used in European broadcasting network, but so far have not been studied extensively for their propagation characteristics. In the following, we show that each propagation model has its particular shortcomings and may not be used independently for TVWS databases in any case.

Section 4.1 is organized as follows. Section 4.1.1 reports on TV band measurement campaign in Aachen (Germany), Section 4.1.2 presents the results of the TV band measurements in Skopje (Macedonia), Section 4.1.3 contains the adjacent channel interference measurements from TV towers to WSDs, in Section 4.1.4 results from ATC radar measurement in Macedonia are presented, and finally Section 4.1.5 gives the measurements findings on radar spectrum occupancy in Sweden.

4.1.1 TV bands measurement campaign in Aachen, Germany

In order to determine the combined signal strength from multiple TV transmitters, we have conducted a measurement campaign in the city of Aachen, a mid-sized German town at the border to the Netherlands and Belgium. Aachen exhibits features similar to many other older European cities with a circular cultivation and strict separation of industrial, residential, and shopping areas. As often found in cities from pre-medieval and medieval times, the main agglomeration is surrounded by a natural elevation (cauldron layout), which causes additional shadowing for transmitters outside the city area.

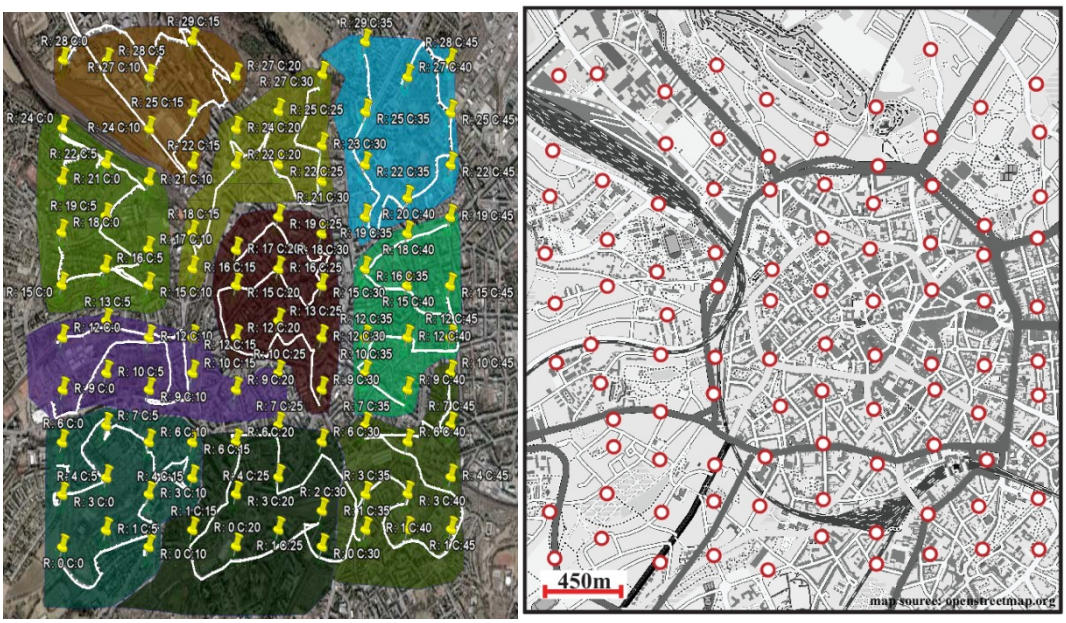

Figure 4-1 Measurement locations in the city of Aachen, Germany. Figure (a) shows the measurement locations (yellow markers) and corresponding walk paths taken on each of the 10 campaign days marked by the colored regions. Figure (b) shows the measurement locations with respect to the city's street layout

We have conducted measurements in the TV bands at 96 roughly equidistant locations in a 2.5km x 3km regular grid, depicted in Figure 4-1(b) as red circles. Locations were manually chosen to fulfill the following requirements:

- Each location was in a separate point of the 3-arc second terrain data we were using for the later processing
- No two locations were at line-of-sight to avoid waveguiding effects leading to correlated shadowing
- No location was at line-of-sight with the transmitter

A ten-day measurement campaign was required to cover the large city area with customized measurement equipment. At each measurement point, the measurement setup collected samples for approximately 27 minutes to average over fading and short-lived changes in the environment such as parked cars or walking-by pedestrians. At each location, GPS measurements were taken to improve the accuracy of location determination. For further localization improvements, also photographs were taken and compared against official street maps provided by the state of Northrhine-Westphalia in which Aachen lies.

The specifications of the measurement setup are listed in Table 4-1. Besides a high-precision spectrum analyzer with low residual noise floor, we used a mast-mounted antenna construction with a biconical antenna. The selected antenna showed almost constant gain within the VHF and UHF bands and hence made it particularly suited for this campaign. Furthermore, we designed a manual tilting mechanism to adjust the antenna for vertical polarization plane, see Figure 4-2. Samples were created with the smallest possible resolution of the hardware, combined and averaged to remove modulation artifacts and the noise floor.

Table 4-1 Measurement setup for the model verification campaign

Spectrum analyzer	**Rohde & Schwarz FSL 6**
Displayed average noise	-162 dBm/Hz
Preamplifier	20 dB
Resolution bandwidth	300 kHz
Sweep points	251 per sweep
Sweep time	420ms per sweep
Number of sweeps per location	1000
Center frequency	Sweep 1: 514 MHz Sweep 2: 586 MHz
Frequency span	75.3 MHz
Detector	RMS
Repeatability	0.05 dB/99 %
Antenna	**Aaronia BicoLOG 30100**
Form factor	Biconical
Antenna height	1.8 meters
Gain (typ.)	1 dBi
Mechanical tilting precision	+- 5 degrees
Other components	
Cable losses (typ.)	0.3 dB @ 500 MHz
Reported channel noise floor (typ.)	-91.95 dBm (+- 0.91 dB)

Figure 4-2 Measurement setup with mechanical tilting mechanism, mounted on wooden mast.

4.1.1.1 Measured primary system configurations

In the city of Aachen, three independent multi-transmitter networks could be detected with our measurement equipment. Their towers are shown in Figure 4-3, with the red square marking the area in which measurements were conducted. The transmitters build broadcasting-specific Single Frequency Networks (SFNs), which serve the same channel bouquet. They exploit the guard interval in the OFDM broadcasting signal and the equalizer of the TV receiver hardware to improve coverage and alleviate holes in the coverage region. Information on the transmitters was made available to us through the local regulator.

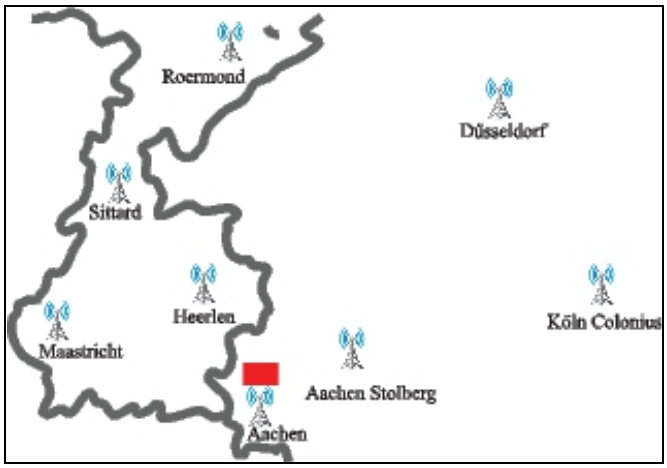

Figure 4-3 TV transmitters detectable in the studied region (red).

Statistics on measured signal strength are shown in Table 4-2. The Aachen SFN is the closest one to our study area. Two channels of this network have been included which show a 2 dB difference in the received median power. The network itself consists of two towers located in the South-West and North-East. We found by initial testing with a directional antenna that the lower-powered tower is the dominant signal provider. The tower acts as a gap filler in the SFN configuration and is supposed to cover the Aachen city area which is partially shadowed from the other transmitter. The signal variability over different measurement locations is of the same magnitude as has been reported earlier in literature for similar configurations.

We additionally included the Dutch SFN for the region of Zuid-Limburg in the measurement campaign. Compared to the Aachen SFN, this network is considerably more complex. It features four transmitters with high directivity. As you will note in Figure 4-3, the towers' main purpose is to cover a spike-shaped region in the Netherlands. The position of the towers spans an angle of arrival region between 280 and 350 degrees. Not surprisingly, the channel variability in this network is up to 4 dB higher than in the two-transmitter case. We consider this to be caused by the multi-transmitter configuration where the main arrival paths of multiple towers can exhibit independent shadow components. The last SFN we were able to observe in the area is composed of two towers in the larger cities of Köln and Düsseldorf. They are furthest from the study area and reasonable reception of their signal is achieved only in elevated locations of the study area. Within the shadowed center region, the low received power hence does not significantly vary, causing low standard deviation when compared to other scenarios.

Table 4-2 Single-Frequency Networks measured in Aachen study region

					Channel power statistics					
	CH	Freq.	Serving towers	TX power	Distance	Max.	Min.	Med.	90th prctl.	10th prctl.	Std. Dev.
		[MHz]	[No]	[dBW]	[km]	[dBm]	[dBm]	[dBm]	[dBm]	[dBm]	[dB]
Aachen SFN											
	26	514	2	37 43	2.2 13.0	-29.2	-63.7	-50.6	-38.8	-59.0	6.78
	37	602	2	40 47	2.2 13.0	-29.5	-64.3	-52.1	-40.4	-58.2	6.79
Limburg SFN											
	24	498	4	46 43 43 43	10.9 29.4 47.3 30.6	-42.8	-81.8	-71.5	-53.1	-79.1	9.61
	34	578	4	43 40 43 43	10.9 29.4 47.3 30.6	-44.3	-85.4	-73.5	-55.3	-81.9	9.84
Düsseldorf SFN											
	29	538	2	47 43	70.5 64.5	-59.7	-89.9	-83.2	-74.3	-87.6	5.77

For visual inspection, we depict the received signal strength in the study area in Figure 4-4. The geographical peculiarities described above are dominating the received signal variations. Hills in the North and South of the study area become particularly visible in this plot due to their better reception of transmitters located far from the study region. We were able to measure up to 25 dB difference in the power of the center region compared to the outer areas if, e.g., the Limburg SFN was considered.

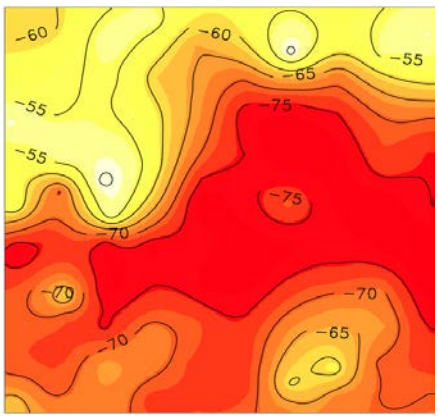

(a)Channel 24 of Limburg SFN

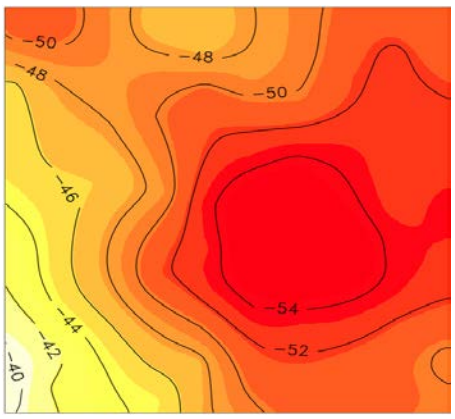

(b)Channel 26 of Aachen SFN

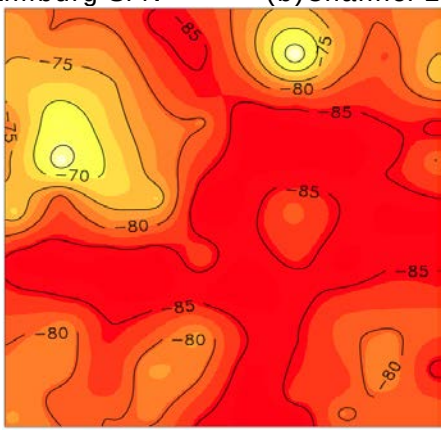

(a) Channel 29 of Dusseldorf SFN

Figure 4-4 Measured signal strength in Aachen study area.

4.1.1.2 Prediction errors of empirical propagation models

To validate the estimation precision of propagation models destined to be used in future geolocation databases, we calculated the predicted received power based on transmitter information provided to us by the national regulator and compared it to the retrieved signal powers. For each SFN we first calculated the received signal power from each single tower and subsequently added them up. For our measurement setup with low sampling rate in comparison to the signal duration, this is a reasonable approach. The models used in this validation process are standard models in broadcast planning, namely the ITU P.1546-3 model for large-area coverage, the Longley-Rice Irregular Terrain Model (ITM) which also takes the local terrain into consideration, and the Okumura-Hata model which is considered to be particularly powerful in urban scenarios.

The propagation models show large performance variation for the different transmitter configurations. Most surprising in this respect were the outcomes for the ITU P.1546-3 and Okumara-Hata model when used for the local Aachen scenario. The offset from the real mean power accounted to up to 10 dB, an unacceptable deviation for any protection requirements planning. For the Okumura-Hata model, the standard deviation is in the order of the standard deviation of the base dataset, while for the ITU model the standard deviation is up to 2 dB higher.

Table 4-3 Prediction errors of empirical propagation models.

	ITU P.1546-3		**Longley-Rice ITM**		**Okumura-Hata**	
	Mean error [dB]	Std. Deviation [dB]	Mean error [dB]	Std. Deviation [dB]	Mean error [dB]	Std. Deviation [dB]
Aachen SFN						
26	7.14	8.12	-16.24	8.92	10.31	6.3
37	4.85	8.69	-18.89	9.06	7.83	6.48
Limburg SFN						
24	-2.96	9.21	-9.52	9.32	-2.12	9.19
34	-1.71	9.45	-5.74	9.57	0.14	9.40
Dusseldorf SFN						
29	-4.10	5.82	5.68	5.1	-2.65	5.76

Besides the Longley-Rice ITM model requiring the most extensive specification of the environment by demanding terrain information as well as information on climate, earth curvature, etc., it performed worst in our tests. In the Aachen SFN scenario as well as the Limburg SFN, the model highly overestimated the received signal power. All error moments of the model were larger than those of the simpler propagation models, indicating a considerable discrepancy. A more thorough analysis of the data revealed that the Longley-Rice ITM model entirely failed to capture the signal deterioration in the center region caused by the building structure. Instead, emphasis was put by the model on the general terrain, identifying relative signal strength differences caused by the terrain profile correctly.

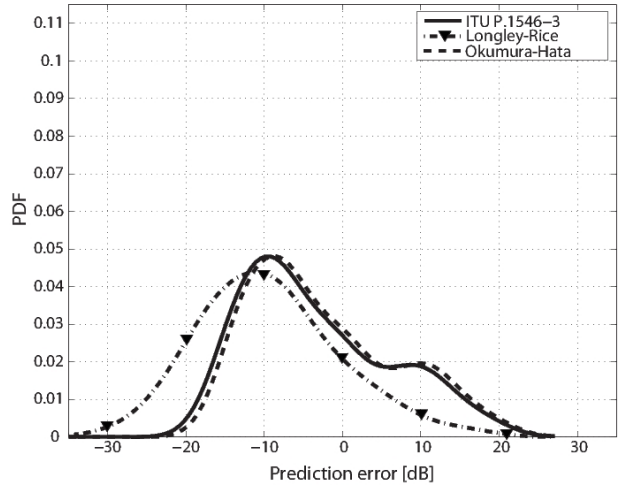

(a) Channel 24 of Limburg SFN

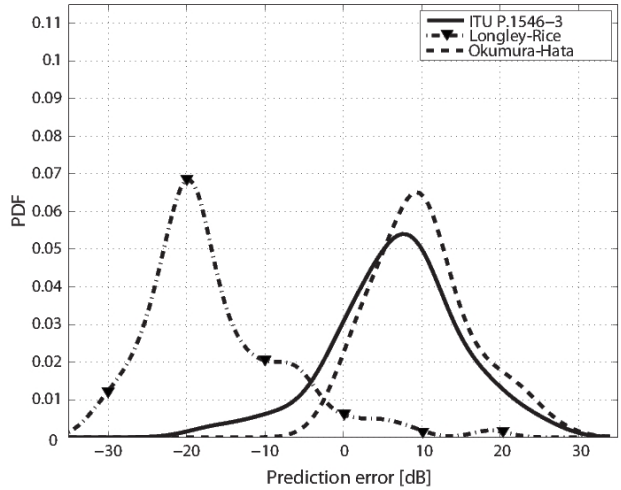

(b) Channel 26 of Aachen SFN

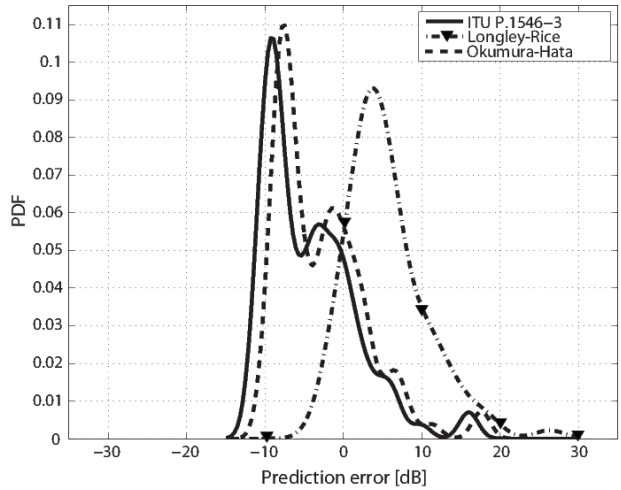

(c) Channel 29 of Düsseldorf SFN

Figure 4-5 Probability density functions of prediction error of empirical propagation models.

In order to study the nature of the errors of the propagation models, we depict in Figure 4-5 the probability density functions (PDF). We notice that in all scenarios, the ITU P.1546 and the Okumura-Hata model show similar shapes of their PDFs. This becomes particularly visible in Figure 4-5(b), where the two models are almost indistinguishable. Furthermore, in the Aachen scenario the error of the models is near symmetrical around

the mean error. We can conclude that the application of a simple offset would have improved the prediction capabilities significantly. Furthermore, we can observe that the Longley-Rice model is seemingly more accurate when mid-range towers are considered. While the model is incapable of providing good estimates in the near-range and the far-away case, the model shows at least similar error tendencies when applied to the Limburg SFN case. The terrain-unaware models perform poorly here, whereby the bimodal behaviour of the PDF points to a problem with the terrain differences (hills vs. city area). We were able to confirm this by further inspection of the regional error distributions.

4.1.1.3 Conclusions on verification of propagation models in Aachen

The QUASAR project has carried out an extensive measurement campaign covering an entire city and various configurations of multi-transmitter scenarios. Due to the particular relevance for secondary exploitation, we have focused on the TV bands for verification of propagation model capabilities.

We have found that empirical propagation models exhibit significant errors when used in complex urban scenarios. Standard models without terrain information such as the ITU P.1546-3 and the Okumura-Hata model tended to underestimate the received power in the proximity of the transmitter, while becoming more accurate when used for mid-range transmitter setups. The further away the transmitters were, the more the models were overestimating the received power. The Longley-Rice ITM, which we considered to be the most accurate one given the multitude of data it is using for estimating, failed to a large extend in the prediction process. We found that urban environments are too challenging for this model, as it has an emphasis on the general terrain, not on obstacles hindering direct LOS reception. All models were unable to estimate local shadowing correctly, resulting in high standard deviations of the error.

Another observation we made when analyzing the probability distributions of the error is, that the standard propagation models may be significantly improved if the mean error was known. This could, e.g., be achieved through small-scale measurement campaigns. We conclude that for secure and robust geolocation databases, drive tests would be a feasible mean of improving accuracy and thereby providing better protection.

4.1.2 **TV bands measurement campaign in Skopje, Macedonia**

For the purpose of simulation results validation, UKIM has performed measurements of TV band at the campus area in Skopje. The measurements were performed at 20 locations which form an ideal grid with step size of 100 meters. Such resolution ensures a relevant comparison of the resulting maps obtained through measurements and simulations. Figure 4-6 presents the measurement locations in Skopje. Simulation results were generated by the Radio Mobile Deluxe (see D5.3 Section 3.3 and [Latkoski2012]), which uses Longley-Rice IMT propagation model.

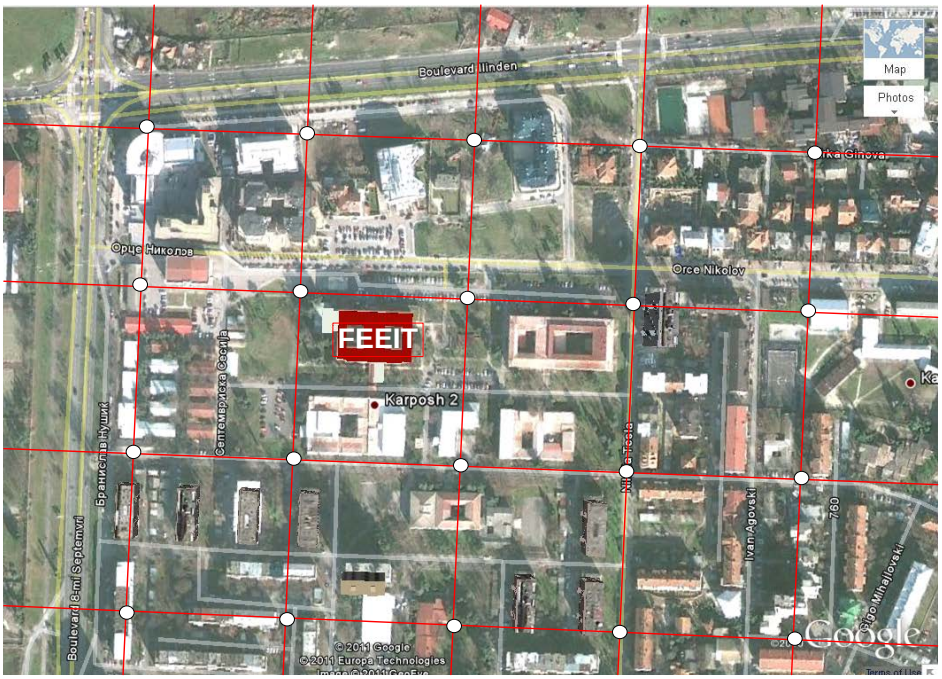

Figure 4-6 Measurement points near UKIM (FEEIT) campus

All measurements were performed outdoors, using horizontally polarized log-periodic antenna positioned directly towards the DTV transmitter location. Almost all measurement sites have LOS with the transmitter location (on the neighbouring Vodno hill). Also, this part of the city has small and medium sized buildings. Table 4-4 contains the configuration parameters of the spectrum analyzer.

Table 4-4 Measurement parameters

Parameter	Type / Value
Spectrum Analyzer	Anritsu Handheld analyzer
Resolution Bandwidth (RBW)	1 MHz
Input Attenuation	0 dB
Detector	RMS
Sweeptime (SWT)	5000 ms
Sweep Points (MP)	551
Number of sweeps	10

4.1.2.1 Results

Figure 4-7 presents the current state of the UHF band in Skopje. It contains three distinguishable digital television channels and many analogue broadcasting signals. This verifies the simulation results regarding low availability of secondary spectrum in Skopje reported in the case study for Macedonia in Section 2.5 of this deliverable.

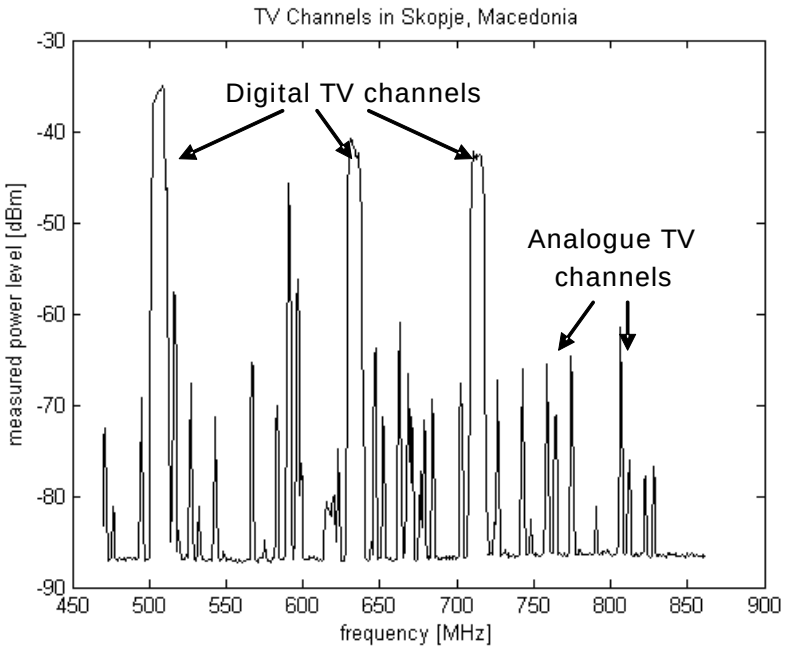

Figure 4-7 Measured spectrum in Skopje (UHF band)

For the purpose of simulation results accuracy validation, as well as propagation model validation, Figure 4-8 provides the absolute difference in the signal power obtained by measurements and simulation in each of the measurement points specified in Figure 4-6, and for each of the digital TV channels. The results reveal that the absolute difference is smaller than 10 dB. Obviously, the difference between the measured and simulated receiving TV signal power takes both positive and negative values. Additionally, at most of the measurement points the absolute difference is either positive or negative for all three digital channels at the same time. Only in few locations some of the channels have positive and some negative value for the absolute difference in the signal mean power (see Figure 4-8).

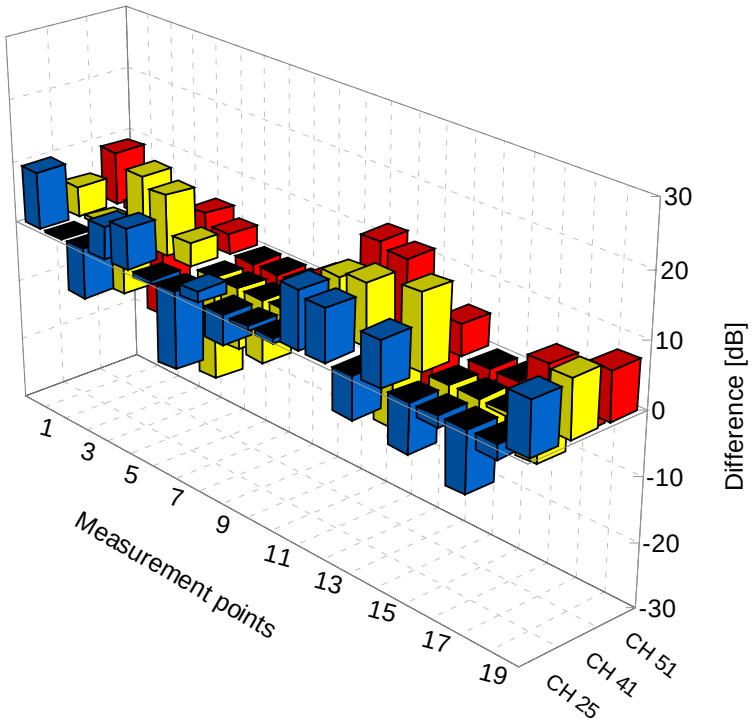

Figure 4-8 Absolute difference between measured and simulated TV signal mean power

4.1.2.2 Summary on measurements in Skopje

The measurements of TV band conducted in Skopje revealed that the current state of digital switchover process involves an existence of both digital and many analogue channels. This severely lowers the amount of secondary spectrum available in Skopje. On the other hand, the measurements proved the satisfactory accuracy of the used simulation framework in case of small and medium sized building surrounding areas and an existence of almost always LOS to the TV transmitter site. The absolute difference in power levels is within tolerable limits and manly is defined by the micro-topology of the measurement points, i.e. existence of buildings, trees, etc.

4.1.3 **TV bands measurement campaign in Gävle, Sweden: Adjacent channel interference from TV towers to WSDs measurement**

An extensive work has been done to model and measure the interference from white space devices (WSD) into the TV active channels such as the research done in [Gosh11]. However, the interference between WSD and TV channels is mutual and from WSD point of view this issue arises more when we come closer to the TV tower due to the high TV transmission power which leads to a considerable impact of out of band radiation (spectrum leakage) of TV OFDM signal and inter-modulation products. Therefore, filters requirements for WSDs are to be addressed carefully.

4.1.3.1 Purpose

The main aim of this measurement campaign is to evaluate the interference that TV signal would inject into the different adjacent channels at different distances. When SUs utilize TVWS, it is of a great importance to study the interference coming from the TV transmitter to the SUs. Adjacent channel interference is due to imperfections in the transmitter. Especially, non-linearities in the power amplifier will result in a leakage into

the adjacent channel. Moreover, the non-linearities will also cause intermodulation distortion.

4.1.3.2 Geographic area

Measurements are done indoor and outdoor at 6 different locations in Gävle, Sweden marked as L1-L6 as shown in **Error! Reference source not found.**.

Table 4-5 Measurement locations

Location	Description	GPS coordinates
L1	Next to the DVB antenna (outdoor only)	60.6400 N, 17.1322 E
L2	In a supermarket	60.6417 N, 17.1428 E
L3	In the City centre	60.6734 N, 17.1395 E
L4	A School	60.6689 N, 17.1514 E
L5	An apartment	60.6904 N, 17.1198 E
L6	At a University (HiG)	60.6692 N, 17.1210 E

Below map shows those locations of the measurements.

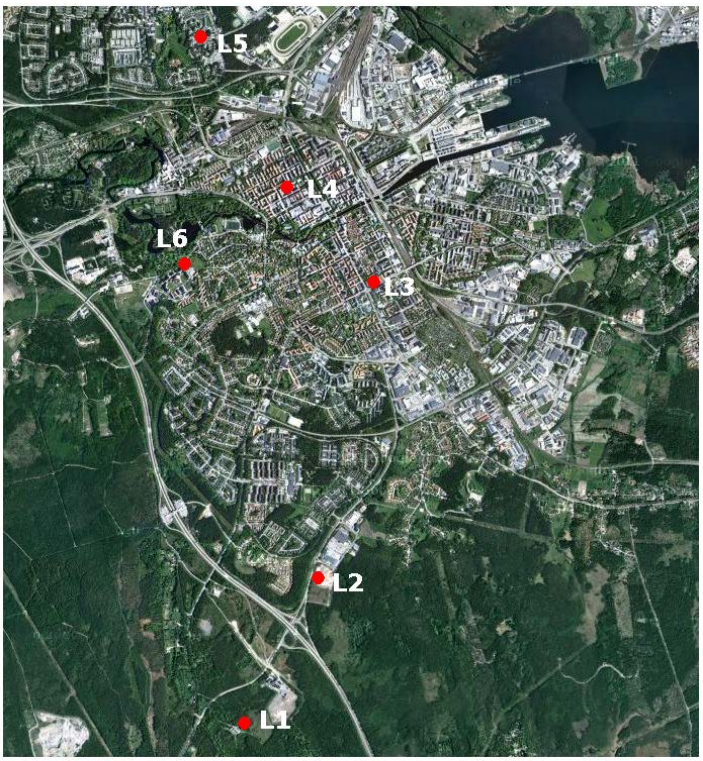

Figure 4-9 Locations for the measurements in Gävle

4.1.3.3 Frequency range

Six TV channels in UHF are used in Gävle, those are channels 24, 27, 30, 32, 46, 50 besides channel 9 in VHF which is out of the concern of this measurement. (The channels are at the frequencies: 206, 498, 522, 546, 562, 674, 706 MHz).

4.1.3.4 Measurement set-up and parameters

This section handles the measurements setup and parameters used to carry out the measurements campaign.

Figure 4-10 shows the measurement setup which consists of:

1. Antenna to capture the signals in UHF TV broadcasting band;
2. A spectrum analyzer to evaluate the signal captured by the antenna;
3. PC to control the spectrum analyzer and to save the measurements data.

Figure 4-10 Measurement setup.

In Table 4-6 are the parameters used during the measurements.

Table 4-6 Measurement parameters

Parameter	Type / Value
Spectrum Analyzer	Anritsu MT8221B BTSMaster
Antenna	R&S HE200 (RF Module 2)
Resolution Bandwidth (RBW)	300 KHz
Preamplifier	On
Input Attenuation	0 dB
Detector	RMS
Sweeptime (SWT)	840 ms
Sweep Points (MP)	551

4.1.3.5 Measurements procedure

For each location (both indoor and outdoor) four measurements have been carried out as follows:

1. The whole TV broadcasting band has been captured with the spectrum analyzer;
2. The power in channels 24-33 is measured;
3. Power in Channel 37 (randomly picked up) is measured and taken as a reference value for the noise floor all over the band since channel 37 is not an adjacent channel for one of the utilized channel by the TV transmitter.

Adjacent channel interference is measured on channel 29 and 31, i.e. the spectrum leakage from channel 30 to its first adjacent channels.

4.1.3.6 Results

4.1.3.6.1 Adjacent channel interference from the TV to the WSDs

In Figure 4-11 is a snapshot of the measured spectrum in channel 30 in location L2 (outdoor) where the noise floor and the channel boundaries are shown, accordingly the amount of injected interference from this channel to its adjacent channel can be observed.

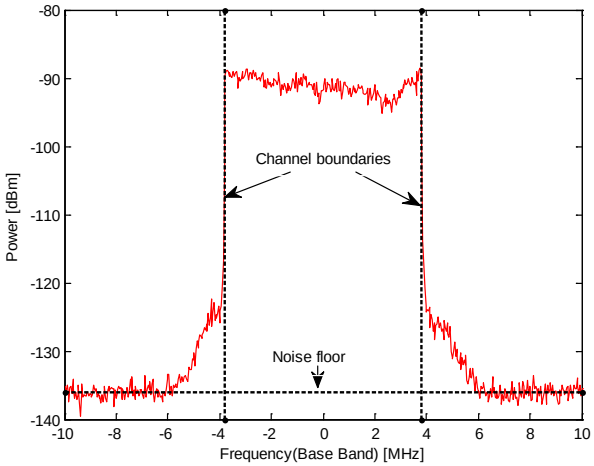

Figure 4-11 Spectrum on channel 30 in location L2 (outdoor)

For each location the channel with the strongest measured power is labeled as channel *N* and the received power on its two adjacent channels (N-1 and N+1) above the noise floor have been recorded as in Table 4-7.

Table 4-7 Power on Channels N-1 and N+1 above the noise floor for all measurement locations

Measurement Location	Power on Channel (N-1) above the noise floor [dB]	Power on Channel (N+1) above the noise floor [dB]
L1	11.27	11.8
L2 Outdoor	3.91	7.32
L2 Indoor	1.01	0.20
L3 Outdoor	5.90	6.38
L3 Indoor	0.45	0.12
L4 Outdoor	4.76	10.53
L4 Indoor	0.29	0.44
L5 Outdoor	2.10	1.32
L5 Indoor	0.68	0.71
L6 Outdoor	6.05	1.96
L6 Indoor	1.76	2.85

4.1.3.6.2 Intermodulation products interference in TVWS

Intermodulation products components for two transmission channels having frequencies f_1 and f_2 appears in frequency f_{IM}' as in

$$f_{IM} = |(i) f_2 + (j) f_1|,$$

where $i,j=0,\pm1,\pm2,\pm3,\ldots$ are integers, such as $|i|+|j|=m$, $m>1$. Even order intermodulation (that is m is even) will fall outside the frequency range of the DVB-T, moreover, when i an d j are both positive, will also fall outside the frequency range of the DVB-T. Odd order intermodulation will decrease as m increases. Highest impact will be from m=3, which is denoted IM3.

In the case of Gävle TV transmitter the IM3 products are in the following channels: 21, 22, 28, 33, 34, 36, 37, 40, 42, 54, 60, 62, 65, 68 (474, 482, 530, 570, 578, 594, 602, 626, 642, 738, 786, 802, 826, 850 MHz). Measured results for all outdoor locations are presented in Figure 4-12. Some of the IM3 channels are pointed out. In Table 4-8 the IM3 falls in channel 40 (626 MHz) for all measurement locations are presented.

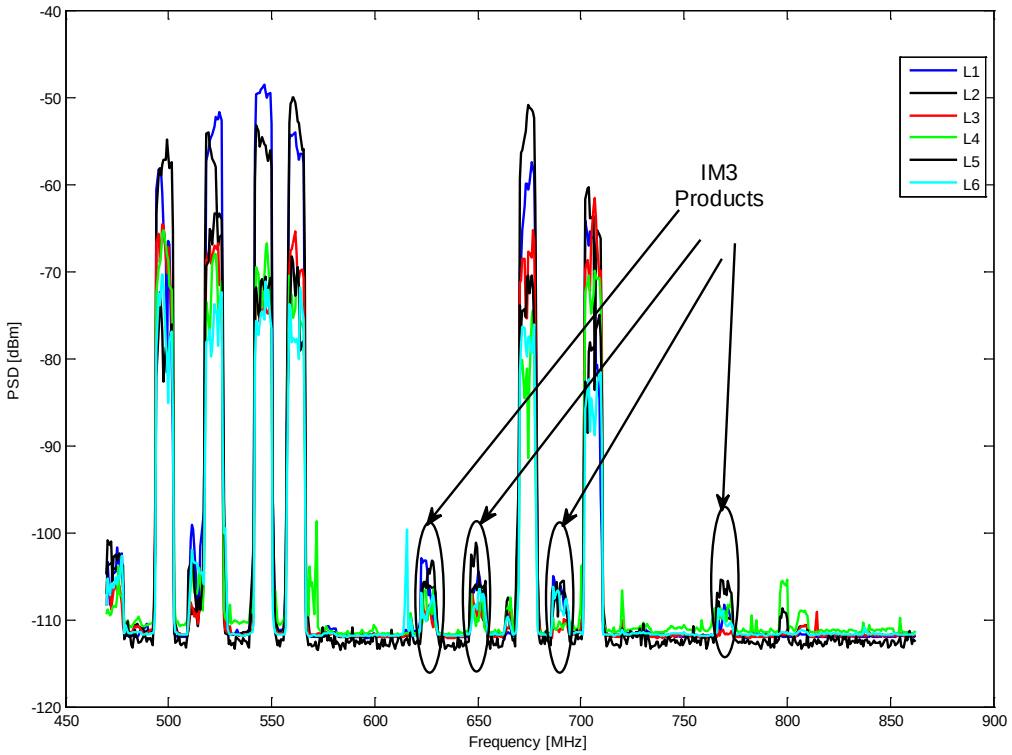

Figure 4-12 Spectrum occupancy for the whole DVB-T band in outdoor locations

Table 4-8 Measured IM3 product falls into channel 40

Measurement Location	Received power above the noise floor [dB]
L1	5.6
L2 Outdoor	6.2
L2 Indoor	0.3
L3 Outdoor	3.8
L3 Indoor	0.5
L4 Outdoor	4.1
L4 Indoor	0.2
L5 Outdoor	7.5
L5 Indoor	0.0
L6 Outdoor	4.7
L6 Indoor	0.3

4.1.3.7 Discussion on measurements in Gävle

From the results in Figure 4-12 and Table 4-8 it can be concluded that both the spectrum leakage and the Intermediation products impacts seriously for outdoor operation and they become more and more when the WSD operates closer to the TV transmitter, consequently, the WSDs occupying first adjacent channels for active TV channels or those channels where intermodulation products exist should compensate for this effects. Increasing WSD transmission power can overcome the problem; however, protecting the TV transmission from harmful interference is a severe consideration [Obregon10].

4.1.4 **Measurement of ATC (Air Traffic Control) radar in Skopje, Macedonia**

Measurements were conducted on 10.11.2011 near Alexander the Great Airport in Skopje, Macedonia. The ATC radar signals were measured with non-real time Anritsu handheld spectrum analyzer and a vertically polarized AOR-5000 discone antenna.

The ATC radar parameters are the following:

- site height level: 308 m above the MSL (mean sea level),
- rotations per minute: 15,
- Tx power: 19 kW,
- Assigned frequencies: 2775 MHz and 2825 MHz,
- Mechanical tilt: 3.5 degrees,
- Maximum range: 60 Nm ≈ 111 km.

The measurement points are located according to the following map.

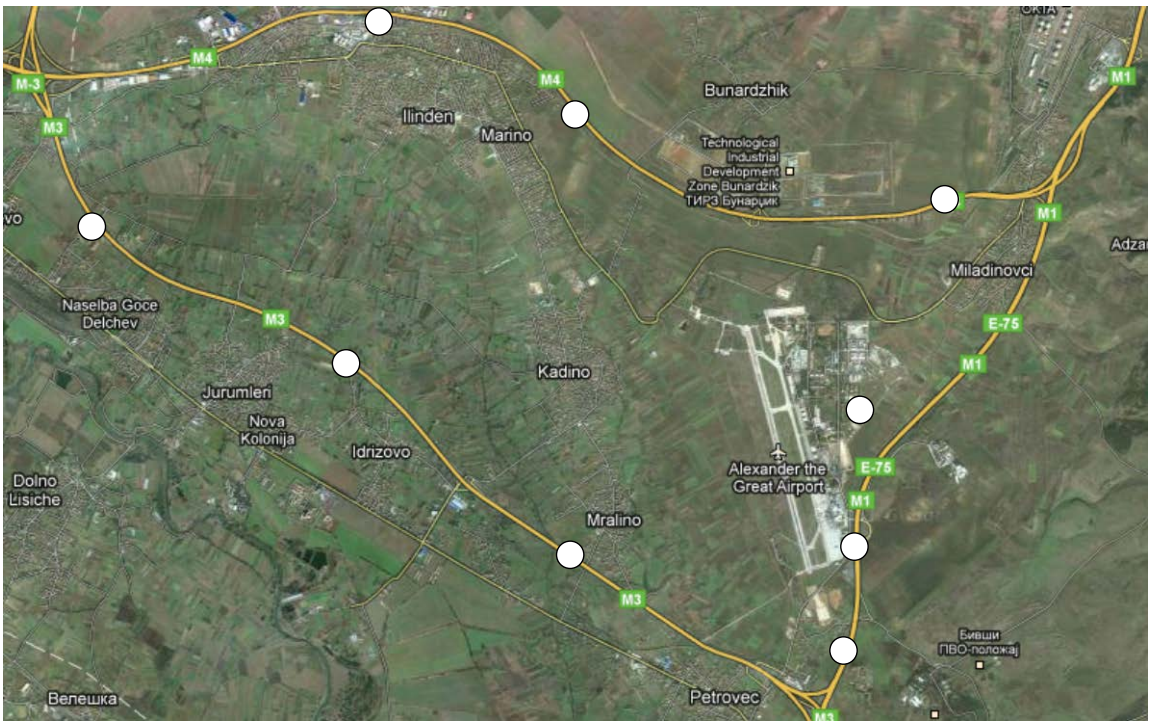

Figure 4-13 Measurement point near the ATC radar in Skopje

All measurement points are located on almost the same altitude (288m above the sea level), which is lower compared to the radar site.

The measured results present the receiving power level at each measurement point for both assigned radar frequencies, as presented in Figure 4-14.

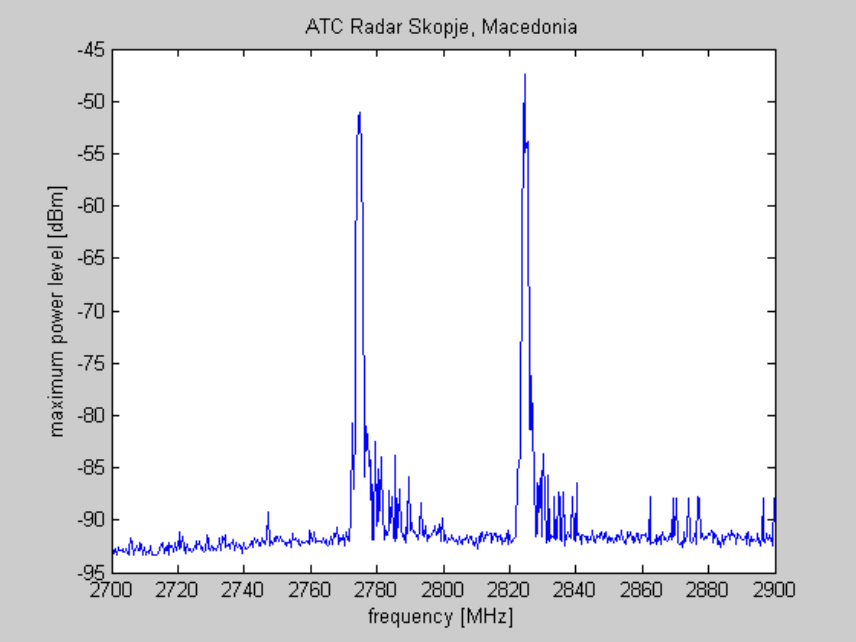

Figure 4-14 Measurement result from a single point (maximal power level in dBm)

As the measurement instrument could not provide real time measurements (each sweep takes approximately 1.24 seconds, and the radar antenna rotates 15 times per minute), the measured peaks in time domain are not regular (see Figure 4-15).

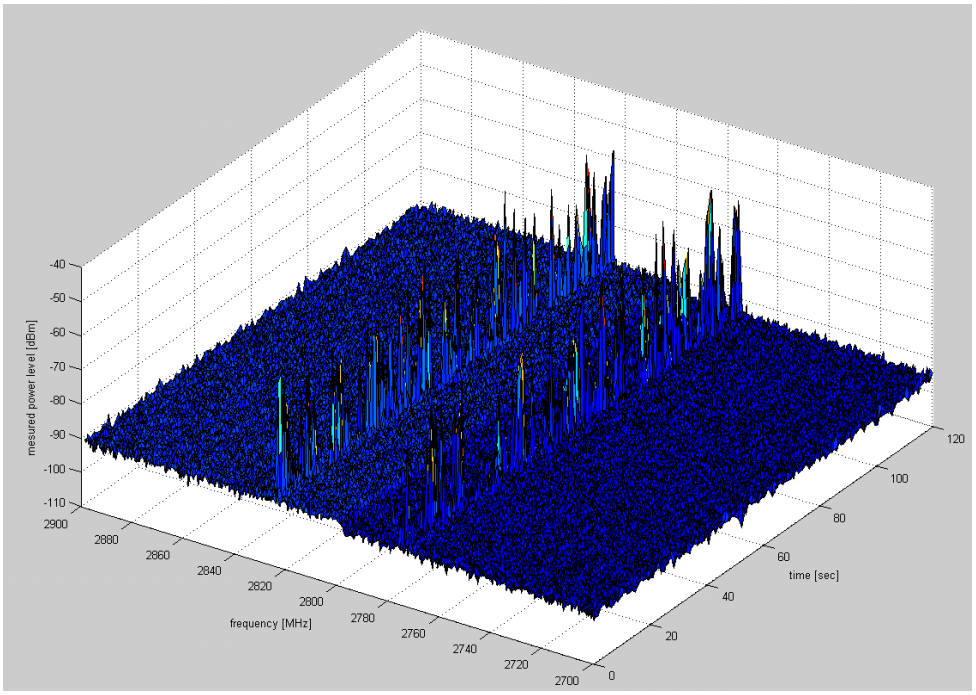

Figure 4-15 Measurement result from a single point (in both frequency and time domain)

Based on the measurements we provide empirical results which present the receiving power decay as a function of distance to the radar (Figure 4-16).

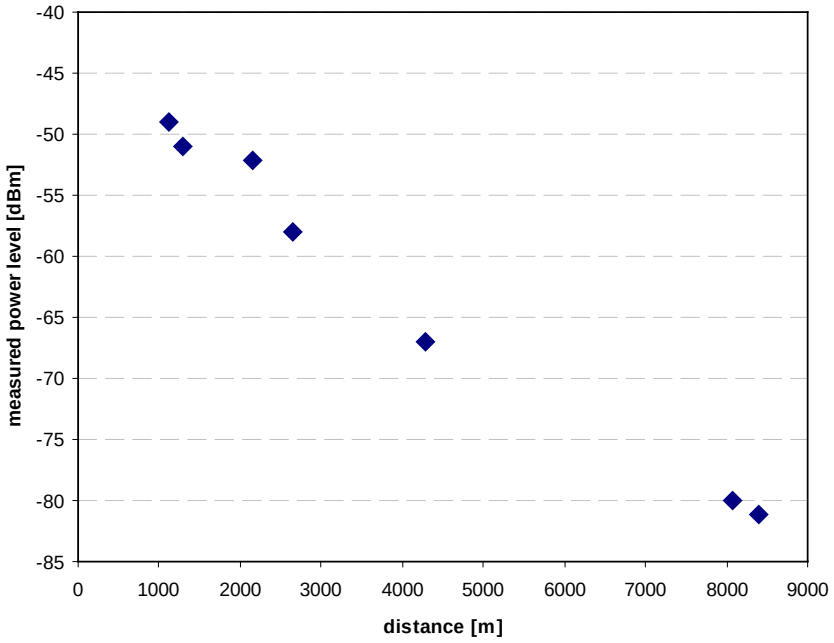

Figure 4-16 Measured power level as a function of distance

4.1.4.1 Summary on ATC measurements in Skopje

The radar band dedicated for air traffic control can be used for low power secondary communications. The measurements reveal that if the secondary users are located below the radar location site level and at a distance of at least 10 km from the radar site, the signals from the radar are almost undetectable. At such locations the ATC radar signals are below -90 dBm, which can be explained by the vertical tilt of the radar antenna of 3.5 degrees upwards, besides its high transmission power.

On the other hand, the measurements proved the accuracy of the Radio Mobile software in predicting the radar signals propagation. For more details on this topic please refer to [Karamacoski12] and [D53].

4.1.5 **Measurements on Radar spectrum occupancy in Sweden**

Tempo-spatial usage (radiation) pattern for radars is a fundamental factor in determination the spectrum opportunities in radar spectrum, hence, this measurements campaign in Sweden aims at assessing the radar signal strength as a function of the distance from the radar ground station antenna and the activity factor (time dependant signal strength). The measurements are performed in three different radar bands: Distance Measuring Equipment (DME), Air traffic control (ATC) radar, and weather radar.

4.1.5.1 Purpose

The main motivation for this measurement campaign is to assess the radar signal strength as a function of the distance from the radar ground station antenna and the activity factor (time dependant signal strength).

4.1.5.2 Geographic area

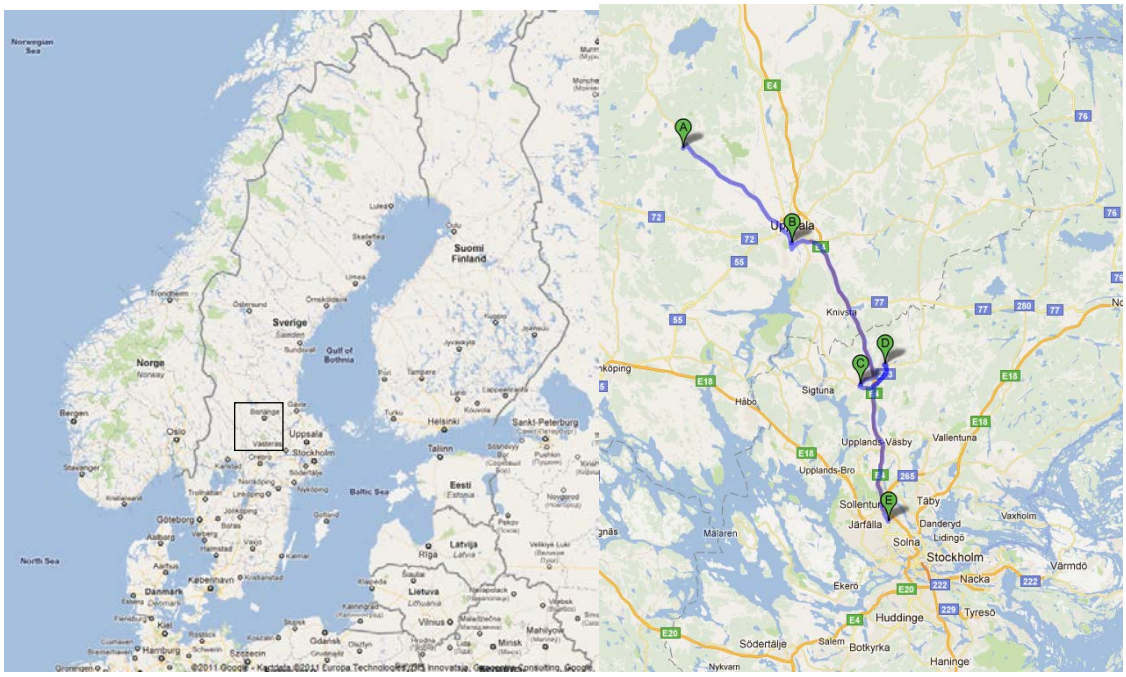

Figure 4-17 The region for radar measurements.

4.1.5.3 Radar locations

- DME in the surroundings of Arlanda airport (Position D)
- Air traffic control (ATC) radar north of Uppsala (Position A)
- Weather radar in the surroundings of Arlanda airport (Position D)

4.1.5.4 Measurement locations

Measurements were performed for all three radars in five outdoor locations.

- Near the ATC Radar (Position A) at a GPS coordinates of 59.8911 N, 17.3075 E
- In Uppsala (Position B) at a GPS coordinates of 59.8406 N, 17.6456 E
- In Marsta (Position C) at a GPS coordinates of 59.6217 N, 17.8589 E
- Arlanda Airport (Position D) at a GPS coordinates of 59.6389 N, 17.9031 E
- Kista (Position E) at a GPS coordinates of 59.4050 N, 17.9450 E
-

In addition, two more measurements were done:

- Indoor measurements in Kista for the DME. Due to weak signals in the outdoor measurements, other radar bands were omitted.
- Complementary measurement in the ATC band a few kilometers north of the ATC antenna at a GPS coordinates of 59.9994 N, 17.3044 E

4.1.5.5 Radar parameters

The measurements have been done in three DME, ATC and weather radar having the parameters as in Table 4-9, Table 4-10, an Table 4-11. In position D there are five DME stations having different IDs, those are: ARL, ANE, ANW, ASW and ASE.

Table 4-9 DME stations parameters

ID	ARL	ANE	ANW	ASW	ASE
Interrogation freq (from airplane)	1131 MHz	1104MHz	1081 MHz	1108 MHz	
Reply Freq. (from ground)	1194 MHz	1167 MHz	1144 MHz	1045 MHz	1052 MHz
Antenna Location	59 39 12,4N 17 54 51,9E	59 41 38,3N 18 03 35,6E	59 42 47,8N 17 51 09,2E	59 35 15,7N 17 49 10,9E	59 38 13,9N 17 57 26,5E
Transmission Power	1000 W	100	100	100	100
Pulse width	12 μs	12 μs	30 μs	30 μs	30 μs

Table 4-10 Air traffic control radar parameters

Frequency and hopping pattern	F_1 2764.05 MHz, F_2 2804.97 MHz, F_3 2845 MHz. Jumps from sweep to sweep between F_1, F_2, F_3
Location	Coordinates: X: 6652279,9, Y: 158391,2
Transmission power	22 kW
Vertival Antenna rotation pattern	12 rpm
Horizontal Antenna rotation pattern	Fixed, with a 2.4° lobe
Pulse width	The radar transmits two different pulse lengths 10μS and 100μS

Figure 4-18 shows the ATC radar spectrum and the three hopping frequencies.

Figure 4-18 ATC Radar spectrum

Table 4-11 Weather radar parameters

Frequency	5.605 GHz
Location	59.655N, 17.949 E

The weather radar is rotating both horizontally and vertically and this rotation pattern will be extracted from the measurements.

4.1.5.6 Measurement setup

The measurement setup consists of:

- Directional antenna working on DME spectrum and Omni directional one working on air traffic control radar spectrum and weather radar band.
- Rohde & Schwarz FSVR real time spectrum analyzer.
- PC to control the analyzer and capture the measurements data
-

The figure below depicts the measurement setup.

Figure 4-19 Measurement setup

4.1.5.7 Results and discussion

This Section contains the measurements results obtained for DME, ATC and weather radar in Sweden.

4.1.5.7.1 DME

Figure 4-20 and Figure 4-21 show the DME inter-negotiation signal sent by the airplane and the reply signal from the ground station respectively in Marsta (position C) for ARL DME. Both signals are captured over a 30 minuets. From Figure 4-20 and Figure 4-21 it can be seen that both inter-negotiation and reply signals do not have a specific tempo-spatial usage pattern in frequency domain. Having unspecific usage pattern for DME signals can be explained by the nature of DME operation as the airplanes pass randomly over a specific location and the ground station stays quite unless there is an inter-negotiation from an airplane where the replay signal starts to be sent. Accordingly, it can be concluded that a tempo-spatial database based spectrum opportunities cannot be built for a DME system. Moreover, the inter-negotiation signal strength cannot be predicted over any location since airplanes move everywhere, however, ground stations

are stationary and therefore the replay signal is distance dependant. Figure 4-22 verifies having inter-negotiation signal everywhere as it shows the spectrum of inter-negotiation band over time in Uppsala (position B) and it can be seen that it is very similar to the one obtained in Marsta (position C). Never the less, the replay signal measured in Uppsala (position B) depicted in Figure 4-23 is 'noise only' signal as the measurement position is far from the ground station. To investigate the DME signal strength in indoor environments, 40 MHz spectrum of DME spectrum is measured as in Figure 4-24 where it can be noticed that the received signal is still strong and having random pattern.

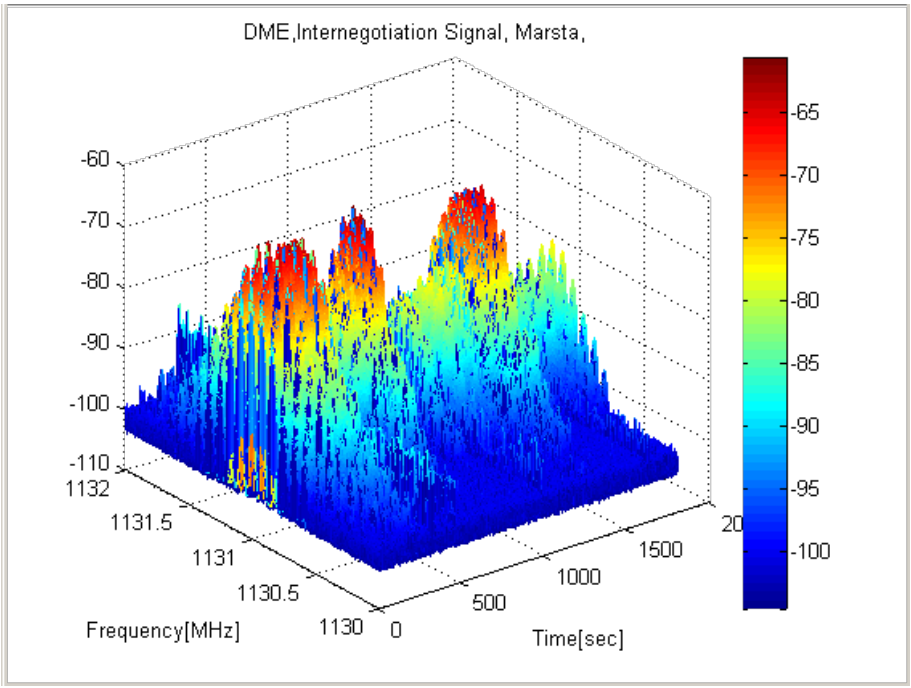

Figure 4-20 DME Inter-negotiation signal captured in Marsta (location C) for ARL DME

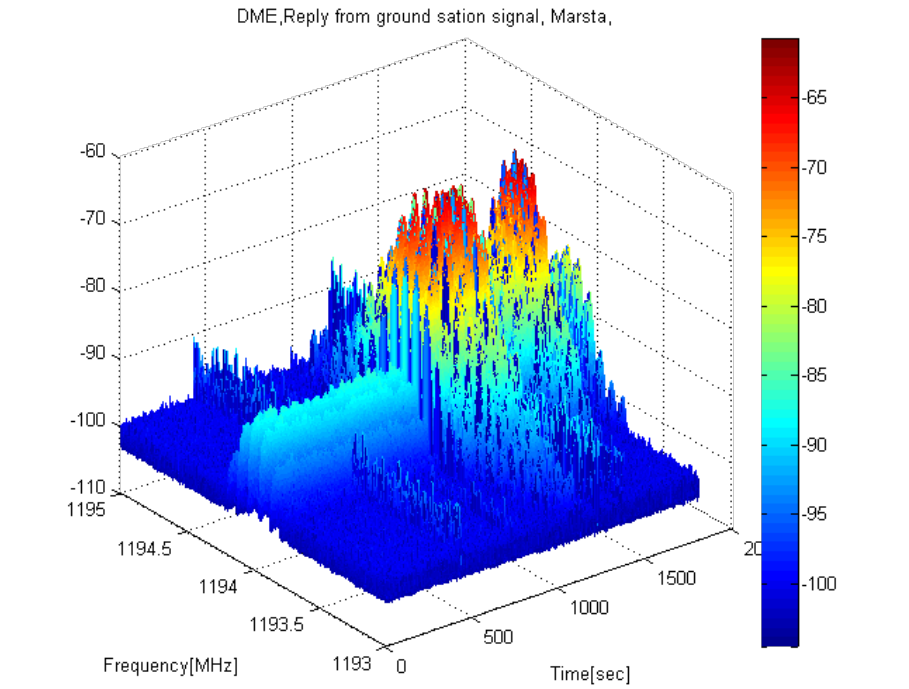

Figure 4-21 DME reply signal captured in Marsta (location C) for ARL DME

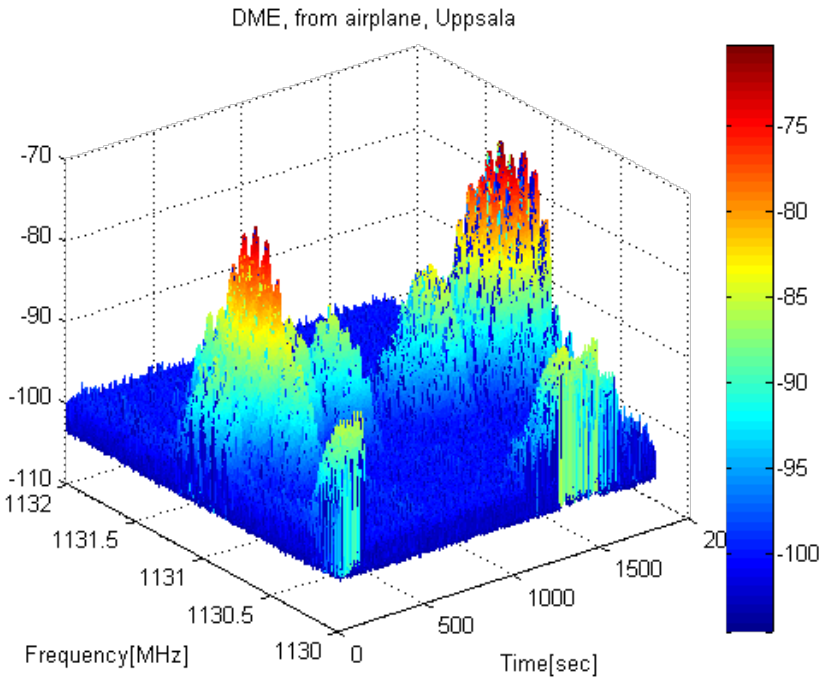

Figure 4-22 DME Inter-negotiation signal captured in Uppsala (location B) for ARL DME

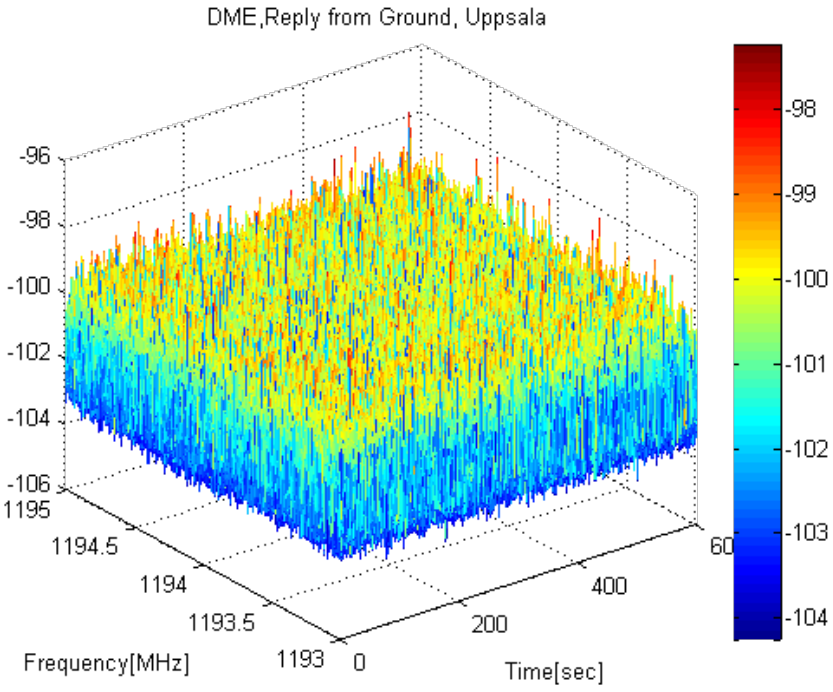

Figure 4-23 DME reply signal captured in Uppsala (location B) for ARL DME

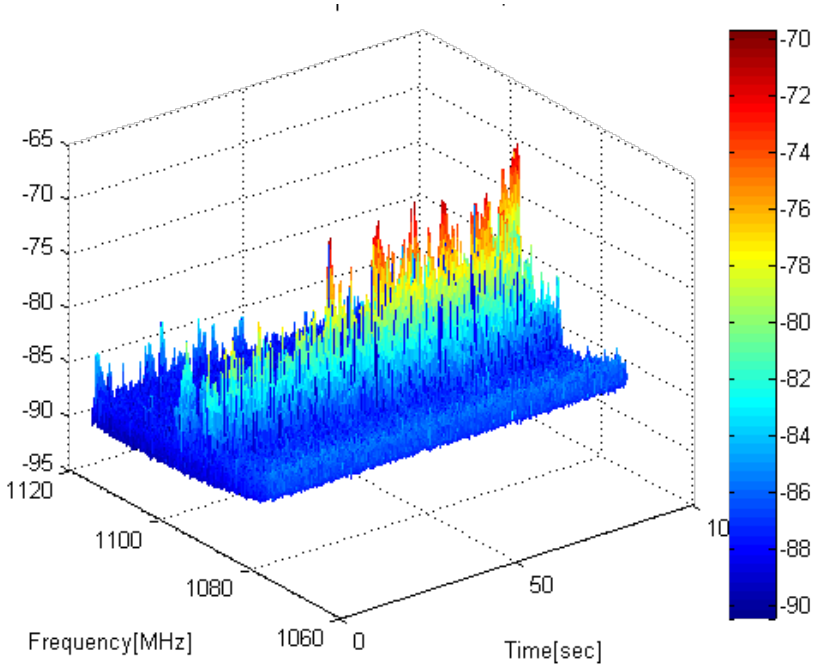

Figure 4-24 40 MHz of the DME spectrum captured in indoor location in Kista (position E)

4.1.5.7.2 ATC radar

For ATC radar the measurements results very close to the radar (i.e ≈ 100 meters away from the radar- position A) are shown in Figure 4-25 where it can be observed that the signal is very strong all the time during the three minutes of measurements, hence, utilizing the ATCR is not doable in such close distances.

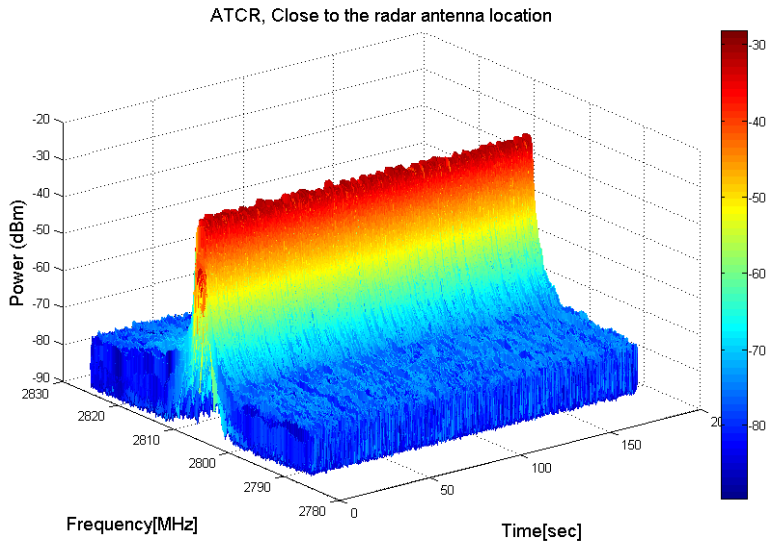

Figure 4-25 Received signal around ATCR spectrum very close to the radar

Figure 4-26 presents the measured spectrum of the ATC radar signal at allocation aparted by ≈ 3 kilometres from the radar antenna. The signal peaks are extensively spread over time due to the short full rotation period for ATC radar antenna which is 5 seconds.

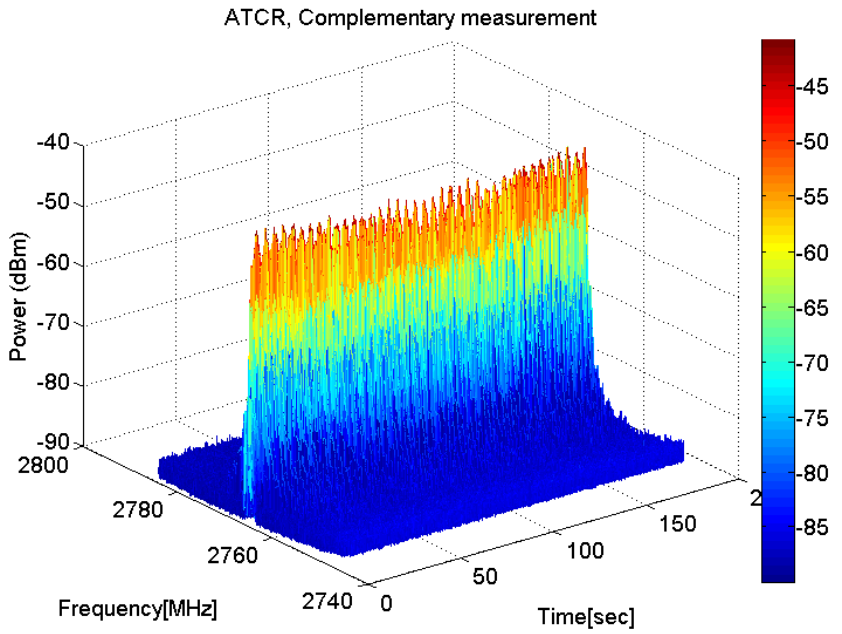

Figure 4-26 Received signal around ATCR spectrum around 3 kilometers far from the radar

In Marsta (location C) the measured signal is illustrated in Figure 4-27 which looks like 'noise only signal' where the ATC radar spectrum seems to be 'free of use'.

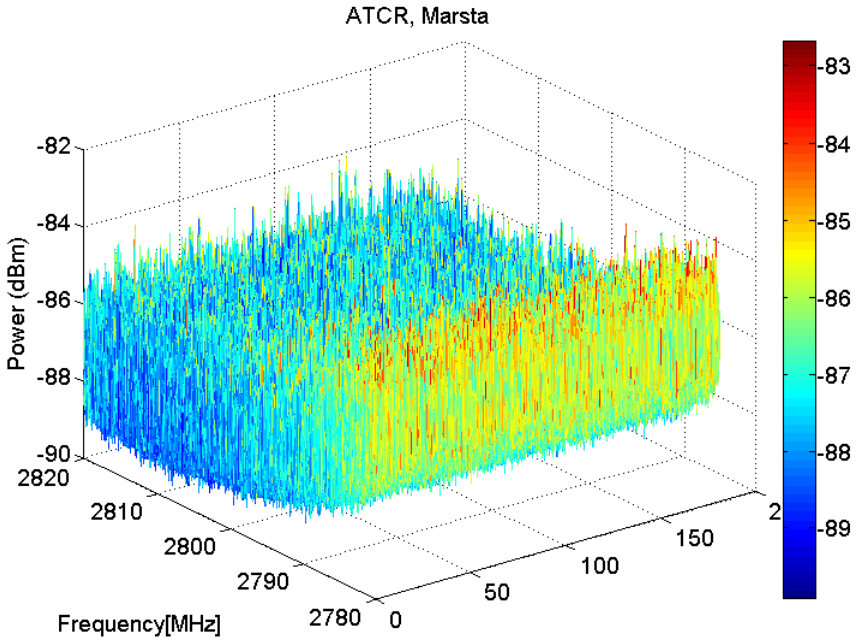

Figure 4-27 Received signal around ATCR spectrum in Marsta (position C)

4.1.5.7.3 Weather radar

The weather radar spectrum in Arlanda airport (position D) is shown in Figure 4-28 where two big peaks can be noticed and smaller ones exists also. The big peaks corresponds to the points in time where the rotating weather radar antenna faces the measurements antenna both horizontally and vertically while the small peaks are captured when the radar antenna faces the receiver antenna vertically and points

towards another direction horizontally. The time period where the rotating radar antenna points to a specific point both horizontally and vertically is found to be ≈ 5 minutes.

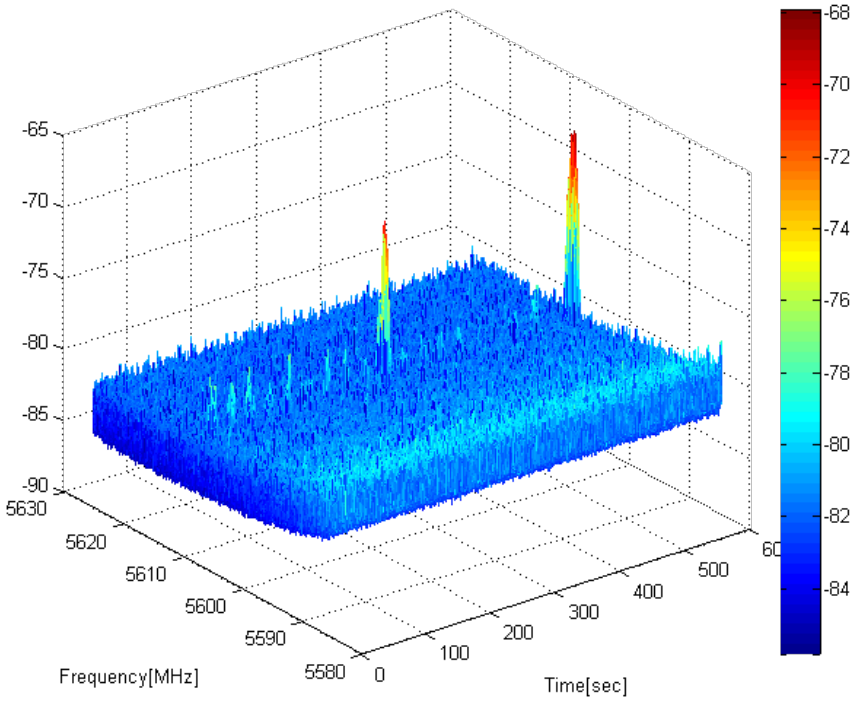

Figure 4-28 Received signal in weather radar spectrum in Arlanda airport (position D)

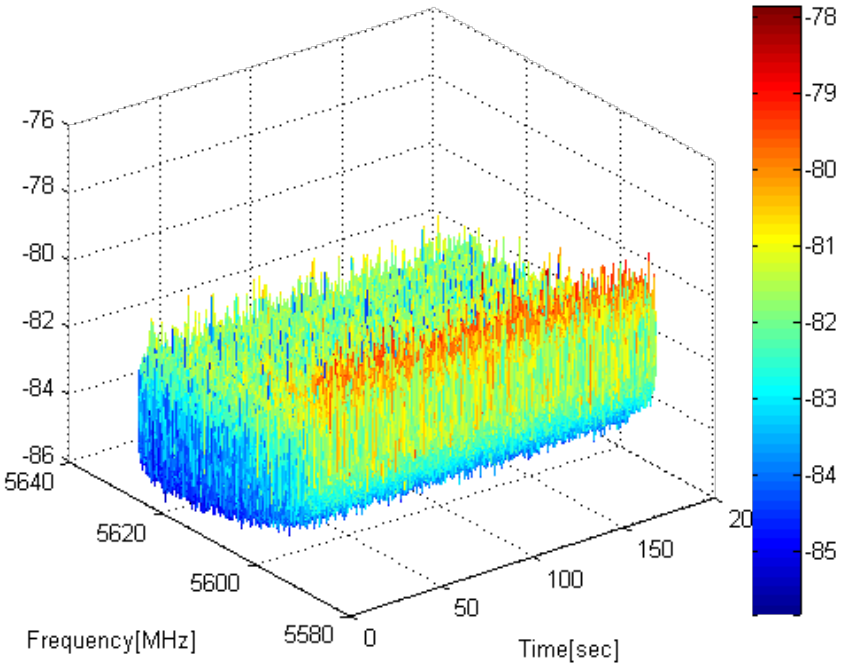

Figure 4-29 Received signal in weather radar spectrum in Uppsala (position B)

Figure 4-29 shows the received signal for the weather radar in Uppsala (position B) which seems to be 'noise only signal' due to the separation distance between the radar and the measurement location.

It can be concluded that the spectrum opportunities offered in the weather radar band are higher than the ones in DME and ATC radar bands due to the high period of rotation for weather radars which leads to the ability of utilizing it for long periods even close to the radar antenna.

4.2 **Co-existence measurements**

Previous studies [Beek11][Randhawa06][Randhawa07][Obregon10][Stuber09] have quantitatively and qualitatively analyzed the accessible spectrum for secondary use for different geographical areas and studied the interference constraints the primary system poses on such secondary systems to allow the undistracted operation. It is likely that secondary users or WSD will identify and use TV White Spaces (TVWS) without causing any unfavourable impact on the primary user. In order to ensure co-existence of the primary and secondary systems, detailed studies on the effects of white space devices on the DVB-T reception are needed.

We study the co-existence of a WSD and a DVB-T receiver through measurements and analyze the effects on the performance of the DVB-T reception in the presence of WSD interference. Our measurements are diverse covering the effects of different locations, power and frequency. We consider different power levels of WSD interference and different RF attenuations of the TV signal at the receiver. The location analysis covers the antenna discrimination by testing two types of receiving antennas and two types of antenna polarizations at the transmitting WSD. The filter receiver capabilities are tested in the frequency dimension against Co-Channel Interference (CCI) and the Adjacent Channel Interference (ACI). One of the most important parameters for evaluation of the performance of a DVB-T system is the carrier-to-noise (C/N) ratio required for good reception. The ETSI DVB-T standard [ETSI04] provides simulated minimum C/N values required for quasi-error-free (QEF) reception. Outdoor measurements [Angueira04] and laboratory tests [Schramm04] have showed that the proposed thresholds are in fact too conservative and therefore should be adjusted. These studies were confined either to the outdoor case or to an indoor controlled environment with laboratory generated DVB-T signals and using a channel emulator.

4.2.1 **Measurement setup**

In order to obtain the different performance parameters of the DVB-T received signal, an indoor measurement campaign was accomplished by implementing and analyzing different set-up configurations.

The measurements were carried out in a typical office environment in Aachen, Germany. In the Aachen region there is influence from several Single Frequency Networks (SFNs). In our measurements we were able to demodulate channels from SFNs in the Netherlands and Belgium, but as expected the Aachen SFN was the one with the highest influence. This SFN has two towers located in direction South-West and East of the office building respectively. Further information about the different configuration parameters and locations of the SFNs is publicly available by the German regulator [BNetzA12].

The general set-up for measurements is shown in Figure 4-30. An Agilent Technologies E4438C ESG vector signal generator serves as a WSD source interferer.

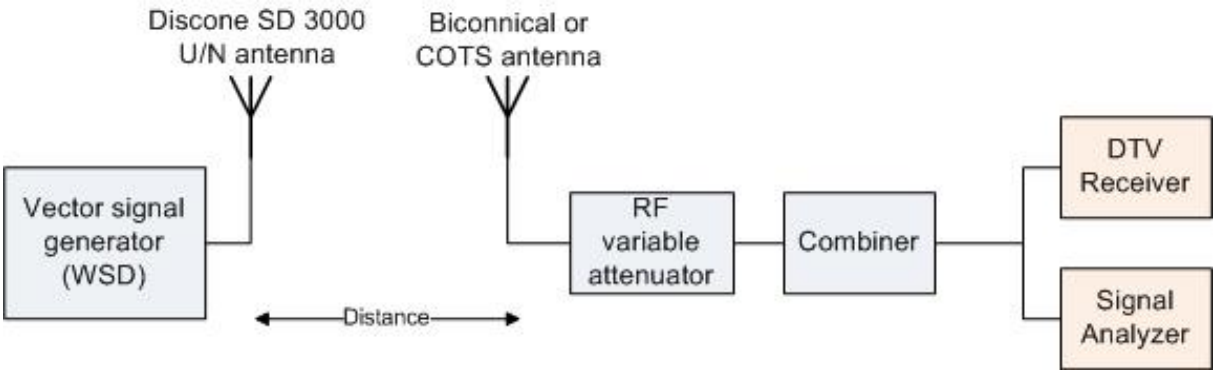

Figure 4-30 General measurement setup

The transmitting antenna is a Discone SD 3000 U/N unidirectional wideband antenna with good transmission capabilities in the TV channel band. This antenna can be mechanically adjusted to change its polarization properties. The transmitting antenna and the signal generator are illustrated in Figure 4-31. The main configuration parameters of the interference signal are included in Table 4-12.

Table 4-12 General configuration of the interfering signal

Parameter	Value
Signal Bandwidth (W)	8 MHz
Modulation Scheme	simple 64 Multitone or QPSK signals
Maximum output power	20dBm

Figure 4-31 Transmitting antenna and signal generator

At the receiver side either a commercial off-the-shelf (COTS) TV antenna or a biconical antenna were used. The COTS antenna is a very cheap UHF/VHF/FM DVB-T chamber set-top antenna with high directivity, and the biconical antenna is the Aaronia BicoLOG 30100, which is a high precision EMC biconical antenna (radial isotropic) that shows almost constant 1dBi (typ.) gain within the frequency range of the DVB-T channels. This suitable antenna is specified for the frequency range between 30 MHz and 1GHz with gains between -39Bi to 1dBi (typ.). The two antennas are depicted in Figure 3.

Figure 4-32 Receiving antennas

The receiving antennas are connected trough a variable RF step attenuator to a Rohde&Schwarz ETL TV analyzer with DVB-T/H option firmware installed (see Figure 4). This is a high precision, universal multi-standard platform for the analysis of TV signals through real-time demodulation. It combines the functionality of a TV and FM (radio) signal analyser, a video and MPEG TS analyser and a spectrum analyser in a single instrument. It also allows the implementation of different TV standards according to the firmware option used.

Figure 4-33 R&S TV Analyzer

4.2.2 **DVB-T Signal spatial variability**

Initially, five different indoor locations were selected. The number and type of channels correctly demodulated highly differed depending on the location of the DVB-T receiver and type of receiving antenna used.

In Figure 4-34, we include the received power level for each of the 49 channels. In this case, the whole setup was placed in a room with a single window facing outdoors to the 220° SW (location 1). When the COTS antenna was used; its orientation was towards the direction of this window and we measured each channel for 15 minutes.

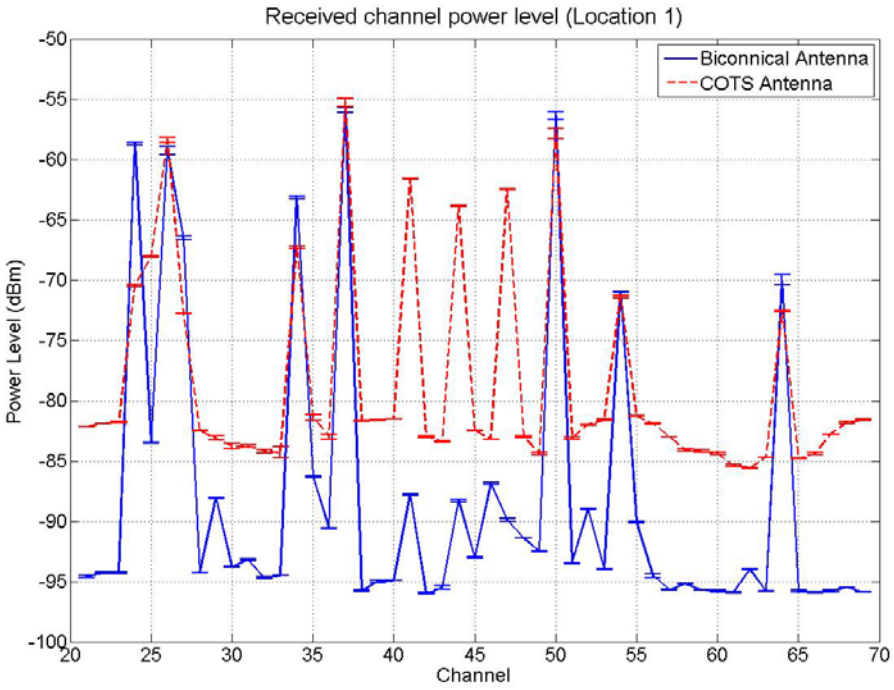

Figure 4-34 Received channel power level at location 1

In location 1, with the biconical antenna the TV analyzer was able to demodulate eight channels (24, 26, 27, 34, 37, 50, 54, and 64). These are the three channels with transmitters in Aachen (26, 37, and 50) and the rest are five channels from transmitters in Heerlen (Netherlands). With the COTS antenna also eight channels were correctly demodulated (25, 26, 34, 34, 41, 44, 47, and 50) this includes the three Aachen channels plus four channels from Genk (Belgium) and channel 34 from Heerlen.

In Figure 4-35 and Figure 4-36, we present the received channel power levels achieved with two different type of receiving antennas without any additional interference at two different locations. Location 2 is in a room with the window facing 125° SE and location 3 is in another room but now facing 345° NW.

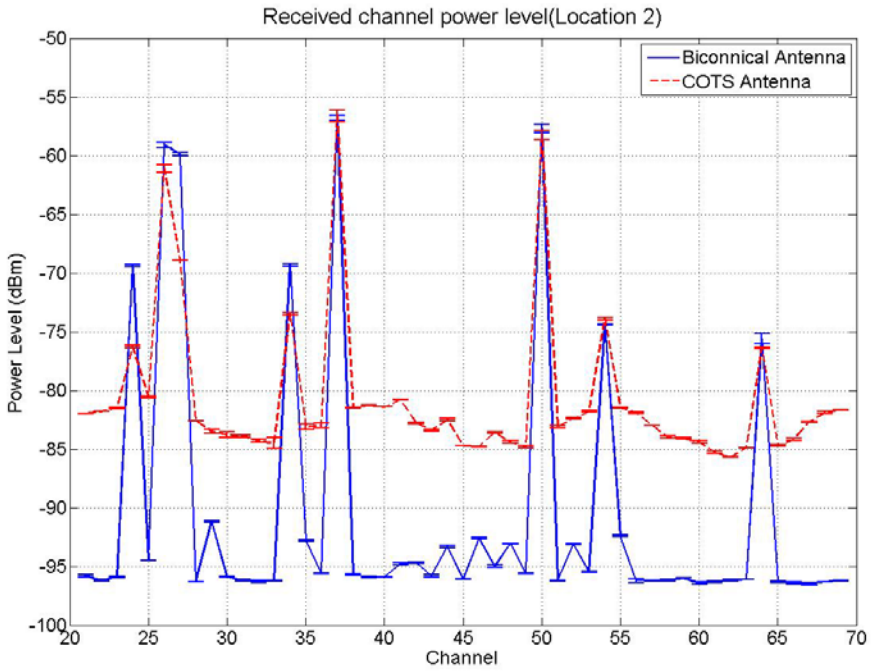

Figure 4-35 Received channel power level at location 2

When we moved the TV receiver to these other two locations and when using the biconical antenna, the same eight channels as above were demodulated. For the case of the COTS antenna fewer channels were demodulated correctly. The common channels that were always demodulated with this antenna are only the three Aachen channels.

We can clearly see how the reception highly depends on the placement of the TV receiver and the orientation of the room's window. This effect is even higher for the COTS antenna because of its directivity characteristics. We can also see the better performance achieved with the biconical antenna in terms of noise floor.

When comparing the reception quality at the three different locations in the ground floor, we found that the best results were achieved in Location 1. In this room we found not only the highest received power levels, but also the other performance parameters were better.

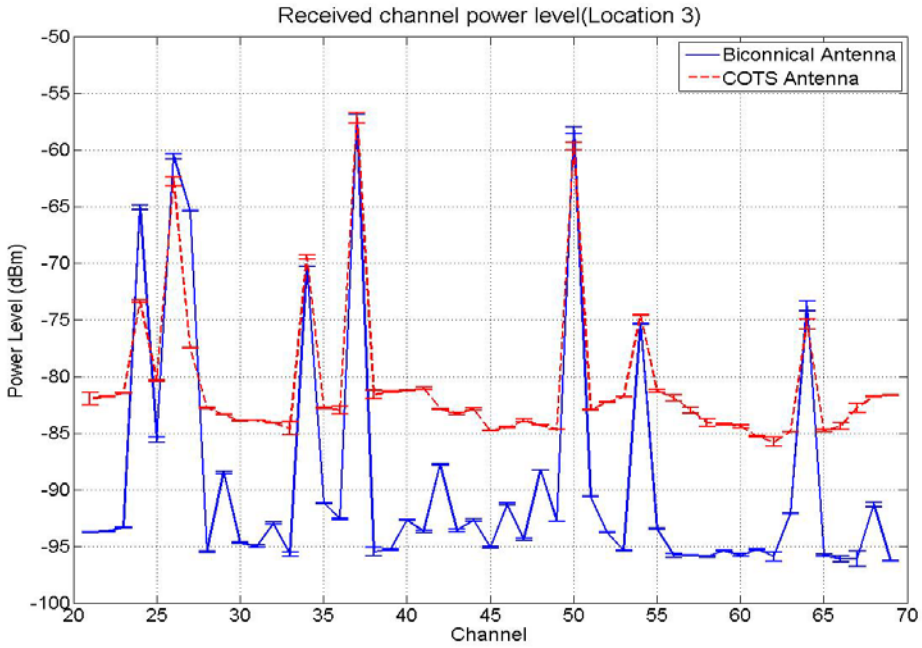

Figure 4-36 Received channel power level at location 3

When we compare the received power level of the channels when using the biconical antenna we see that the power level stays within a 5dB range. When the COTS antenna is used we obtained higher differences. We can say that in terms of power level we have very stable results. This is clear from the very small error bars obtained in all the plots.

As mentioned above the only 3 channels that were correctly demodulated in all measurement locations and with both type of antennas were the Aachen channels, therefore we present some performance parameter for these channels without any induced interference. In this case, we measured each channels for 20 minutes. In Figure 4-37 we compare the Modulation error rate (MER) for these three channels. The MER is a measure of the signal-to-noise ratio (SNR) in a digitally modulated signal. The rms value of the MER is calculated from the average power of the signal and for N number of symbols is defined as:

$$MER(dB) = -10\log_{10}\frac{\frac{1}{N}\sum_{j=0}^{N-1}\left|meas(j)-ref(j)\right|^2}{E\left\{\left|ref(j)^2\right|\right\}}$$

Where, *meas(j)* is the j-th symbol received and *ref(j)* is the j-th symbol of the ideal transmitted signal. For MER calculation only payload carries are used, and we can clearly see how the best MER is always obtained for channel 37, followed by channel 50 and the worst results are for channel 26. The MERs are obtained by finding the relationship between the rms value of the payload data and the effective error without reduction, contrary to the SNR measurements where the reduced effective error is used. As expected the COTS antenna had worse performance, in general we found differences between 2 and 4 dB in favour of the biconical antenna.

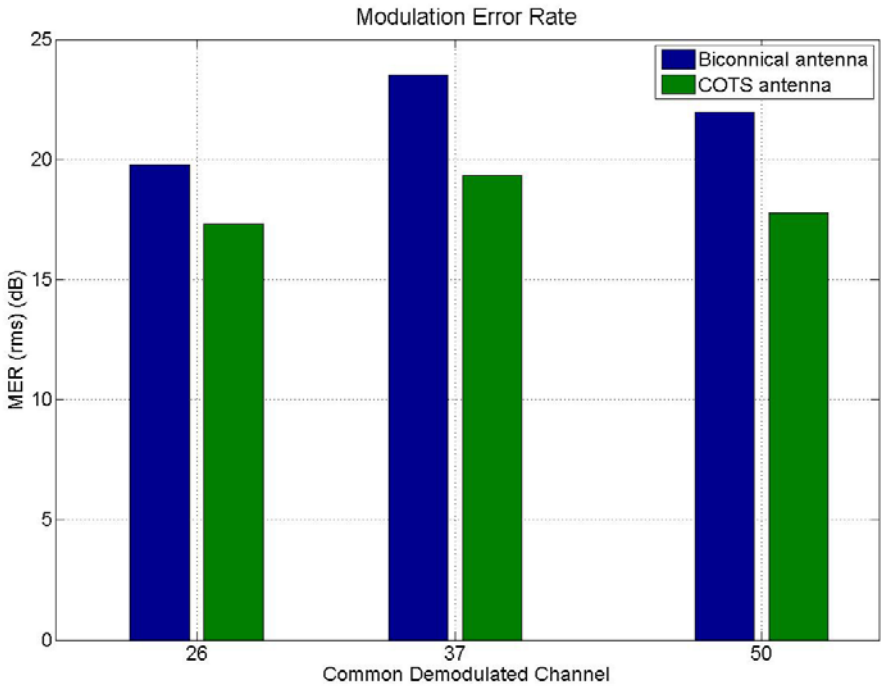

Figure 4-37 MER for the common demodulated channels

In Figure 4-38 we show the measured Error vector magnitude (EVM). This is related to the MER and ρ, where ρ is the correlation between the two signals. The error vector is the difference between actual received symbols and ideal transmitted symbols. The EVM is the average power of the error vector, normalized to signal power. Thus, EVM and MER are proportional and the former is calculated as:

$$EVM(\%) = \sqrt{\frac{\frac{1}{N}\sum_{j=0}^{N-1}\left|meas(j) - ref(j)\right|^2}{\max_j \left|ref(j)^2\right|}} * 100$$

As expected opposite values with respect to the MER are obtained. Thus, the higher percentage values are measured for channel 26 followed by channel 50 and finally 37. The differences between the COTS and biconical values lay in the range of 1.5% to 2.3%.

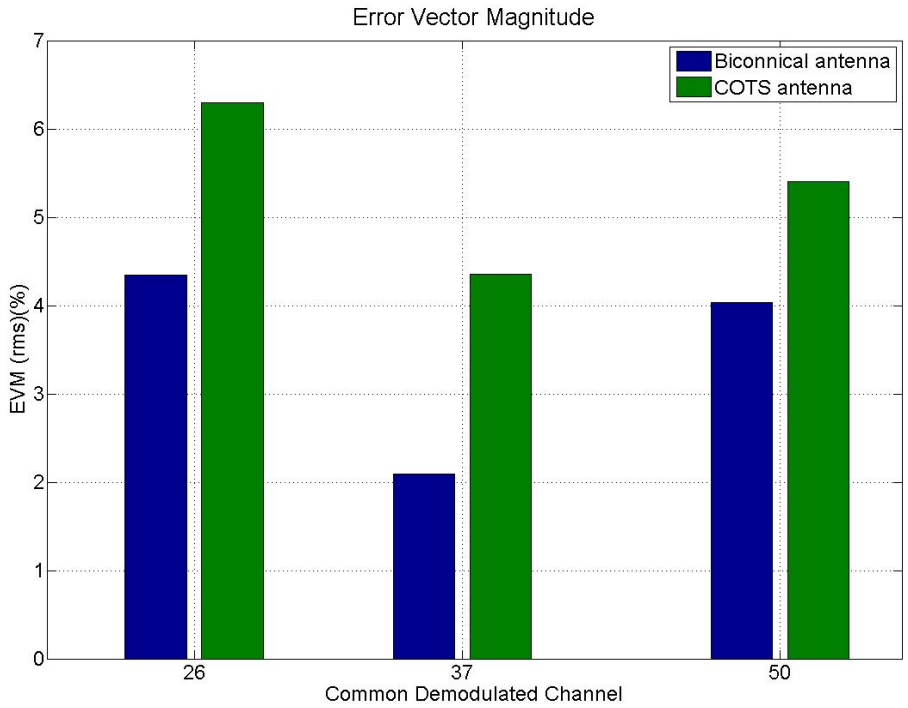

Figure 4-38 EVM for the common demodulated channels

In Figure 4-40, we show the comparison of the different type of BERs, The three points of measurement after demodulation are included. BER measurement is a general objective test for digital communication systems. In the receiver link of video broadcast systems, BER is defined at several points as shown in Figure 4-39. There are three types of BER tests in the performance evaluation of digital video receivers:

- BER before Viterbi: Bit error ratio before Viterbi decoder in the Forward Error Correction (FEC) (inner) decoder, implemented at 1 in Figure 4-39.
- BER before Reed-Solomon (RS): Bit error ratio before Reed Solomon (outer) decoder, implemented at 2 in Figure 4-39.
- BER after RS (outer) decoder: it is implemented at 3 in Figure 4-39; If an MPEG2 packet is erroneous at least 9 bits are erroneous in the corresponding MPEG2 packet. Therefore, this value is derived from the packet error ratio as:

$$BER\_after\_RS = PER * \frac{9}{8*188} = \frac{PER}{167{,}111}$$

In Figure 4-40, we show the BER measurement for the three Aachen channels under normal operation by performing a sliding BER calculation. The results illustrated were achieved once the test receiver checked 1000 blocks, each comprising 107 bits. It is clear the efficiency of the Viterbi FEC, in which at a code rate of 2/3 for channels 26 and 50 and ½ for channel 37. It corrects raw BERs (i.e. before Viterbi) from values in the order of 10^{-3} to values before RS FEC below $2.0*10^{-4}$ which is considered as a well known estimate for good quality reception as seen in results obtained for the BER after RS which are almost quasi-error free (QEF). As with all previous parameters, BERs showed how channel 37 is the one with the best performance.

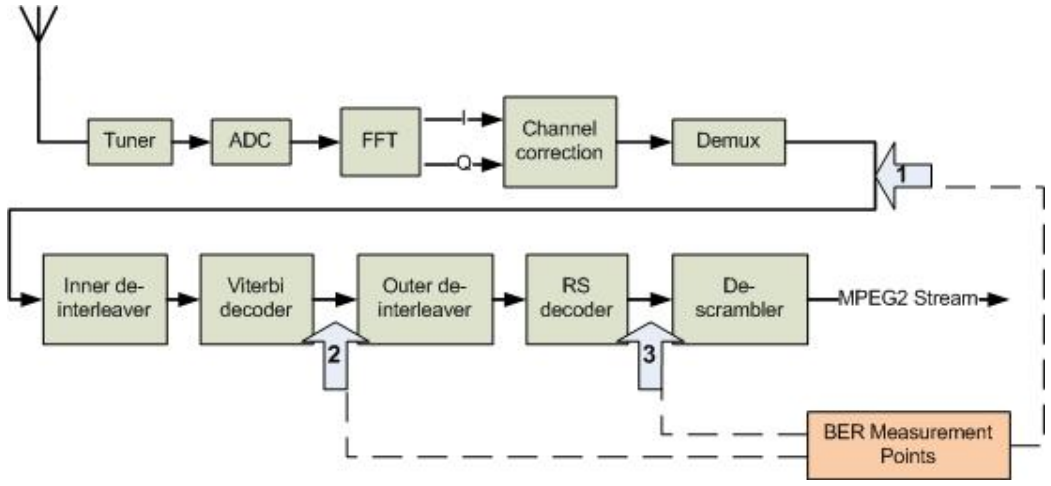

Figure 4-39 BER Measurement points in a digital video receiver

As a common rule and without any additional induced interference, we established that channels 26, 37, and 50 from the Aachen SFN provided the best performance characteristics at all considered locations. For this reason we focus the rest of our study on these three channels. Their main configuration parameters are included in Table 4-13.

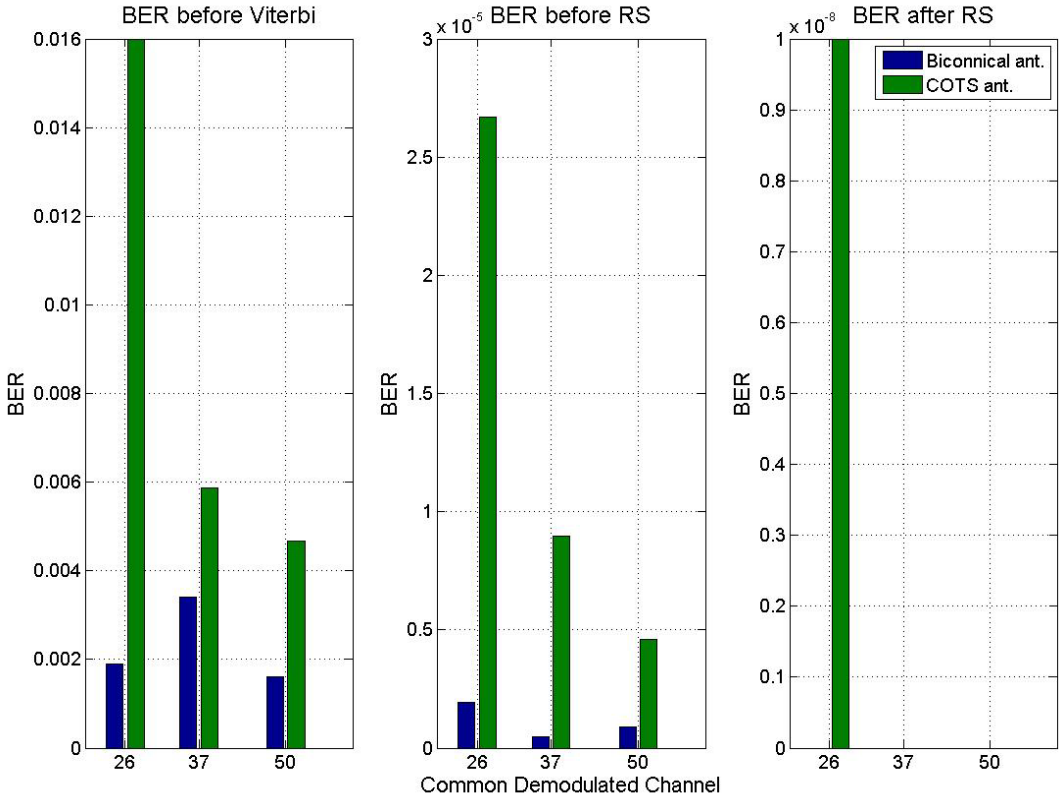

Figure 4-40 Different BERs for the common demodulated channels.

Table 4-13 Configuration of the DVBT-T channels measured at an institute in Aachen

Aachen SFN	Center frequency (MHz)	Modulation	Code rate	Guard interval	Serving tower	Distance to institute (km)	Transmit power (dBW)
Channel 26	514	16-QAM	2/3	1/4	Aachen	5.16	**37**
					Aachen Stolberg	12.76	**43**
Channel 37	602	64-QAM	1/2	1/4	Aachen	5.16	**40**
					Aachen Stolberg	12.76	**47**
Channel 50	**706**	**16-QAM**	**2/3**	**1/4**	**Aachen**	**5.16**	**40**
					Aachen Stolberg	**12.76**	**47**

Three of the chosen indoor locations were on the ground floor and two additional measurement points were included in two offices located in the third floor of the building.

Initially, each channel was measured for 20 minutes alternately using two types of receiving antennas. Signal performance parameters were stored every second. The receiving antenna was placed to achieve the best possible reception which was found to be next to the single window available at each of the rooms. The COTS antenna was oriented towards the window. The main resulting statistics for the channels of interest in addition to the orientation and altitude of the locations are listed in Table 2. By means of these results, the DVB-T signal variation for indoor reception can be analysed. For the same floor, channel power values lie within small ranges, the biggest span of 4.4 dB was found for channel 26 at the ground floor. Channel 26 always has the lowest mean received power level with on average 4.3 dB less than channel 37 and 2.6 dB less than channel 50.

Table 4-14 Power and spectrum measurements of selected DVB-T channels at different indoor locations

CH	Antenna	Location														
		1. (220° SW) Ground floor			2. (125° SE) Ground floor			3. (345° NW) Ground floor			4. (220° SW) 3rd. floor			5. (125° SE) 3rd. floor		
		P_c	σ_p	σ_s	P_c	σ_p	σ_s	P_c	σ_p	σ_s	P_c	σ_p	σ_s	P_c	σ_p	σ_s
26	Biconical	-59.3	0.334	3.98	-59.9	0.245	4.23	-60.6	0.234	3.76	-56.9	0.423	3.01	-57.8	0.278	2.72
	COTS	-58.4	0.193	4.56	-61.1	0356	4.78	-62.8	0.424	3.91	-56.7	0.321	3.11	-58.4	0.435	2.91
37	Biconical	-55.9	0.205	4.04	-56.8	0.209	4.97	-57.3	0.344	3.87	-52.4	0.332	2.76	-51.8	0.367	2.65
	COTS	-55.3	0.312	4.78	-56.6	0.498	4.14	-57.2	0.464	4.03	-53.1	0.447	2.99	-54.5	0.412	2.78
50	Biconical	-56.4	0.332	4.01	-57.7	0.343	5.03	-58.3	0.298	4.32	-54.2	0.446	2.68	-55.6	0.251	2.83
	COTS	-57.9	0.406	4.23	-58.3	0.412	4.98	-59.7	0.352	4.46	-55.3	0.363	2.83	-56.4	0.456	2.51

Pc(dBm): Mean power channel, σp(dB): Standard deviation of the channel power, and σs(dB): Standard deviation of the channel spectrum.

This effect is clear for having lower transmitter powers. For similar conditions but different receiving antennas, the mean received channel powers exhibit very similar absolute values with on average 1.13 dB differences. The effect of moving the TV

receiver to different locations within the same floor has a greater influence on the COTS antenna due to its directional properties. Location 1 is oriented towards the closest transmitting tower and therefore exhibits the best reception quality; for the same reason Location 3 has the worst reception quality and in these cases we have a mean drop in the received channel power of 1.5 dB when the biconical antenna is used and 2.7 dB for the COTS antenna case. Measurements on the third floor report better performance; on average a gain of 2.54 dB on the received channel power is achieved.

It is a common practice to use different propagation models to study the DVB-T portable reception inside buildings [ETSI97][Ladebusch06]. The ideal case is modelled by the Gaussian channel which is characterized by a single direct signal path between the transmitter tower and the TV receiver. Here, the only disturbance affecting the reception is the internal noise of the receiver. In a real indoor environment this model is too simple and not longer applicable. When there is not a single path and effects like multipath or fading are commonly present, two other propagation models are considered.

In addition to AWGN, the Ricean channel model takes into account the effects of multipath caused by echoes of the signal. In this model there is a stronger and predominant component. This component counts for most of the influence and therefore the other multipath components do not contribute much to the impairments found in the reception. The other model is the Rayleigh channel in which the multipath components are strong such that cannot be neglected, sometimes these components even have higher amplitudes than the main path or a direct signal path is simply not present.

Multipath effects were always found in the measurements. In the set-up used, the receiving antennas were always fixed and even in this case the power fluctuated because of the continuous change in the field strength. In order to analyse the multipath intensity, the standard deviation of the received spectrum σ_s was computed and presented in Table 3. Previous studies [Weck97][Angueira04] have measured the impulse response of the channel and found that there is a correspondence between the type of channel and the ranges of the standard deviations of spectrum of the received OFDM signal. Thus we could classify the type of channel according to the measured σs based on the setup used en each of the locations analyzed.

Values of σs lower than 1 dB are attributed to a Gaussian channel. Furthermore, values in the range of 1 to 3 dB are credited to Ricean channels and values higher than 3 dB to Rayleigh channels. Under this characterization, we found both Rician and Rayleigh behaviours in all the indoor measurements points used. All of the measurements carried out in the ground floor exhibit Rayleigh channel characteristics, while most of the measurements in the third floor show Rician properties.

The ETSI DVB-T standard [ETSI04] provides minimum C/N values for different types of reception configurations. These simulated figures are based on theoretical hypotheses associated to Rician and Rayleigh channel models. Moreover, the proposed values do not take into account any implementation margins. Hence, previous studies [Schramm04][Martinez09] carried out similar measurements and concluded that the thresholds proposed in the standards are too conservative and should be adjusted. The proposal of appropriate C/N thresholds requires first of the choice of a proper evaluation criterion. There are several degradation criteria to asses the interference in digital systems, some of the most common are [ECC148][Agilent08].

- Reference Bit Error Ratio (BER). The QEF criterion in the DVB-T standard defines good quality reception if there is less than one uncorrelated error event per hour. This corresponds to a reference Bit Error Ratio (BER) before Reed Solomon of $2 \cdot 10^{-4}$ [ETSI04].
- Picture failure point (PFP). Point where an observed spurious picture is present carried during a given period.

- Subjective failure point (SFP) usually useful in mobile reception which is not our case.
- Audio failure. Number of detected audio errors in a defined period

To our knowledge most of the studies and measurements reports in the literature have being based on subjective criteria, specially the PFP. This is mostly due to the fact of the impossibility to establish the BERs or the MPEG transport stream errors in commercial TV receivers.

For the case of indoor portable reception some authors [Martinez09][Faria05][Burrow06] claim that the previous criterion is not longer valid when error bursts occur due to the high and rapid variation of the channel. For these circumstances the Erroneous Seconds Ratio of 5% (ESR_5) assessment criterion was proposed [ITU04]. This is an objective method that has also shown a high correlation with other subjective reception quality criteria [Faria05]. In the ESR_5 the total measurement period is divided into intervals of 20 seconds each. An interval block is marked as good if there is not more than one second error (5% of the interval time) in the MPEG-TS packet. The ESR_5 can be calculated by taking the ratio between the number of correct 20-seconds blocks to the total number of blocks evaluated. If this ratio is bigger than 0.99, then the reception quality is considered correct.

$$ESR_5 = \frac{Number\_of\_good\_blocks}{Total\_number\_of\_blocks}$$

The C/N thresholds evaluated in this study are associated to failure points based on these QEF and ESR_5 objective criteria. For this purpose, attenuation levels were adjusted in steps of 1 dB. For each step, the duration of the C/N measurement was 10 minutes. Different BER before RS values were measured, each one associated to a C/N value, Figure 4-41 shows by way of an example the usual relationship found for channel 37 at Location 1. In order to calculate the QEF and the ESR_5 points, a linear interpolation and least-squares fit of the measured values were used respectively. The different measurement points were grouped according to their channel characteristics. The median values found are included in Table 4-15.

Table 4-15 C/N Thresholds for Rician and Rayleigh channels locations

Modulation	16-QAM		64-QAM	
Code rate	2/3		1/2	
Criterion	QEF	ESR_5	QEF	ESR_5
Propagation Channel	Minimum C/N (dB)	Minimum C/N (dB)	Minimum C/N (dB)	Minimum C/N (dB)
Rice	13.58	12.13	17.54	16.28
Rayleigh	16.79	15.37	19.89	18.76

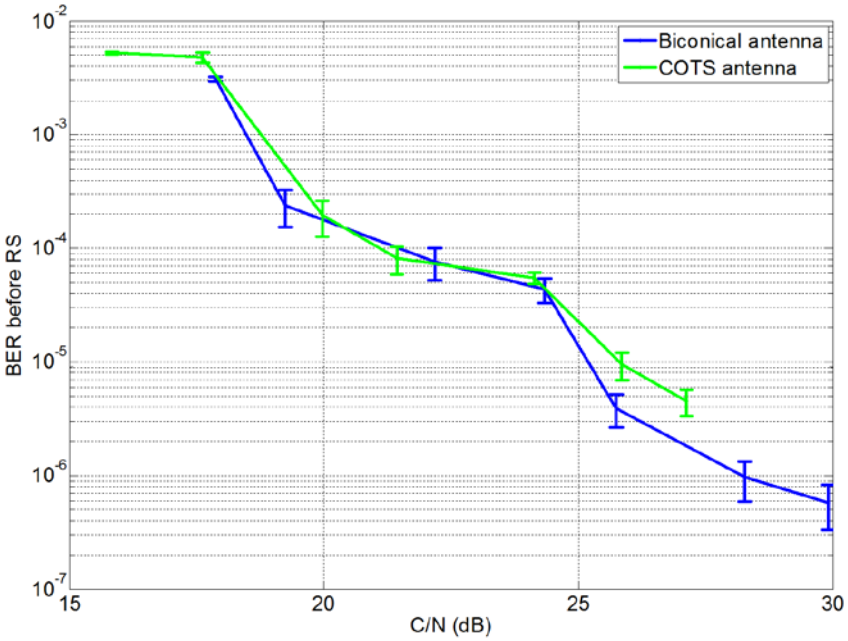

Figure 4-41 BER before RS vs C/N for channel 37 using two different receiving antennas at location 1

Independently from the modulation, code rate, and channel properties; the standard deviations stay almost constant with a value of around 1 dB. It is confirmed that the standardized values are too low. For the Rice propagation channel we found QEF C/N values which are 1.98 dB (16-QAM 2/3) and 2.84 dB (64-QAM 1/2) higher than the recommended by the ETSI [ETSI04]. For the Rayleigh case these differences are much higher 2.69 and 3.89 dB respectively. This is attributable to the fact that in these types of channels bit errors are more prone to occur in heavy bursts, and thus BER measurements are less indicative. Therefore the QEF criterion is less accurate to reflect the reception quality.

Additionally, as mentioned before the standardized values do not take into account implementation losses of receivers. We can also conclude that the common 3 dB value proposed for compensation for example in [CEPT97] is also too high. In [Schramm04] other thresholds based on measurements and for the particular case of static Rayleigh channels are available; these values are very similar to the results provided here. The differences on average of less than 0.8 dB corroborate the proposed figures.

The trade-off in terms of desired quality of service and immunity against errors for particular channel configuration is evident. For example, a 64-QAM scheme channel has the highest data rate but it also has greater susceptibility to communication errors. Furthermore, in [Martinez09] values based on ESR_5 criterion are offered for the case of 64-QAM 2/3 in Ricean and Rayleigh channels; these thresholds are on average 3.17dB higher than the results found in our measurements for the 64-QAM 1/2 case. This proves how the smallest code rate available of 1/2 provides the best choice in terms of robustness against errors.

The significant increase in the C/N thresholds obtained is not only due to multipath effects associated to a typical urban environment and the indoor measurement set-up itself, but also to the fact of multiple transmitter reception. Conducted theoretical studies and laboratory based measurements [Poole01] showed that receivers increase their required C/N thresholds when several transmitters from the same SFN are being

received with significant levels as it occurs in Aachen. It is clear that the QEF criterion is more demanding than the ESR_5. On average, the minimum C/N value that fulfils the QEF criterion is 1.31 dB higher than the value needed in ESR_5. This is expected since according to [Schramm04] in laboratory measurements for static Rayleigh channel, the ESR_5 criterion is satisfied at a BER of $2 \cdot 10^{-3}$.

4.2.3 **Analysis of WSD interference**

4.2.3.1 Co-channel interference measurements

Conducted indoor CCI interference measurements were carried out by implementing several set-ups. The WSD interfering signal is either a 64 Multitone or a QPSK 8 MHz modulated signal and its center frequency was configured according to the channel of interest following the parameters in Table 4-12.

The WSD transmitting antenna was mechanically adjusted to both vertical and horizontal polarizations and as in the previous section the two different types of available receiving antennas were tested. Initially, a fixed distance of 2 meters between the WSD and the TV receiver was used and the WSD transmitting power level was adjusted within the [−30, 20] dBm range in 5dBm steps, each measurement lasted for 5 minutes. Subsequently, the same experiment was repeated but now simultaneously introducing RF attenuations in 1dB steps for each of the WSD transmitting power levels. Finally, the WSD was set to transmit maximum output power (20 dBm) and was moved along a straight line in 50 cm steps towards the TV receiver starting from an initial position 5 meters away.

Each of these set-ups provided different SINR values. To establish the error-free time, the total measurement period was divided into intervals of 20 seconds as already described in the previous section. The relationship between error-free time and SINR has the shape of a Gaussian cumulative distribution with a 5% significance level, in Figure 4-42 a typical plot for a particular channel and set-up is shown.

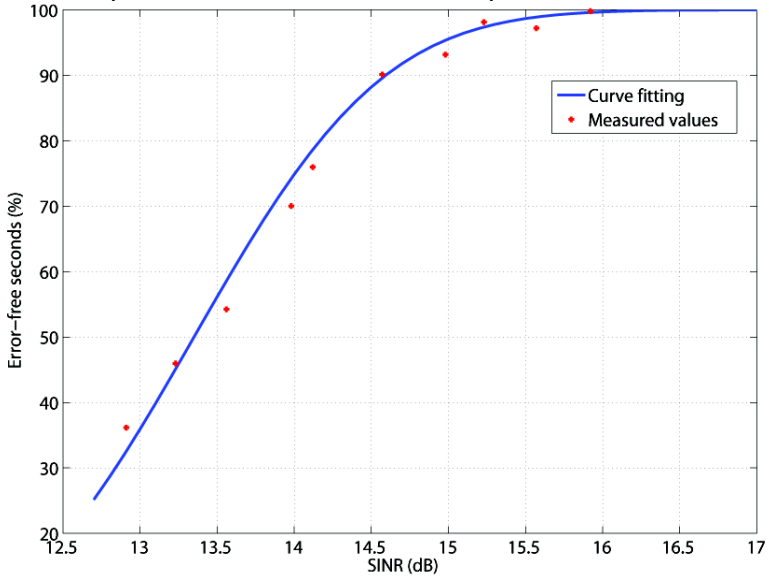

Figure 4-42 Percentage of error-free seconds vs SINR for channel 26 with QPSK WSD co-channel vertical polarized interference and using the biconical receiving antenna.

The Protection Ratio (PR) for a given configuration was estimated by using a least-square fit of a Gaussian cumulative distribution such that a 99% service threshold was achieved. In Table 4-16 several PRs are presented for different scenarios under CCI.

Independently from the type of interferer used, the TV receiver met the PR requirements proposed in [ITU06]. For portable indoor reception (PI), the ITU proposed Co-channel PRs limits of 16 and 19 dB for the 16-QAM 2/3 and 64-QAM 1/2 variants respectively. From Table IV it can be seen that different modulation schemes of the DVB-T signal require different PRs. In general 64-QAM requires a higher PR in the range from 1.91 to 3.04 dB with respect to 16-QAM. In this case, the TV receiver is more tolerant to interference because the 64-QAM modulation requires less interference to change symbol states and therefore produce demodulation errors.

Table 4-16 CCI Protection Ratios based on ESR5 criterion for different combinations of interferers/polarizations and receiving antennas.

WSD Interferer		Multitone		QPSK	
Polarization interferer		V	H	V	H
Modulation Code rate	Receiving antenna	Minimum C/N (dB)	Minimum C/N (dB)	Minimum C/N (dB)	Minimum C/N (dB)
16-QAM	Biconnical	15.01	14.74	15.61	14.93
2/3	COTS	14.65	13.35	15.43	14.15
64-QAM	Biconnical	16.92	17.54	18.32	17.97
1/2	COTS	16.73	16.12	17.86	17.32

When comparing the results for channels 26 and 50 that use the same modulation scheme but different operating frequencies, tests showed that the receiver performance was very similar regardless of the tuned receiver frequency. Additionally, the TV receiver was more susceptible to QPSK interference than to Multitone interference, but the results are still to a large extent similar since the spectral properties of the interfering signals are also comparable. Due to the vertically-polarized TV transmitters available in the area, cross-polar CCI always produces less harmful effects in the reception. This can be seen in the higher PRs required when co-polar CCI was applied. We found a greater effect of the CCI on the biconical antenna; this performance is expected given its radial isotropic radiation pattern. This antenna was installed and constantly controlled such that it maintained its omni-directional properties in the horizontal plane. The interference is less harmful for the COTS antenna as it is evident in the more relaxed PRs obtained. This effect is anticipated because the interferer was always located behind the antenna and opposite to its direction of maximal directivity.

The directivity characteristics of the COTS antenna can be seen in further experiments achieved in which we followed a circular path with a 2m radius around the TV receiver. The WSD had QPSK modulation and a fixed transmission power of 15dBm we followed measurements during 5 minutes at each 45°. The 0° reference was placed towards the window of the room, in this case this direction is towards 220° SW. As seen in Figure 4-43, since the biconical antenna has omnidirectional properties in the horizontal plane, we see almost constant performance independently of the angle of incidence, as

expected there is some degradation in the MER when the WSD is placed in the middle of the receiver and the room window. The degradation in the performance parameters when using the COTS antenna is clearer in the figure below.

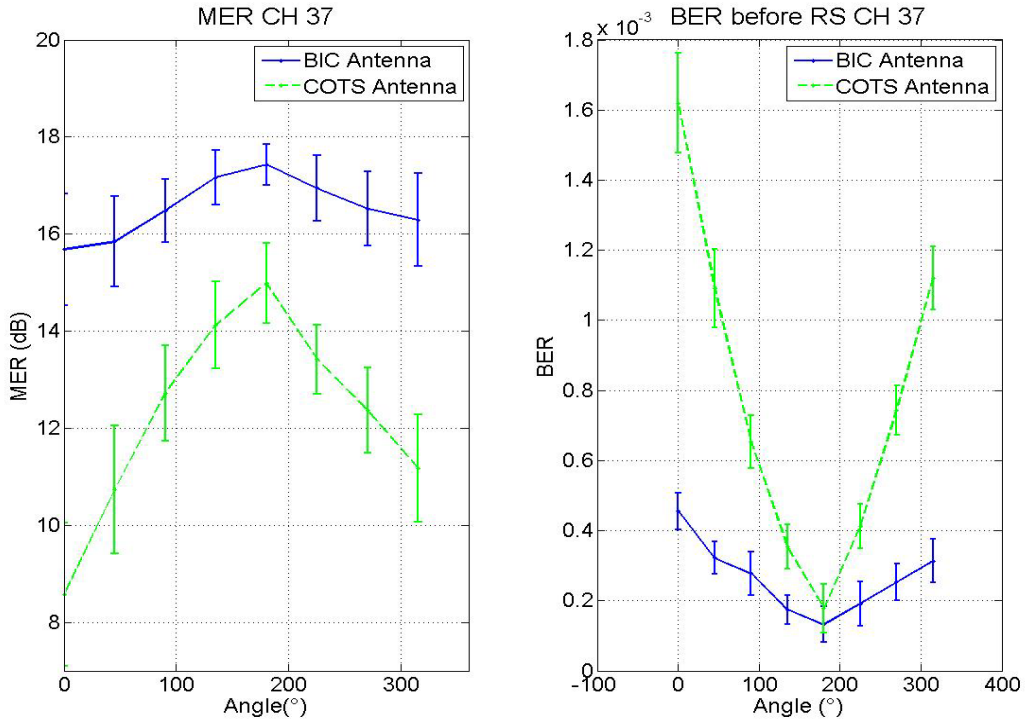

Figure 4-43 MER and BER before RS for channel 37 with co-channel interference with transmitting power of -15dBm and different angles of incidence to the receiver antenna.

In addition, the ESR_5 criterion was satisfied for any WSD receiver distance longer than 2.5m for the biconical antenna and 2m for the COTS antenna. Although, PRs are smaller when the COTS antenna is used, the WSD power level required to produce such disturbance was lower in comparison to the biconical antenna. This outcome can be seen clearer in Figure 4-44. Here, the Modulation Error Rate (MER) is plotted versus the QPSK WSD power level for different channels and particular set-ups. The MER provides a "figure of merit" of the received signal. This figure is calculated to include the total signal degradation likely to be present at the input of the TV receiver. It can be seen that with the biconical antenna higher levels of interference power can be tolerated. These results confirm previous results in terms of performance for the different channels analysed.

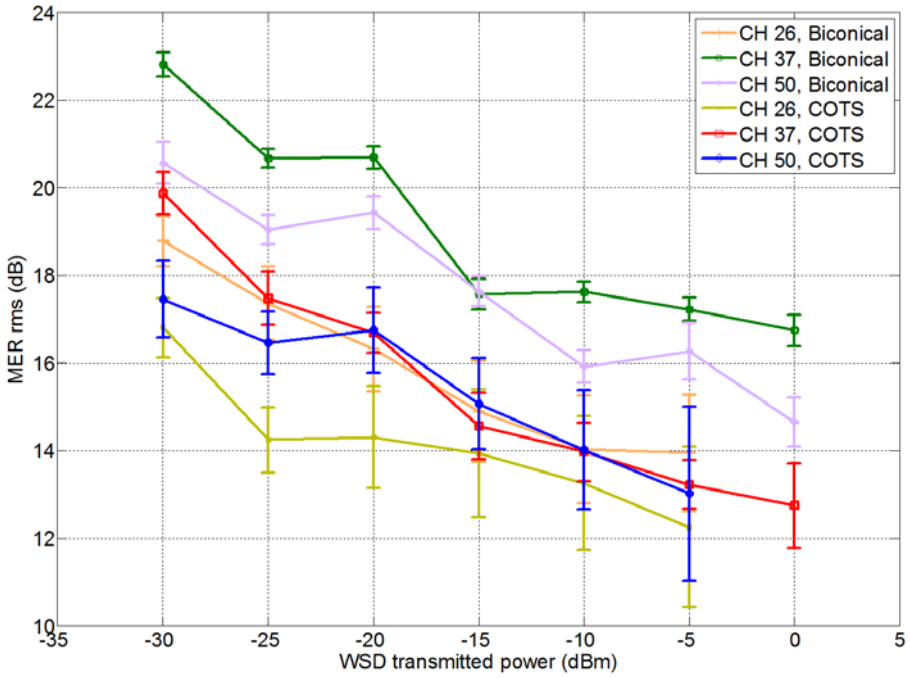

Figure 4-44 MER vs. interference power of the QPSK vertically-polarized WSD for different channels for both types of receiving antennas.

In these scenarios, it was confirmed that QEF criterion provides less accurate results. It is shown in Figure 4-45 for channel 26 how the QEF criterion provides reasonably different results for relatively similar conditions. Similar results were obtained in all other cases. Given the fact that block errors were frequent especially for low values of SINR, we found that the use of the QEF criterion cannot provide suitable values.

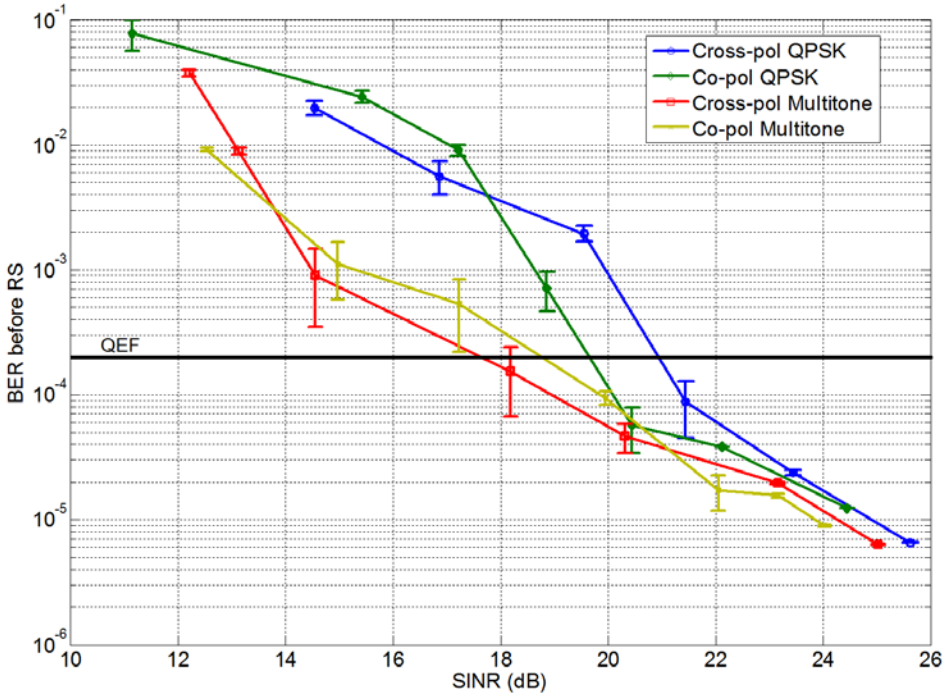

Figure 4-45 BER before RS vs. SINR for channel 26 using the biconical receiving antenna with different WSD CCI conditions.

4.2.4 **Conclusions on coexistence measurements**

The overall goal of this study was to contribute trough measurements in real indoor environments towards analysing the performance effects on DVB-T reception in the presence of a low-power WSD interferer. The results presented are an extension to other studies for obtaining C/N and PR thresholds for achieving right quality reception. Contrary to most of other studies the values proposed are based on objective criteria and were carried out on real indoor environments rather than in controlled or laboratory scenarios.

It was showed that between two convenient objective criteria analysed, the QEF criterion is more demanding than the ESR_5. Measurements confirmed that on average, the minimum C/N value that fulfils the QEF criterion is 1.31 dB higher than the value needed in ESR_5. Additionally, it was exhibited that the minimum QEF C/N values proposed in standards are too low. For indoor portable reception, it was found that for Rice propagation channels the C/N thresholds are 1.98 dB and 2.84 dB higher than the standardized values for 16-QAM 2/3 and 64-QAM 1/2 cases respectively. For the Rayleigh case, estimated values are even higher; 2.69 and 3.89 dB respectively. Values proposed based on ESR_5 criterion were corroborated with a single similar study which is available only for the Rayleigh case.

In an indoor environment and in presence of WSD interference, the QEF criteria did not provide suitable values. When multipath effects are present, the ESR_5 criterion is more appropriate to assess the TV reception quality. The PRs found always fulfilled the requirements proposed by the standards and can be consulted in Table 5. Due to the vertically-polarized TV transmitters available in the area, the co-polar interference always caused the most adverse effects. Furthermore, tests showed that for equivalent configurations the channel frequency does not play an important role in terms of performance evaluation. The use of an expensive biconical receiving antenna does not improve in a greater manner the TV reception quality; it was found that the overall quality of the receiver plays a major role.

4.3 **Shadowing**

4.3.1 **Equipment**

4.3.1.1 Introduction

This chapter presents the equipment used in the Shadow Correlation Measurement Campaign. In order to measure the shadow correlation, we have to transmit constantly a signal with the least power and frequency fluctuations possible, so as the collected data to be unbiased and thus reliable. We measure the RMS received power in different locations. The data are fitted in the large scale propagation model and from this we extract the shadow field, that is the residuals of the fitting. Then we proceed to the spatial statistical analysis of the shadow field that lead to the shadow correlation estimations.
Here, we describe the transmitter and receiver chains. The license that was issued for our purposes, permits a transmition of 4 Watts of power in different frequency bands. We chose to start our measurements with a frequency close to the DVB-T bands, that is 485 MHz and we currently continue to higher frequency bands.

4.3.1.2 Transmitter

The transmitter consists of the following components listed below.

The signal generator: We use the Agilent E4438C ESG Vector Signal Generator configured to generate a continuous wave of up to 30 dBm or 1 Watt of RF output power at a specified by user center frequency.

The Kuhne-Electronic KU PA BB 5030 A Power Amplifier: As mentioned above, the maximum output power we are allowed to transmit is 4 Watts and that was achieved by using the KU PA BB 5030 A Power Amplifier connected to the RF output of the signal generator, which can give only 1 Watt of RF power. The power amplifier with input power of 3 mW (4.77 dBm) and a typical gain of 32 dB gives the required output power that is fed to our antenna. A power supply of 24 V- 26 V DC is necessary for the power amplifier to work.

The Mini-Circuits VLF-490 Filter: The power amplification produces harmonics that must be suppressed. The frequencies of the harmonics are given by the formula:

$$n * f_{\text{center frequency}}, n = 2,3,4,\ldots$$

and in the case of 485 MHz the harmonics appear in:

a. 970 MHz.
b. 1455 MHz.
c. 1940 MHz.
d. 2425 MHz. That is in 2.4GHz ISM band, etc.

This problem is tackled by adding in the system the Mini-Circuits VLF-490 filter. The filter suppresses up to 40 dB the harmonic frequencies, without suppressing the signal in the center frequency of 485 MHz.

The SBA 9113-515 Omnidirectional Broadband Antenna: We used both at the transmitter and the receiver side the SBA 9113-515 Omnidirectional Broadband Antenna. As it can be seen by the manual [Schwarzbeck12], this antenna has omni directional characteristics from 450 MHz up to 3200 MHz and can cover also future measurement campaigns in different frequencies such as 1.7 GHz and 2.6 GHz. In 480MHz the Half Power(3dB) Beamwidth is equal to 90 degrees, for the E plane and in the H plane the antenna radiates isotropically.

4.3.1.3 Receiver

The receiver consists of the following components listed below.

The SBA 9113-515 Omnidirectional Broadband Antenna: The antenna used is the same with the antenna used at the transmitter.

The FSL6 Spectrum Analyser: The spectrum analyser used is the Rohde & Schwarz FSL6. The device settings are given in [RS12. There are different kind of detectors featured in FSL6. As noted in [Rauscher01], the average detector determines the average value of the power of the signal by using the linear level scale, so that the higher level of signal power are subjected to greater compression due to the calculation of the average in the dB scale. On the other hand, the RMS detector allows measurement of the actual power of the input signal without being spoiled by its temporal characteristics, and this is why we used the RMS detector as the main detector while collecting and analysing our data.

The Data Acquisition System: We used a laptop connected to the spectrum analyser through ethernet connection. The data collection and storage was done by a Matlab implemented software. The software uses Matlab Toolbox and Agilent Instrument Control Libraries. We also stored the measurements for the Average and the Auto Peak detectors, so as to be able later on to investigate the impact of the detector used on the results.

The Positioning System – Localisation: In order to measure the position of a measurement we tried first to use GPS. Although GPS is easy to use, it does not provide the accuracy needed. That is why we used the Digital Orthophotos 20 (DOP 20) created by the State of Aachen ("Stadt Aachen"). Digital Orhtophotos (DOP) are aerial vertical photographs that after digitazation are through digital processing enriched with geographical data, such as coordinates and data used to blend neighbour DOPs, and

then are saved as image files enriched with geographical data, namely geotiff files. The DOP 20 files can be opened by any free licence geotiff reading program and provide a position accuracy of 20cm.

Table 4-17 Summary of the Configuration of the Spectrum Analyzer

Filters in Span	Centre Frequency	Span	Sweep Time
501	485 MHz	5.01 MHz	0.05 sec

4.3.2 **Measurements**

In this chapter we present the procedures with which the measurements were conducted. Measuring the shadowing, requires first to estimate the local average of the power in every measurement point, so as to minimize the fast fading effect (or the multipath effect on the signal). More than 1000 measurement points were used with two different measuring techniques. Along with the measurements, there was also a reference receiver in Line of Sight (LoS) with the transmitter, so as to ensure the stability of the transmitted power, and from this the consistency of our dataset. Initial extensive calibration ensures the fitness of the transceiver chain for the fine-grained measurements we conducted.

4.3.2.1 No-Local-Average Measuring Approach

The first way of averaging out fast fading used, was to measure the Received Power in every measurement point for 1 min. This time period is enough to cancel any effects caused by the channel in a small-scale region, namely fast fading, due to relative motion between the receiver and transmitter, or by the movement of the objects in the channel. The distance between the measurement points is 5 meters except the first 60 measurement points that have a distance of 2 meters between them. The measurement points of the first approach are depicted in Figure 4-46.

Figure 4-46: Measurement Points of No-Local-Average Approach.

4.3.2.2 Local-averaging-out Measuring Approach

Lee [Lee85] states that the local average power of a signal in a given position can be accurately measured by averaging at least 36 i.i.d. power measurements in a distance of 40λ. In this local-averaging-out campaign we measured for 1 min (200 sweeps of the Spectra) while moving across a distance of 40λ, that is 24 meters at 485 MHz. The distance between the measurement points is 5 meters. It is obvious that if we just measured every λ, some of these measurements would be common for different measurement points. That is why we chose to measure continuously for the above mentioned distance and make 200 power measurements while moving. These 200 measurements are not i.i.d. but the error introduced is small. Figure 4-47 provides the map of the local-averaging-out measurement point approach.

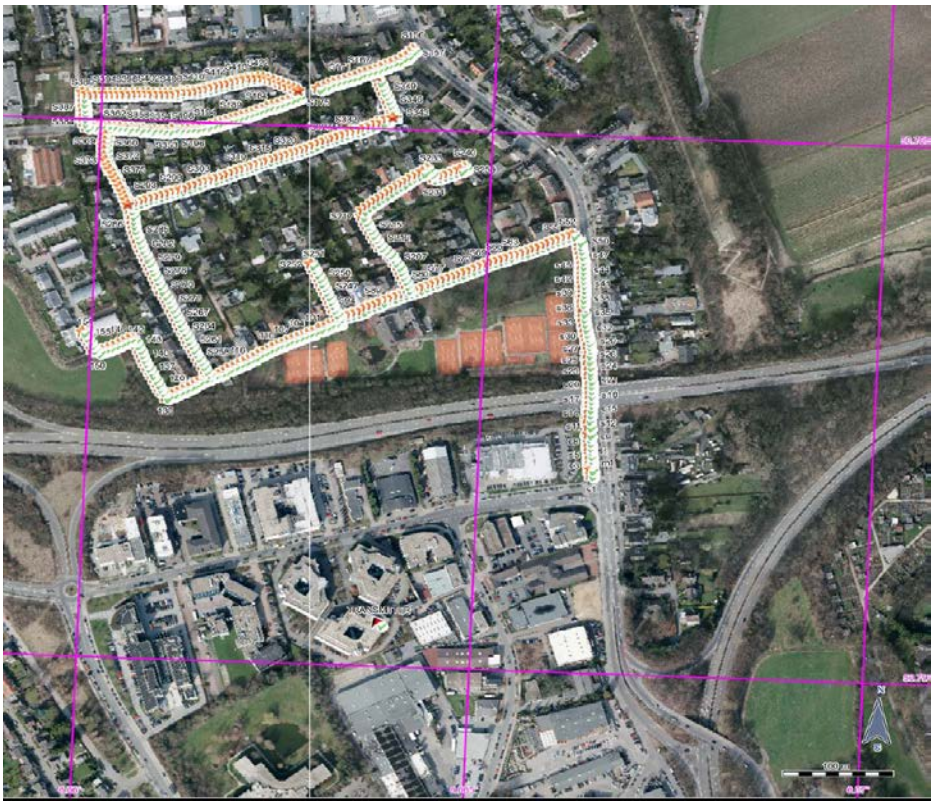

Figure 4-47: Measurement Points of Local-averaging-out Approach.

4.3.3 **Analysis**

In the following we describe how the shadow field was extracted from the dataset and then how the geospatial analysis was carried out. In order to convert the received power P(x) into the corresponding shadow field, we need to subtract the large scale propagation losses. The shadow field extraction is followed by the spatial statistics analysis. There are two types of spatial statistics analysis that are used here. The "Classical Geostatistics" and the Maximum Likelihood Variogram Estimation.

Propagation models assume path losses to be caused by three main contributing factors:

- Large Scale Path Loss (distance-based signal power deterioration)
- Shadow Fading
- Multipath Fading

During the measurements multipath fading due to the overlay of multiple scattered copies of the same signal should be averaged out. The only factors that should contribute in the propagation model is thus the zero mean normal distributed shadowing and the Large Scale Path Loss.

$$PL(dBm) = \underbrace{10g\log_{10}(distance)}_{deterministic-known} + \underbrace{Shadowing}_{wanted} + \underbrace{FastFading}_{averaged\ out}.$$

First step is to fit the curve $c+10g\log_{10}(d_i)$ to our data, where d_i is the distance between the i^{th} measurement point and the transmitter.
After determining c and g, the shadow field is given by

$$S(x_i) = P(x_i) - (c+10g\log(d_i))$$

4.3.3.1 Analysis with methods from geostatistics

In this approach the methods-of-moments and the least squares methods are used in order to estimate the semivariogram. The semivariogram is a function that describes the spatial correlation of a spatial random field. It is analogous to the variance of the values of the field between two different locations, i.e.

$$\gamma(s,t) = \frac{1}{2}var(Z(s) - Z(t))$$

In case of second order stationary random field, we can define the autocovariance as

$$\gamma(h) = C(0) - C(h) \ .$$

Where var is the variance, Z(▪) is the random field realization, s and t are two locations, h is the distance between s and t and C(▪) is the autocovariance. Due to stationarity, the distance h is merely the Euclidian distance between any two points s and t. Using data derived through the measurement campaign, the *empirical semivariogram* is derived. The derivation requires quantization of intervals between points and definition of the maximum correlation distance (which is usually the largest inter-point distance).

Th experimental semivariogram is in the following mapped to a *theoretical semivariogram* by means of finding the best-fit in terms of the residual error [Cressie93], [Gelfand10]. A robust estimator for this purpose in the sense of sensitivity to outliers is [Schwartz05]

$$\overline{\gamma}(h_u) = \frac{\left\{\frac{1}{N(H_u)}\sum_{s_i - s_j \in H_u}\left|S(s_i) - S(s_j)\right|^{1/2}\right\}^4}{0.914 + \left[0.988/N(H_u)\right]},$$

where $u = 1,\ldots,k$

4.3.3.2 Maximum Likelihood Variogram Estimation

Except classical geostatistics, we employed the model-based geostatistics in order to analyse the data. Model-based geostatistics is the term used in [Cressie80] to describe the use of stochastic models and likelihood-based methods to estimate the parameters of the variograms. However, maximum likelihood semivariogram estimation method is susceptible to non Gaussianities, and that is a reason that one must be careful when applying it. Last but not least, the method should be repeated many times with a grid of initial values so as to reduce the probability to find an estimation that minimises the negative log-likelihood function only locally.

There are two well known maximum likelihood analysis methods in spatial statistics. The first analysis method is the Maximum Likelihood Estimation (MLE), in which we estimate the m-vector of parameters, θ , given the covariance function of the Shadow Field, by maximising the log likelihood function.
The second analysis method is the Restricted or Residual Maximum Likelihood (REML) Estimation that reduces the bias of the MLE estimators. In REML the log likelihood is associated with the error contrasts, a number of linearly independent linear combinations of the observations [Gelfand10].

4.3.4 **Results**

4.3.4.1 Results of the no-local-average approach of measuring

For the first approach of measuring as described in section 4.3.2.1 the marginal distribution of the shadow field is depicted in Figure 4-48. Although the marginal distribution is fitted in a normal distribution with mean $\mu=\pm0.264857$ and $\sigma^2=35.3552\pm0.0351795$, one can realise that there is almost no correlation between them. The above is verified by the Figure 4-49 that is the experimental variogram of these data.

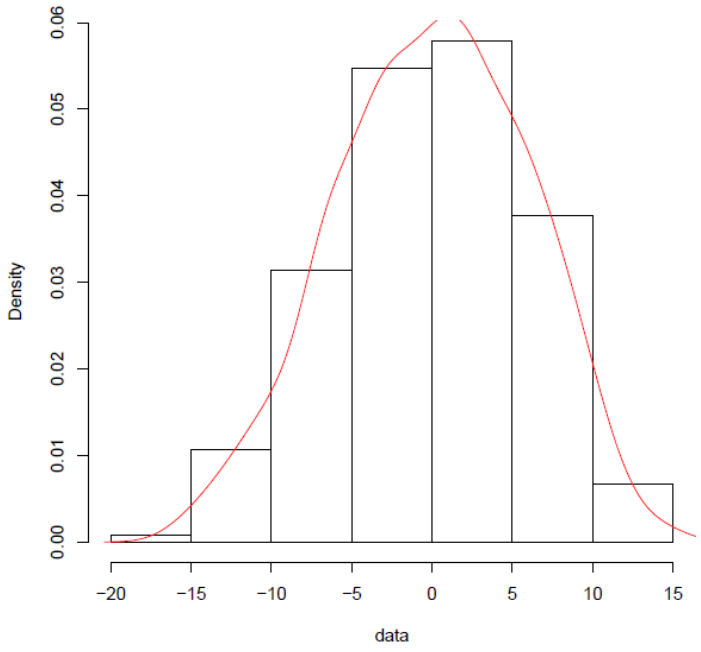

Figure 4-48: Marginal Density of Shadow Field without Local Averaging of the Received Power.

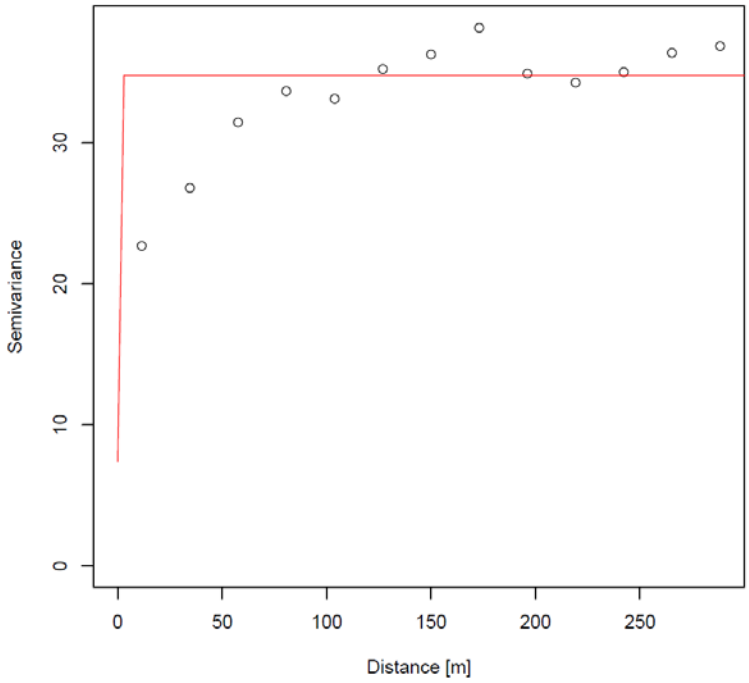

Figure 4-49 Empirical semivariogram of non-local-average method (best-fit theoretical semivariogram is shown for comparison in red)

4.3.4.2 Software-averaged measuring approach

In this approach we used the data from the previous measuring technique but we added a pre-analysis step. We averaged the received power in the distance of 40λ for every measurement point. For example, the received power on the first measurement point is the average RMS received power measured in the first 12 measurement points (as the distance between the measurement points is 2 m and 2*12=24m=40λ), the received power for the second measurement point is the average RMS received power meausured in the 12 measurement points from measurement point number 2 to measurement point number 11 etc. After the 60th measurement point we average every 5 measurement points (as the distance between the measurement points is 5 m and 5*5=25m>24m=40λ for 485 MHz).

As shown in Figure 4-50, there are areas with shadow correlation as the values of shadowing measured in neighbour measurement points, belong to the same quantile of the normal marginal distribution (have the same colour). Although this is a good sign for our measurement campaign the marginal distribution clearly not Gaussian, as can be seen in Figure 4-51. The fitting shows that the shadow field follows the normal distribution with mean equal $\mu=\pm 0.179299$ and variance equal to $\sigma^2=16.042\pm 0.0153735$. The variogram of these data and the estimated exponential theoretical fit can been seen in Figure 4-51. From this fit we estimated the range to be $\varphi=66.06$m.

Another useful parameter is the practical range defined as the range in which the correlation factor becomes equal to 0.05. The estimated practical range is 197.9m.

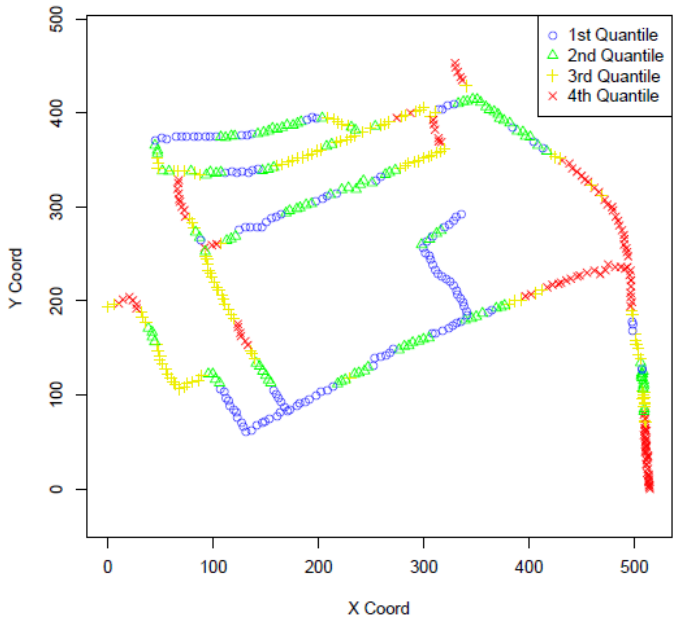

Figure 4-50: Shadowing Field of the Software-averaged Method of Measuring.

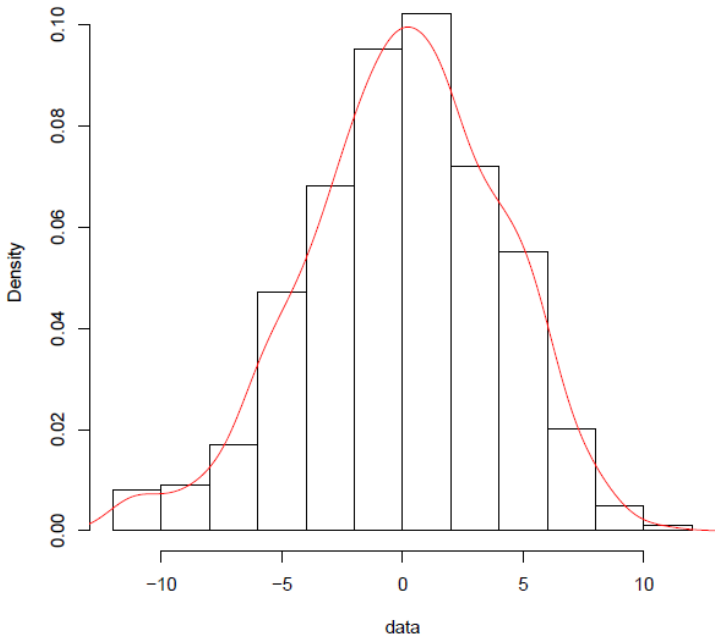

Figure 4-51: Marginal Density of Shadowing Field of the Software-averaged Method of Measuring.

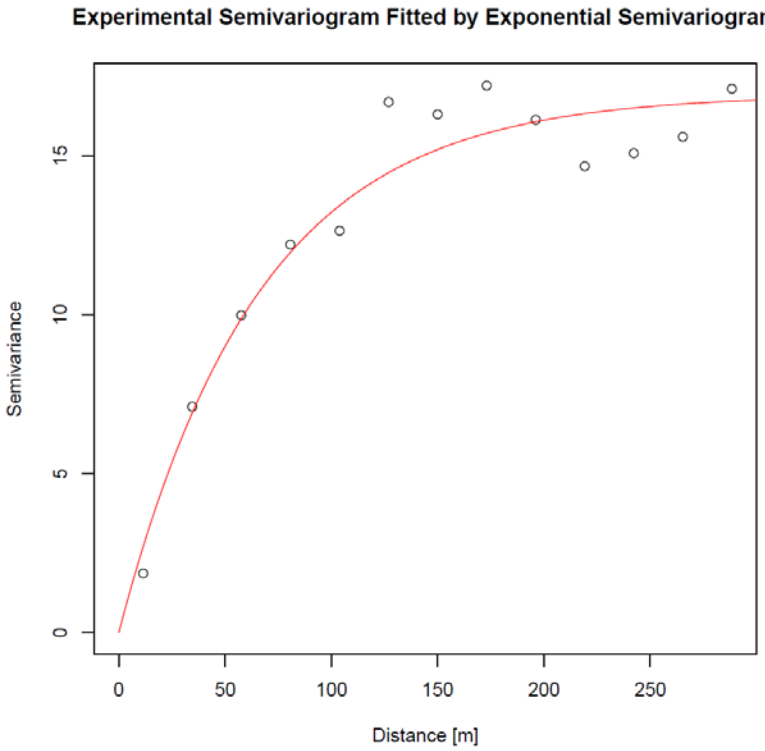

Figure 4-52: Semivariogram of the software-averaged method of measuring (for comparison, the fit to an exponential semivariogram is shown in red).

4.3.4.3 Results of the local-averaging-out approach of measuring

In Figure 4-53 and Figure 4-54, we show the results of the local-averaging-out measuring campaign. Here, one can see that we also have shadow correlation between neighbour measuring points. Shadowing follows a normal distribution, where $\mu = \pm 0.175042$ and $\sigma^2 = 13.1445 \pm 0.0153$.

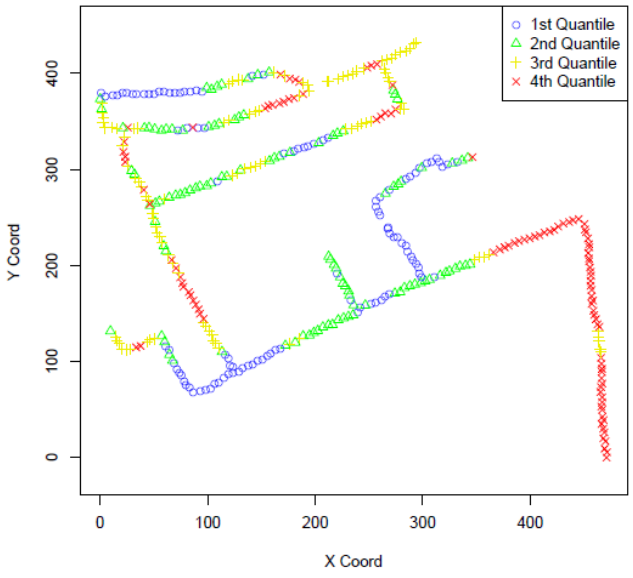

Figure 4-53: Shadowing Field of the Local-averaging-out Method of Measuring.

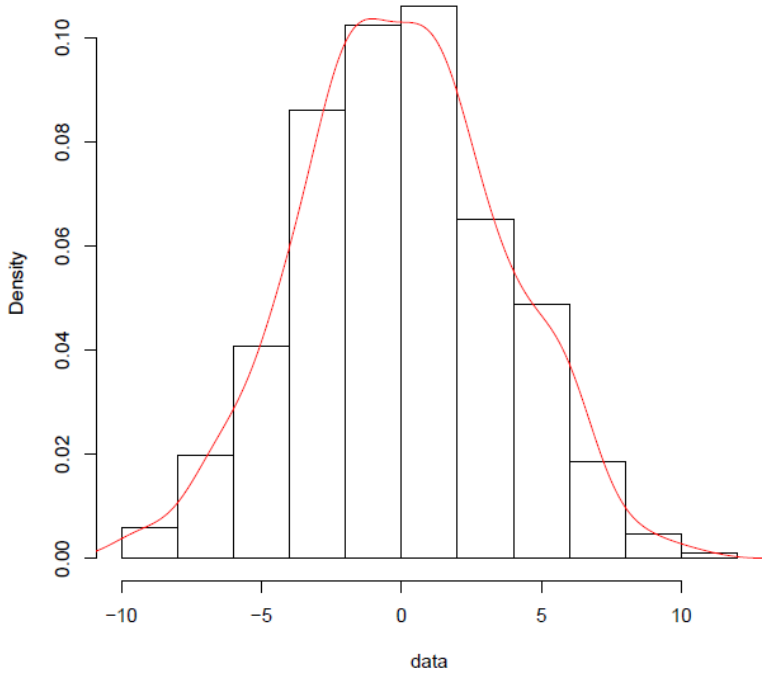

Figure 4-54: Marginal Density of the Local-averaging-out Method of Measuring.

4.3.4.4 Estimation of best-fit theoretical semivariogram

In Table 4-18 we depict the most importand estimated parameters and in Table 4-19 we show the RSS and the Chi-Square goodness of their fit. All the fit estimations have similar values. However, it can be seen that the exponential fit succeeds the best goodness of fitting score both in RSS and X^2 goodness of fit.

Table 4-18: Estimated parameters of theoretical semivariograms

Name	Practical Range [m]	nugget	k	φ[m]	σ^2
Cauchy	279.888	1.184	1	64.211	12.638
Matern	202.218	0.894	1	50.573	12.530
Exponential	284.567	0	-	94.991	14.470
Gaussian	130.049	1.627	-	75.137	11.096
Spherical	190.614	0.659	-	190.614	12.476
Cubic	182.798	1.639	-	182.798	11.093

Table 4-19: Goodness of fit to theoretical semivariograms

Name	Residual Sum of Squares	X^2 Goodness of Fit
Cauchy	13.682	1.192
Matern	12.345	1.065
Exponential	10.436	0.881
Gaussian	22.545	2.073
Spherical	14.645	1.338
Cubic	23.071	2.122

4.3.4.5 Maximum likelihood analysis

In the following, we analyze the dataset derived through the local-averaging-out measurement approach with MLE and REML methods. We use a grid of initial values so

as to avoid errors due to local minimum that may exist. Last but not least we repeat the estimation many times with a stochastic component algorithm.

In Table 4-20, the results of the two ML estimations are shown. Moreover in Figure 4-55 the fit of the exponential estimation estimated in against the ML and REML fits are depicted. The fits estimated by the maximum likelihood techniques,although they succeed a negative log-likelihood minimisation of -780.224 and -775.884 respectively, do not succeed on fitting the experimental variogram. The main reason are some non-Gaussianities that are present in the shadow field that can be observed in Figure 4-55 and in the quantile-quantile plot in Figure 4-56.

Table 4-20: ML and REML Estimated Parameters

Name	Practical Range [m]	nugget	k	φ[m]	σ^2
MLE	747.613	0.549	-	249.559	25.277
REML	1724.935	0.554	-	575.797	57.453

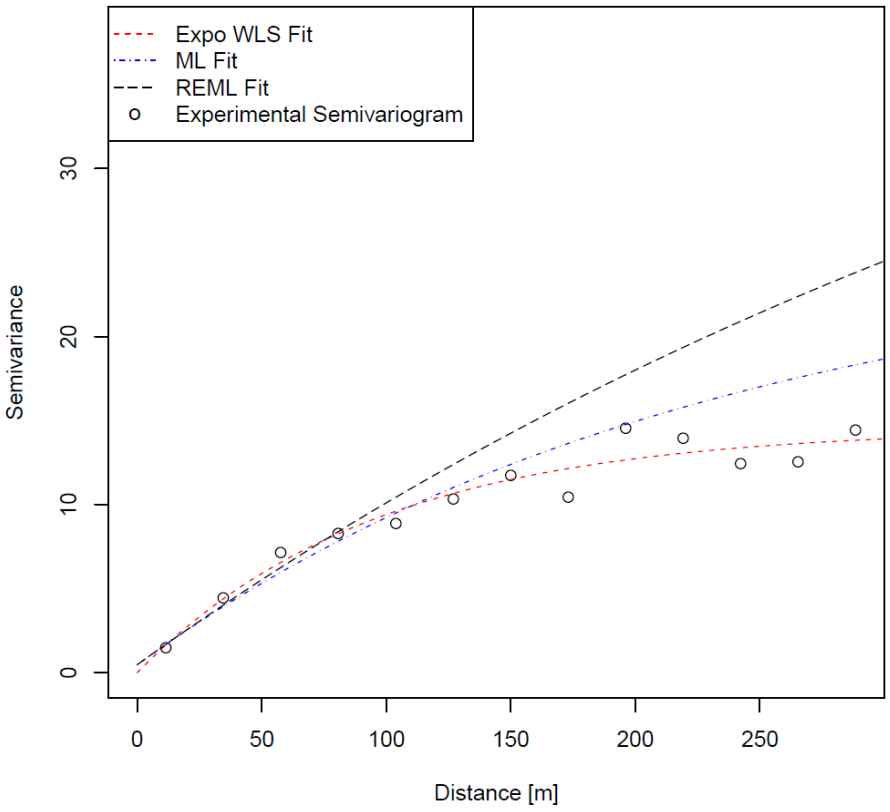

Figure 4-55: Weighted Least Square Fit, Maximum Likelihood Fit, R.M.L.E. Fit.

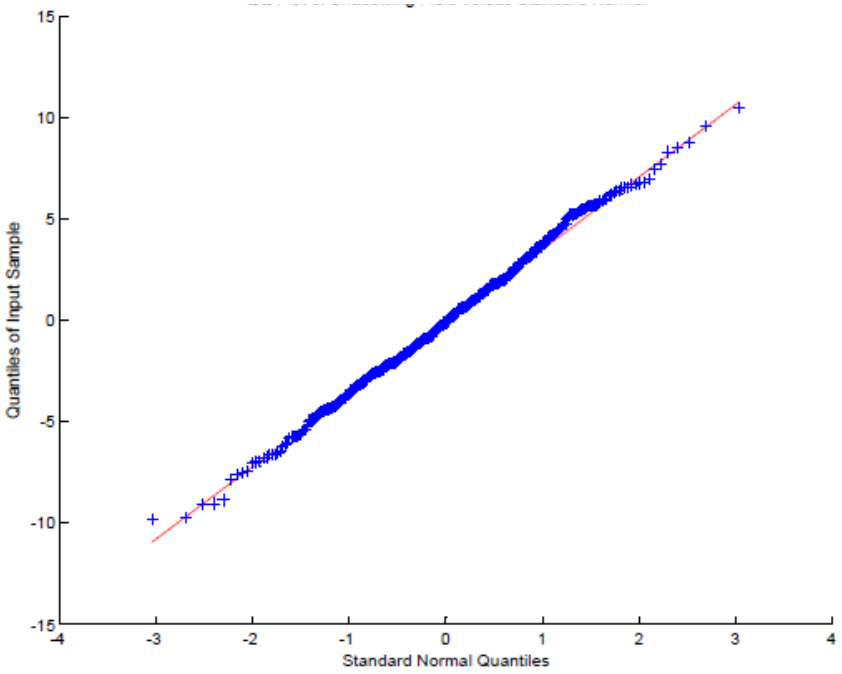

Figure 4-56: Quantile-Quantile Plot of Shadowing Field versus Normal Distribution

4.4 Conclusion on verification measurements

Section 4 reported on conducted spectrum measurements within the QUASAR project. The spectrum measurements serve different purposes starting from propagation model verification, primary and secondary system co-existence along with interference estimation, as well as for shadow correlation calculation and shadowing field modeling.

The measurements revealed that empirical propagation models exhibit significant errors when used in complex urban scenarios. Standard models without terrain information (ITU P.1546-3 and the Okumura-Hata model) tended to underestimate the received power in the proximity of the transmitter, while becoming more accurate when used for mid-range transmitter setups. It was found that urban environments are too challenging for The Longley-Rice ITM, as it has an emphasis on the general terrain, not on obstacles hindering direct LOS reception. All models were unable to estimate local shadowing correctly, resulting in high standard deviations of the error. On the other hand, the Longley-Rice model is suitable for country-wide analysis, not just for the UHF band, but also for the 2.7-2.9 GHz radar band.

Coexistence measurements in the TV receiver configuration revealed the complex effects of antenna configuration and WSD spacing to the perceived signal quality. While theoretical SINR estimates behave as expected in the presence of interfering signals, the effect on MER, PER, and other metrics describing the user-side quality are considerably more complex.

Finally this section presented the findings of the 485MHz shadow correlation measurement campaign, comparing the results obtained by the two basic approaches: No-Local-Average Measuring Approach and Local-averaging-out Measuring Approach.

5 Conclusions

Deliverable D5.4 is the final document reporting the outcomes and findings from the research activities in WP5. In the beginning we gave a short summary of the developed secondary spectrum assessment methodology with a special accent on interference modelling, which is one of the limiting factors for practical realization and implementation of opportunistic secondary systems. Using the assessment methodology, thorough quantitative analysis for finding out exploitable secondary spectrum opportunities were carried out for four use case and a number of countries and different locations in Europe. As a result of these detailed studies several essential findings emerged, which are summarized in section 2:

- Our analyses showed that the aggregate interference considerably reduces the availability of secondary access opportunities for macro-cellular deployments. It is not recommended to try to build a cellular LTE network relying only on TVWS opportunities. It can be observed that TVWS is much better suited for offloading than for stand-alone networks. Contiguous cellular coverage in TVWS is difficult to achieve and the use of TVWS as a capacity booster in limited local areas looks more plausible. It was found that mostly microcells in urban areas with low coverage requirements would benefit from TVWS. Additionally it is worth mentioning that the existing protection rules are not appropriate for cellular SU deployment. Compared to ECC and FCC usage rules, we found out that the power density based secondary power allocation can provide more capacity and protect the primary users more efficiently.
- The investigations of operating Wi-Fi-like multi-user secondary networks in TVWS showed that outdoor operation of such systems was not viable. The estimates of achievable range and rate were based on real estimates of TVWS channel availability from example urban and rural study regions in Germany. It was also found that operation of Wi-Fi-like secondary devices in TVWS might be viable for extending the range in indoor environments in comparison to the existing IEEE 802.11g standard, but only for low-rate applications. From the studies in Macedonia it can be concluded that in urban dense environment significant interference limits the average throughput of a secondary access point to only 1.7Mbps. Comparing with today's Wi-Fi systems operating in the ISM bands this maximal average throughput indicates that the solution will not be competitive alternative to operating in ISM bands.
- A large part of the 2.7-2.9 GHz radar band, used by air traffic control (ATC) radars, is found to be available for dense deployments of low-power secondary users. This in particular applies to secondary users in urban areas, which are typically far from the primary radars. The study of the possibilities of secondary spectrum access to the aeronautical spectrum band (960-1215 MHz), used by distance measurement equipment (DME), have shown that under conservative assumptions a bandwidth of at least 50MHz would be available to a dense deployment of secondary users in any location of Germany or Sweden. Overall the radar and aeronautical bands provides promising opportunities for low-power secondary systems. However there are still large regulatory issues to be cleared out and understood before the opportunities may be realized in practice.

In section 3 for the first time we introduced a software tool that allows assessing the feasibility and utility of secondary spectrum access beyond simple whitespace availability evaluation. The tool is aligned with the assessment methodology developed and provides a unified framework to conduct studies on the performance of secondary systems with dynamic spectrum access and is composed of an extensive primary spectrum usage database, a graphical interface for user interaction, and an interface to a backend for numerical calculations**.** The tool we allow for detailed showcasing of secondary spectrum availability in a desired set-up and could help researchers, industry and regulators to further study secondary spectrum access using the QUASAR methodology.

Finally in section 4 we report on a number of measurement campaigns carried out to study and verify several assumptions and facts taken in modeling when assessing secondary spectrum availability. The spectrum measurements serve different purposes starting from propagation model verification, primary and secondary system co-existence along with interference estimation, as well as for shadow correlation calculation and shadowing field modeling.

For example, we have found that empirical propagation models exhibit significant errors when estimating the received power in complex urban scenarios. The measured data was used to compare the performance of standard models such as ITU P.1546-3 and the Okumura-Hata model as well the Longley-Rice ITM. We found out that urban environments are too challenging for this model, as it has an emphasis on the general terrain, not on obstacles hindering direct LOS reception. All models were unable to estimate local shadowing correctly, resulting in high standard deviations of the error. Tom estimate the shadowing component more precisely we carried out a 485MHz shadow correlation measurement campaign, and the findings comparing the results obtained by the two basic approaches: No-Local-Average Measuring Approach and Local-averaging-out Measuring Approach are presented at the end of this section.

From measurements in Sweden it can be concluded that both spectrum leakage and intermediation products impacts seriously the outdoor operation of a WSD and they become more and more limiting when the WSD operates closer to the TV transmitter. Increasing WSD transmission power can overcome the problem; however, protecting the TV transmission from harmful interference is a severe restriction.

Finally from the measurements campaigns in the radar and aeronautical bands we learned that it is very difficult to reliably estimate the spatio-temporal characteristics of the DME radar, which make the estimation of secondary spectrum opportunity difficult. In the ATC bands it was measured that there can be some opportunities after a certain exclusion region of 10 km in Sweden for example, which is in accordance to the analytical studies.

Acronyms

AP	Access Point
ATC	Air Traffic Control
AWGN	Additive White Gaussian Noise
BER	Bit Error Rate
BS	Base Station
CAPEX	Capital Expenditures
CCDF	Complementary CDF
CCI	Co-Channel Interference
CDF	Cumulative Distribution Function
CEPT	European Conference of Postal and Telecommunications Administrations
CLI	Command Line Interface
COTS	Commercial off-the-shelf
CSMA/CA	Carrier Sensing Multiple Access / Collision Avoidance
DFS	Dynamic Frequency Selection
DL	Downlink
DME	Distance Measuring Equipment
DOM	Document Object Model
DOP	Digital Orthophotos
DSA	Dynamic Spectrum Access
DTT/DTV	Digital Television
DVB-T	Digital Video Broadcasting Terrestrial
ECC	European Communications Committee
EIRP	Equivalent isotropically radiated power
EMC	Electromagnetic Compatibility
ESR	Erroneous Seconds Ratio
ETSI	European Telecommunications Standards Institute
EVM	Error Vector Magnitude
FCC	Federal Communications Commission
GPS	Global Positioning System
GUI	Graphical User Interface
HTTP	Hypertext Transfer Protocol
IEEE	Institute of Electrical and Electronics Engineers
IETF	Internet Engineering Task Force
ISD	Inter-Site Distance
ISM	Industrial, Scientific, and Medical Bands
ITM	Irregular Terrain Model
ITU	International Telecommunication Union
KML	Keyhole Markup Language
LOS	Line-of-Sight
LTE	Long Term Evolution
MAC	Medium Access Control
MC-NKP	Multiple Choice Nested Knapsack Problem
MER	Modulation Error Rate

MLE	Maximum Likelihood Estimation
MSL	Mean Sea Level
NTIA	National Telecommunications and Information Administration
OFDM	Orthogonal Frequency Division Multiplex
OPEX	Operating Expense
PAWS	Protocol for Access to WS databases
PDF	Probability Distribution Function
PER	Packet Error Rate
PFP	Picture Failure Point
PPP	Poisson Point Process
QAM	Quadrature Amplitude Modulation
QEF	Quasi-Error Free
QPSK	Quadrature Phase Shift Keying
REML	Restricted Maximum Likelihood
RMS	Residual Mean Squared
RSS	Residual Square of Sums
SAP	Secondary Access Point
SDK	Software Development Kit
SFN	Single Frequency Network
SFP	Subjective Failure Point
SINR	Signal-to-Interference-And-Noise-Ratio
SIR	Signal-to-Interference-Ratio
SNR	Signal-to-Noise-Ratio
TCP	Transmission Control Protocol
TV	Television
TVWS	TV whitespaces
UHF	Ultra-High Frequency Band
UL	Uplink
URL	Univeral Resource Locator
VHF	Very-High Frequency Band
WLAN	Wireless Local Area Network
WSD	Whitespace Device
XML	Extended Markup Language

References

[Achtzehn11] A. Achtzehn, M. Petrova, P. Mähönen, “Deployment of a Cellular Network in TVWS: A Case Study in a Challenging Environment”, ACM CoRoNet ’11, Las Vegas, NV

[AchtzehnSimic12] A. Achtzehn, L. Simic, M. Petrova, P. Mähönen, “Feasibility of Secondary Networks in TVWS: Quantitative Study of Cellular and Wi-Fi-like Deployments”, submitted to IEEE Journal on Selected Areas in Communication

[Agilent00] Agilent Technologies, “Agilent E4438C ESG Vector Signal Generator Data Sheet”, 2000, online: http://cp.literature.agilent.com/litweb/pdf/5988-4039EN.pdf.
[Agilent08] Agilent Technologies, Inc. Application Note “BER and Subjective Evaluation for DVB-T/H Receiver Test“ May 2008.

[Angueira04] P. Angueira et al., “DTV reception quality field tests for portable outdoor reception in a single frequency network,” in Broadcasting, IEEE Transactions on, vol.50, no.1, pp. 42-48, March 2004.

[Beek11] J. van den Beek, J. Riihijärvi, A. Achtzehn, and P. Mähönen, “UHF white space in Europe - a quantitative study into the potential of the 470-790 MHz band,” in New Frontiers in Dynamic Spectrum Access Networks (DySPAN), 2011 IEEE Symposium on, pp.1-9, May 2011.

[BNetzA12] German Federal Network Agency, “DVB-T transmitter database,”, 2012, online: http://www.bundesnetzagentur.de

[Burow98] R. Burow et al., “On the performance of the DVB-T system in mobile environments,” in Global Telecommunications Conference, 1998. GLOBECOM 98. The Bridge to Global Integration. IEEE, vol.4, no., pp.2198-2204, 1998.

[CEPT97] The European Conference of Postal and Telecommunications Administrations (CEPT), “The Chester 1997 Multilateral Coordination Agreement relating to Technical Criteria, Coordination Principles and Procedures for the introduction of Terrestrial Digital Video Broadcasting (DVB-T),” Multilateral Coordination Agreement, Resolutions, Supplementary Information, Chester, July 1997.

[Cressie80] Cressie, N. and Hawkins, D.M., “Robust Estimation of the variogram”, IEEE Journal of the International Association for Mathematical Geology, 1980.

[Cressie93] Cressie, N, and Noel, A.C., “Statistics for Spatial Data Revised Edition”, John Wiley and Sons INC., 1993.

[D11] Jonas Kronander (editor), “Models, Scenarios, Sharing Schemes”, QUASAR deliverable D1.1, June 30, 2010

[D13] Seong-Lyun Kim, Jan Markendahl (editors), “Business Impact Assessment”, QUASAR deliverable D1.3, June 30, 2012.

[D43] Konstantinos Koufos (editor), “Combined secondary interference models”, QUASAR deliverable D4.3, March 30, 2012

[D51] Marina Petrova, Andreas Achtzehn (editors), “Model Integration and Spectrum Assessment Methodology,” QUASAR deliverable D5.1, March 31, 2011.

[D52] Ki Won Sung (editor), “Methods and tools for estimating spectrum availability: case of single secondary user,”, QUASAR deliverable D5.2, December 31, 2011.

[D53] Ki Won Sung (editor), “Methods and tools for estimating spectrum availability: case of multiple secondary users,” QUASAR deliverable D5.3, March 31, 2012.

[Diggle98] Diggle, P. J., and Tawn, J. and Moyeed, R.A., “Model Based Geostatistics”, Journal of the Royal Statistical Society: Series C (Applied Statistics), issue 3, vol. 47, pp. 299–350, 1998.

[Dudda12] T. Dudda and T. Irnich, “Capacity of cellular networks deployed in TV White Space,” submitted to DySPAN 2012.

[ECC148] Electronic Communications Committee (ECC) within the European Conference of Postal and Telecommunications Administrations (CEPT) ECC Report 148, “Measurements on the performance of DVB-T receivers in the presence of interference from the mobile service (especially from LTE)”, June 2010.

[ECC159] Electronic Communications Committee (ECC) within the European Conference of Postal and Telecommunications Administrations (CEPT) ECC Report 159 , “Technical and Operational Requirements for the possible operation of Cognitive Radio Systems in the White Spaces of the Frequency Band 470-790 MHz”, 2011.

[ETSI97] European Telecommunications Standards Institute (ETSI), “Digital Video Broadcasting (DVB); Implementation guidelines for DVB terrestrial services; Transmission aspects,” TR 101 190, V1.1.1, 1997.

[ETSI04] European Telecommunications Standards Institute (ETSI), “Digital Video Broadcasting (DVB); Framing structure, channel coding and modulation for digital terrestrial television,” EN 300 744, V1.5.1, 2004.

[ETSI08] European Telecommunications Standards Institute (ETSI), “Broadband Radio Access Networks (BRAN); 5 GHz high performance RLAN; Harmonized EN covering the essential requirements of article 3.2 of the R&TTE Directive,” Dec. 2008.

[Faria05] G. Faria, “DVB-H : Digital TV in the hands!,” in Teamcast, Amsterdam: IBC05, 2005.

[FCC10] Federal Communications Commission, “In the matter of unlicensed operations in the TV broadcasting bands: Second memorandum opinion and order”, Tech. Rep. 10-174A1, 2010

[FCCDB12] Federal Communications Commission, “TVWS database System Tests and Requirements”, 2012, online: http://transition.fcc.gov/oet/whitespace/guides/TVWS_Database_Tests.doc

[FinnTerrain] Digital elevation terrain data for North Eurasia, Available at: http://www.viewfinderpanoramas.org/dem3.html#eurasia

[Gelfand10] Alan E. Gelfand, Peter J. Diggle, Montserrat Fuentes, Peter Guttorp,. Handbook of Spatial Statistics. s.l. : Chapman & Hall/CRC, 2010.

[Ghosh11] Ghosh, C.; Roy, S.; Cavalcanti, D.;, "Coexistence challenges for heterogeneous cognitive wireless networks in TV white spaces," *Wireless Communications, IEEE* , vol.18, no.4, pp.22-31, August 2011.

[Gulati2010] K. Gulati, B.L. Evans, J.G. Andrews and K.R. Tinsley "Statistics of Co-Channel Interference in a Field of Poisson and Poisson-Poisson Clustered Interferers," IEEE Trans. on Signal Processing, vol. 58, no. 12, Dec. 2010

[ITM82] G.A. Hufford, A.G. Longley, and W.A. Kissick. A guide to the use of the Irregular Terrain Model in the area prediction mode. Technical Report 82-100, NTIA, 1982.

[ITU04] International Telecommunication Unit (ITU), "The ESR5 Criterion for the Assessment of DVB-T Transmission Quality," ITU WP6E, Document 6E/64-E, April 2004.

[ITU06] International Telecommunication Unit (ITU), "FINAL ACTS of the Regional Radiocommunication Conference for planning of the digital terrestrial broadcasting service in parts of Regions 1 and 3, in the frequency bands 174-230 MHz and 470-862 MHz (RRC-06)," RRC-06, Geneva, June 2006.

[ITU07] ITU-R M.2112, "Compatibility/sharing of airport surveillance radars and meteorological radar with IMT systems within the 2 700-2 900 MHz band," 2007.

[Karamacoski12] J. Karamacoski, P. Latkoski, L. Gavrilovska, "On Estimation Aspects of WLAN Secondary Spectrum Availability in ATC Radar Band", 18th European Wireless Conference (EW 2012), Poznań, Poland, April 18-20, 2012.

[Kingman1993] J. Kingman, "Poisson Process," Oxford University Press, 1993.

[Kronegger10] Dieter Kronegger, "EU Telecom Flash Message 44/2010", May 22, 2010.

[Ladebusch06] U. Ladebusch and C. Liss, "Terrestrial DVB (DVB-T): A Broadcast Technology for Stationary Portable and Mobile Use," in Proceedings of the IEEE, vol.94, no.1, pp.183-193, January, 2006.

[Latkoski2012] P. Latkoski, J. Karamacoski, L. Gavrilovska, "Availability assessment of TVWS for Wi-Fi-like secondary system: A case study", 7th International Conference on Cognitive Radio Oriented Wireless Networks – CROWNCOM 2012, Stockholm, Sweden, June 18–20, 2012.

[Lee82] Lee, William C. Y.,. Mobile Communications Engineering: McGraw Hill Higher Education, 1982.

[Lee85] Lee, William C. Y, "Estimate of Local Average Power of a Mobile Signal", IEEE Transactions on Vehicular Technology, 1985.

[Martinez09] A. Martínez et al., "Analysis of the DVB-T Signal Variation for Indoor Portable Reception," in Broadcasting, IEEE Transactions on, vol.55, no.1, pp.11-19, March 2009.

[Matlab12] The MathWorks, “MATLAB – The Language for Technical Computing”, 2012, online: http://www.mathworks.com

[MatlabCLI12] The MathWorks, “MATLAB Command Line Interface and Automation Server”, 2012, online: http://www.mathworks.com

[MFC12] Microsoft, “Microsoft Foundation Classes Library”, 2012, online: http://msdn.microsoft.com/en-us/library/d06h2x6e%28v=vs.71%29.aspx

[NETSDK12] Microsoft, “The .NET 2.0 Software Development Kit”, 2012, online: http://www.microsoft.com/en-us/download/details.aspx?id=19988

[Obregon10] Obregon, E.; Lei Shi; Ferrer, J.; Zander, J.; , "Experimental verification of indoor TV White Space opportunity prediction model," *Cognitive Radio Oriented Wireless Networks & Communications (CROWNCOM), 2010 Proceedings of the Fifth International Conference on* , vol., no., pp.1-5, 9-11 June 2010.

[Obregon12] E. Obregon, K.W. Sung and J. Zander, "Availability Assessment of Secondary Usage in Aeronautical Spectrum," submitted to DySPAN 2012

[PAWS12] IETF, “Protocol to access WS databases”, 2012, online: http://datatracker.ietf.org/wg/paws/charter/

[Poole01] R. Poole, “The echo performance of DVB-T receivers,” in EBU Technical Review, no. 288, pp. 19, April 2001.

[Randhawa06] B. Randhawa, I. Parker, A. Ishaq, and Z. Wang, “RF Measurements to Quantify 3G and WiMAX Mobile Interference to DVB-T Receivers,” ERA Technology Ltd, Ofcom. December 2006.

[Randhawa07] B. Randhawa and S. Munday. “Conducted Measurements to Quantify DVB-T Interference into DTT Receivers,” ERA Technology Ltd, Ofcom. October 2007.

[Rappaport02] Theodore S. Rappaport. Wireless Communications: Principles and Practice 2 Edition: Prentice Hall, 2002.

[Rauscher01] Rauscher, C., Janssen, V. & Minihold, R. Fundamentals of Spectrum Analysis. Fundamentals of Spectrum Analysis. s.l. : Rohde & Schwarz GmbH & Co. KG,, 2001.

[SE4311] ECO WG SE43, “Technical and operational requirements for the possible operation of cognitive radio systems in the whitespaces of the frequency band 470-790 MHz”, Tech. Rep. ECC 159, 2011

[Simic12] L. Simic, M. Petrova, P. Mähönen, “Wi-Fi, but not on Steroids: Performance Analysis of a Wi-Fi like Network Operating in TVWS under Realistic Conditions”, accepted to IEEE ICC’12

[Stuber09] G. Stuber, S. Almalfouh, and D Sale, “Interference Analysis of TV-Band Whitespace,” in Proceedings of the IEEE, vol.97, no.4, pp.741-754, April 2009.

[Schramm04] R. Schramm, “DVB-T - C/N values for portable single and diversity reception,” in EBU Technical Review, IRT: Institut F¨ur Rundfunktechnik, April 2004.

[Schwarzbeck12] Schwarzbeck, D. Microwave Biconical Antenna SBA 9113 Manual, 2012, online: http://www.schwarzbeck.de/Datenblatt/k9113.pdf.

[Schwartz05] Mischa Schwartz, Mobile Wireless Communications: Cambridge University Press, 2005.

[Splat12] RF Signal Propagation, Loss, And Terrain analysis tool for the spectrum between 20 MHz and 20 GHz, 2012, online: http://www.qsl.net/kd2bd/splat.html.

[Weck97] C. Weck and Schramm, “Receiving DVB-T: Results of field trials and coverage considerations,” in 20th Int. Television Symp., Record Cable/Satellite/Terrestrial pp. 351360, June 1997.